SPEC_COLL
THESIS
09S.B
H636

THE UNIVERSITY OF ADELAIDE
DEPARTMENT OF GEOLOGY AND GEOPHYSICS

The Pamatta Pass Canyon Complex: Neoproterozoic Wonoka Formation, Flinders Ranges, South Australia.

by Jonathan Higgins, B.Sc.

November 1997

30·7·98

The Pamatta Pass Canyon Complex: Neoproterozoic Wonoka Formation, Flinders Ranges, South Australia.

Jonathan Higgins B.Sc.

Department Of Geology And Geophysics,
University Of Adelaide.

This thesis is submitted as partial fulfilment of the requirements
for the Honours Degree of Bachelor of Science.
November, 1997.

National Grid Reference:-
Orroroo Sheet SI 54-1 (1:250,000 Geological Series.)

Contents.

Terminology.

Abstract.

Introduction.

Chapter 1 - Regional Geology.
- 1.1. Introduction.
- 1.2. Stratigraphic Outline.
  - 1.2.1 The Warrina Supergroup.
  - 1.2.2. The Heysen Supergroup.
    - 1.2.2.1. Umberatana Group.
    - 1.2.2.2. Wilpena Group.
  - 1.2.3. Moralana Supergroup.

Chapter 2 - Previous Investigations.
- 2.1. Introduction
- 2.2 Wonoka Formation Canyon Systems.
  - 2.2.1. Submarine Canyons.
  - 2.2.2. Subaerial Canyons.
    - 2.2.2a. Messinian Event Style Formation.
    - 2.2.2b. Diapirism.

Chapter 3 - The Stratigraphy Of The Wilpena Group.
- 3.1. The Umberatana Group.
- 3.2. The Wilpena Group.
  - 3.2.1. The Sandison Subgroup.
    - 3.2.1.1. The Ulupa Siltstone.
    - 3.2.1.2. The ABC Range Quartzite.
  - 3.2.3. The Aruhna Subgroup.
    - 3.2.3.1. The Wilcolo Sandstone.
    - 3.2.3.2. The Bunyeroo Formation.
  - 3.2.4.Depot Springs Subgroup.
    - 3.2.4.1. The Wearing Dolomite.
      - 3.2.4.1a. The Burr Well Member.
    - 3.2.4.2.The Wonoka Formation.

Chapter 4 - Canyon Geometry.
- 4.1. K1 Geometry.
- 4.2. K2 Geometry.
- 4.3. Palaeogeographic Reconstructions.

4.4. Linked Canyon Systems.

Chapter 5 - Canyon Fill Stratigraphy.
5.1. Introduction.
5.2. K1 Wonoka Formation Stratigraphy.
5.2.1. K1 Unit.
5.3. K2 Wonoka Formation Stratigraphy.
5.3.1. Basal Conglomerates/Olistostrome Unit.
5.3.2. Basal Sands Unit.
5.3.3. Wallplaster Unit.
5.3.4. Burr Well Member.
5.3.5. Wall Slumps.
5.3.6. HU4 Equivalent Unit.
5.3.7. HU5 Equivalent Unit.
5.4. Palaeocurrent Analysis.
5.4.1. K1 Facies.
5.4.2. K2 Facies.

Chapter 6 - Canyon Fill Discussion.
6.1. K1 Wonoka Formation.
6.2. K2 Wonoka Formation.

Chapter 7 - Sedimentological Analysis.
7.1. XRD Mineralogical Analysis.
7.2. XRF Major And Trace Element Analysis.
7.3. Cathodoluminescence Analysis.
7.4. Stable Isotope Analysis.

Chapter 8 - Depositional Model.
8.1 Introduction.
8.2. K1 Canyon Model.
8.2.1. Model 1 - Wilcolo Sandstone Time Deposition.
8.2.2. Model 2 - Late Bunyeroo Time Incision.
8.2.3. Model 3 - Wearing Dolomite Time Incision.
8.2.4. Model 4 - Wonoka Time incision (post HU1.)
8.3. K2 Wonoka Formation.

Chapter 9 - Depositional Model Discussion.
9.1. K1 Wonoka Formation.
9.1.1. Model 1
9.1.2. Model 2.
9.1.2. Models 3 & 4.
9.2. K2 Wonoka Formation.

9.2.1. Messinian Style Event.

Chapter 10 - Structural Geology.
10.1. Folding.
10.2. Cleavages.
10.3. Tectonic History Of The Region.
10.3.1 Pre-Depositional Tectonism.
10.3.2. Syn-depositional Tectonism.
10.3.3. Post Depositional Tectonism.
a) The Cambro-Ordovician Delamerian Orogeny.
b) Other Phanerozoic Movements.

Chapter 11 - Conclusions.

Acknowledgements.

References.

Appendices.

Appendix A:- Geological Map Of The Pamatta Pass Canyon Complex (Enclosed in pocket).
Geological Cross Sections.

Appendix B - Plates And Descriptions.

Appendix C- Analytical Procedures.

Appendix D - Analytical Results.
a) Geochemical Analysis.
b) Stable Isotope Analysis.

Terminology.

Preserved within the study area is evidence for two successive phases of Wonoka Formation canyon incision. The first, termed 'K1' (i.e. Canyon 1), is unique to this location and is preserved on the western side of the canyon incision.

The second phase of canyon incision, termed 'K2', records the development of the canyon systems for which the Wonoka Formation is renowned. The K2 succession bears close affinity to the shelfal strata of the Wonoka Formation and is accordingly correlated with the units described by Haines (1987). Throughout this thesis references to these units will be denoted by the use of the prefix 'H.' For example, Unit 5 of Haines' classification is denoted as 'HU5.'

Other abbreviations are concerned with sedimentary structures or depositional environments. These include:

HCS = Hummocky Cross Stratification.
SCS = Swaley Cross Stratification.
FWB = Fair-weather Wave Base.
SWB = Storm Wave Base.

Abstract.

Deposition of the late Proterozoic Wilpena Group is characterised by numerous sequence boundaries or regional disconformities that reflect the tectono-stratigraphic history of the Adelaide Geosyncline. The most prominent of these are those related to kilometre-sized incised valley systems within the lower Wonoka Formation. Alternative subaerial and submarine origins have been proposed. Recent work substantiates the subaerial model as it accounts for several lines of evidence the submarine model could not adequately answer.

The Wonoka Formation in the Pamatta Pass Canyon Complex was first observed by Binks (1971). Observations made during field mapping support a subaerial origin and record evidence for multiple phases of canyon incision.

A pre-Wonoka Formation phase of deformation (probably related to the Penguin Orogeny in northwest Tasmania, or the Beardmore Orogeny in Antarctica) is interpreted to have existed. Syn-depositional tectonism is likewise attributed to this event. Compressional deformation during the Delamerian Orogeny subsequently deformed the entire sedimentary prism in a complex array of NNE/SSW folds.

Introduction.

The 'Pamatta Pass Canyon Complex' lies approximately 12 km northeast of Carrieton, and 32 km due north of Orroroo in the southern Flinders Ranges. It comprises Umberatana and Wilpena Group sediments forming the White Valley Syncline.

The history of the Wilpena Group is unique in that it records the incision of 'Grand Canyon'-depth channel systems. These canyon systems are subdivided into 2 sets (Haines, 1987), with the majority of models for canyon development being based on the northern system. Much work has been focussed upon these structures as they have a crucial role to play in understanding the dynamic processes affecting the deposition of the Adelaide System.

Despite having been studied for more than 30 years there is still no consensus on their origin. Two primary hypotheses have evolved to explain their origin and infill with current debate centred upon whether the incisions developed subaerially (Eickhoff, 1988; Eickhoff *et al.*, 1988; DiBona, 1989; Von der Borch *et al.*, 1989), or in a submarine environment (Haines, 1987; Jansyn, 1990; Ayliffe, 1992). Field observations support the subaerial, 'drowned river', model of canyon development.

The geometry of the Pamatta Pass Canyon Complex, along with the nature of the canyon fill and the presence of a non-marine limestone precipitated on the eroded walls, leads to the conclusion that fluvial processes played a dominant role in canyon formation. Evidence for two successive phases of fluvial canyon incision and subsequent burial can be found within the study area in the form of the hitherto undescribed 'K1' succession and the well documented 'K2' succession. A minimum 1050 m of Ulupa Siltstone, ABC Range Quartzite, Wilcolo Sandstone and Bunyeroo Formation was eroded by both phases before being infilled by deltaic to shallow-marine sediments. The upper portion of the canyon has been significantly eroded during post-Adelaidean times.

Such a multi-phase model of subaerial canyon incision has important ramifications for the tectono-stratigraphic history of the Wilpena Group. This model requires sea-level fluctuations of more than a purely eustatic nature. However, the somewhat ambiguous nature of the canyon-filling sediments and the possibility of alteration of the crucial wallplaster, coupled with a lack conclusive evidence for a drawdown of tectonic origin has led to the persistence of the submarine model.

The dearth of evidence pertaining to tectonic involvement has significantly hampered the acceptance of the subaerial model. Nevertheless, such a model is necessitated by the failure of its counterpart to adequately accommodate the observed sedimentary and geochemical characteristics of the canyon systems. Previous mechanisms for subaerial canyon development not invoking regional scale tectonic uplift follow two main lines.

The first suggests uplift was generated by extensive salt diapirism observed throughout the Flinders Ranges. The second elaborates canyon development as occurring in response to an evaporitic sea-level fall within an isolated basin (analogous to the Miocene Messinian event that affected the Mediterranean; Christie-Blick et al., 1990). However, the inability of these models to adequately account for several lines of evidence, including shallow-water sedimentary structures and geochemical and isotopic data, has led to their validity being seriously questioned.

Several authors have presented inconclusive evidence for a pre-Delamerian Orogeny phase of folding within the Adelaide Geosyncline (Binks, 1971; Eickhoff, 1988; DiBona, 1989; Jansyn, 1990). Preserved within the study area lies evidence for a phase of tectonism interpreted to have played a crucial role in generating uplift of the required magnitude. The relationships observed within the Wonoka Formation canyon sediments demonstrate that this phase of folding and deformation post-dates deposition of the K1 succession whilst predating the K2 succession. It is inferred to have been responsible for the widespread development of canyon systems throughout the Flinders Ranges. In addition a pre-K1 phase of tectonism is also implied.

It is postulated that successive phases of uplift may by related to either in homogeneous stretching of the lithosphere (Christie-Blick et al., 1990) or cycles of lithospheric extension and thermal subsidence (Jenkins, 1990.) Conversely these tectonic events may be expressions of the Penguin Orogeny of northwest Tasmania or the Beardmore Orogeny of Antarctica. Further work is required in order to substantiate this premise.

LIBRARY

Chapter 1 - Regional Geology.

1.1 Introduction.

The Adelaide Geosyncline (Sprigg, 1952) (Fig.1.1) comprises a thick succession of late Proterozoic 'Adelaide System', and Cambrian syn- and post-rift sediments. Deposition commenced between 1100 Ma to 800 Ma (Preiss, 1987, 1990) and ended with the onset of the Delamerian Orogeny (around 500Ma) that produced an arcuate fold-belt extending from Kangaroo Island to the the Peake and Denison Ranges. For a detailed summary see Rutland *et al.* (1981) and Preiss, (1987).

Modern dissertations classify the Adelaide Geosyncline as describing the development of a passive continental margin rift or failed rift complex (Rutland *et al.*, 1981; Von der Borch *et al.*, 1988, 1992; Preiss, 1987, 1990.) A variety of discrete and multifarious tectono-stratigraphic units have been devised for the Adelaidean with the northern regions interpreted as an aulacogen (Scheibner, 1973) or the failed arm of a 3-arm rift system (Von der Borch, 1980; Gunn, 1984) and the southern portions resembling a passive continental margin setting. Jenkins (1990) relates deposition within Adelaide Fold-Belt to recurring cycles of lithospheric extension and thermal subsidence.

The poorly exposed Torrens Hinge Zone (Thomson, 1969) separates the Adelaide Geosyncline from a correlative, but relatively undeformed condensed section on the Stuart Shelf to the west. A maximum of almost 300 km in width, the northern and easternmost margins are extensively buried by Mesozoic and Cainozoic cover. It trends southwards beneath modern continental shelf sediments before finally being truncated by the present continental margin (Haines, 1987). Lying to the east, the pre-Adelaidean basement complex of the Curnamona Nucleus, with its western margins largely obscured by Phanerozoic sediments, ostensibly presents an eastern boundary for the Adelaidean succession.

1.2 Stratigraphic Outline.

The Adelaidean is subdivided into 3 unconformity bounded supergroups on the basis of tectonic setting, palaeogeography and palaeoenvironments (Fig. 1.2) (Preiss, 1987).

1.2.1 The Warrina Supergroup.

The basal Callana Group marks the onset of syn-rift sedimentation, consisting of evaporitic lacustrine sediments and volcanics that were later involved in widespread syn-depositional diapirism during post-Burra Group time. The succeeding Burra Group, is composed of various alluvial fan, deltaic and lacustrine deposits.

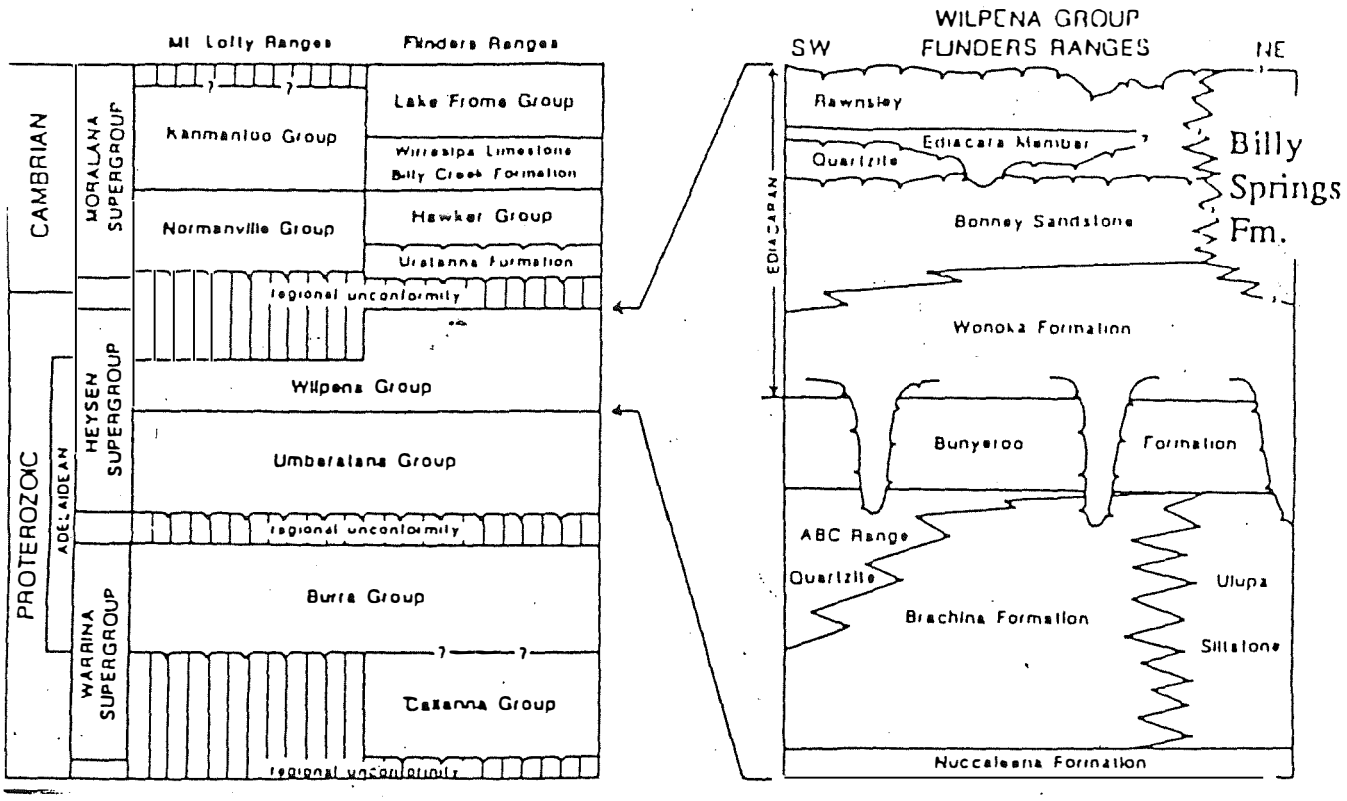

Figure 1.2 Stratal divisions of the Adelaide Geosyncline and the simplified stratigraphy of the formations belonging to the Wilpena Group (modified from DiBona, 1989).

1.2.2 The Heysen Supergroup.

Comprises the Umberatana Group and overlying Wilpena Group, forming the uppermost Proterozoic sequences of the Adelaide Geosyncline.

1.2.2.1 Umberatana Group.

The group includes the Sturtian and Marinoan glaciogenic strata along with the intervening 'interglacial' succession marking the first marine ingression onto the Stuart Shelf during the Adelaidean. These strata broadly correlate with other glacial strata of global extent and form an arbitrary frame of reference for the study area. The Umberatana Group is unconformably overlain by the Neoproterozoic Wilpena Group and together they form the Ediacarian of Cloud and Glaessner (1982).

1.2.2.2 Wilpena Group.

Wilpena Group sedimentation commenced with a marine transgression, followed by clastic progradation from the west across the Adelaide Fold-Belt and onto the Curnamona Nucleus. Wilpena Group sedimentation has been correlated with sequences in the Officer and Amadeus Basins. Moreover, its very extensive distribution elucidates the degree to which the mechanisms controlling sedimentary conditions were remarkably invariable over a very broad expanse (Jansyn, 1990).

Deposition commenced with the Brachina Subgroup (Plummer, 1978), embracing the Nuccaleena Formation, Brachina Formation/Ulupa Siltstone, ABC Range Quartzite and the Wilcolo Sandstone. The subsequent megacycle deposited the Bunyeroo Formation, Wearing Dolomite, Wonoka Formation and uppermost Pound Subgroup.

1.2.3 Moralana Supergroup.

The succeeding widespread Cambrian marine sediments were removed by subsequent erosion in the present study region.

Chapter 2 - Previous Investigations.

2.1 Introduction.

Dalgarno & Johnson (1964) formally defined the Wonoka Formation, mapping its base as the colour change from dominantly maroon to dominantly green shales. Problems with this highly gradational and laterally diachronous boundary (Haines, 1987), coupled with the need for a distinct and regionally significant basal position of the Ediacaran (Jenkins, 1981), led to its redefinition by Gostin & Jenkins (1983). Lowered to the base of the thin, but laterally persistent 'Wearing Dolomite Member' (Dalgarno & Johnson, 1964), this has since been defined as a separate entity by Dyson (1996a), representing a distinct and basinwide lithostrome of regional significance.

Previous studies of the Wonoka Formation have centred largely on its broad sedimentology and stratigraphy, or its localised deposition in large 'canyons.' Haines (1987) subdivided the sequence in the central Flinders Ranges into 11 mappable and lithologically distinct units. The units become ambiguous in the more distal areas of the basin and within the 'canyon' systems. Applying the principles of sequence stratigraphy, DiBona (1989) divided the formation into 9 lithostratigraphic units and 4 unconformity-bounded sequences.

2.2 Wonoka Formation Canyon Systems.

The Wonoka Formation is of great interest to geologists because of the nature of its large-scale unconformities infilled with a unique succession of calcareous and siliciclastic sediments. Coats (1964) first recognised a large-scale slump structure in the Pasty Springs region infilled with thick sequences of Wonoka Formation. Thomson (1969) and Coats (1973) subsequently identified it as a submarine canyon.

Subsequent mapping by various workers (Binks, 1968; Von der Borch *et al.*,1982, 1985, 1989, 1990; Gostin & Jenkins, 1983; Von der Borch & Grady, 1984; Von der Borch *et al.*, 1985, 1989; Haines, 1986, 1987, 1988; Eickhoff, 1986; Eickhoff *et al.*, 1988; DiBona, 1990; Christie-Blick *et al.*, 1990; & Sukanta *et al.*, 1991) has distinguished two separate canyon systems in the northern and southern Flinders Ranges (Fig. 2.1).

2.2.1 Submarine Canyons.

Various authors (e.g. Coats, 1973; Von der Borch, 1982; Haines, 1987; Preiss, 1987) attribute canyon formation to submarine processes.

According to this model, a relative sealevel fall during early Wonoka time diverted large amounts of siliciclastic sediment to the ramp slope. The abrasive action of turbidites and slumping subsequently downcut and laterally eroded the underlying strata. Canyon infilling soon followed, with classic Bouma sequences (Bouma, 1962)

Figure 2.1 Map of the distribution of lower Wilpena Group sediments throughout the Flinders Ranges (after Christie-Blick *et al.*, 1990). The Wonoka Formation canyon systems are listed numerically.

North Flinders Canyon System.
1 - Fortress Hill Canyon Complex.
2 - Shallow incised valley north of Umberatana Station.
3 - Oodnapanicken Canyon.
4 - Depot Springs Canyon.
5 - Patsy Springs Canyon.
6 - Nankabunyana Canyon.
7 - Salt Creek Canyon.
8 - Mucatoona Canyon.
9 - Puttapa Canyon.
10 - Beltana Canyon.

South Flinders Canyon System.
11 - Shallow incised valley west of Buckaringa Hill.
12 - Buckaringa Gorge Canyon.
13 - Yarra Vale Canyon.
14 - Waukarie Creek Canyon Complex.
15 - Pamatta Pass Canyon Complex.
16 - Possible canyon within Waroonee Syncline.
17 - Yunta Canyon Complex.

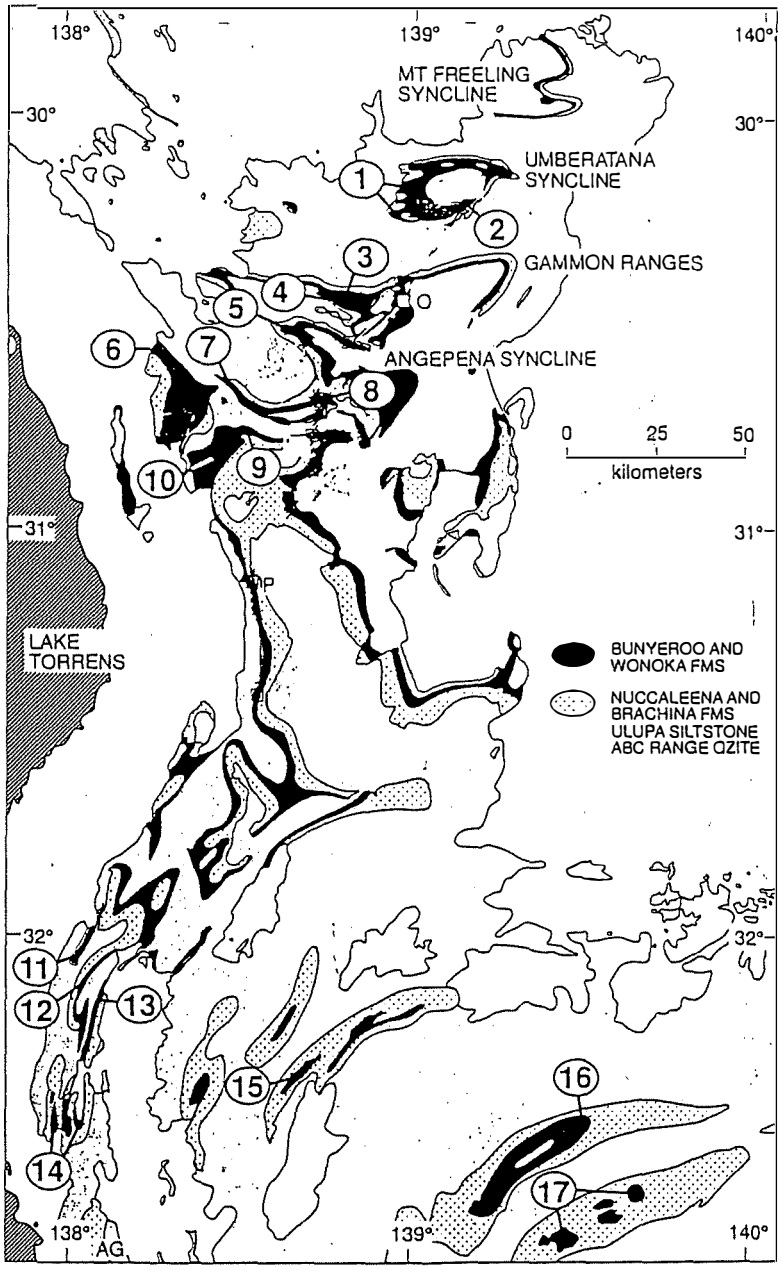
138°
139°
140°
30°
31°
32°
MT FREELING SYNCLINE
UMBERATANA SYNCLINE
GAMMON RANGES
ANGEPENA SYNCLINE
1
2
3
4
5
6
7
8
9
10
11
12
13
14
15
16
17
0
25
50
kilometers
LAKE TORRENS
BUNYEROO AND WONOKA FMS
NUCCALEENA AND BRACHINA FMS
ULUPA SILTSTONE
ABC RANGE QZITE
AG

and deep-water facies associations cited as evidence for a submarine origin (e.g. Haines, 1987; Von der Borch *et al*, 1982, 1985; Jansyn, 1990, Ayliffe, 1992.). Sedimentary textures used to support a submarine origin include HCS, alternating current directions and meandering channels (e.g. Shephard & Marshall, 1973; Piper, 1989; Hesse & Rakofsky, 1992.) The lack of karst topography in the lower Wonoka Formation also casts doubt upon the subaerial model of canyon formation (R.J.F. Jenkins & V.A. Gostin, pers.comm., 1997).

2.2.2 Subaerial Canyons.

Eickhoff, (1988), Eickhoff *et al.* (1988), Von der Borch (1985, 1989), and DiBona (1989), challenged the submarine model, instead proposing a subaerial model for canyon formation.

The occurrence of basal axial conglomerates possessing a distinctly fluvial appearance (Von der Borch, 1985; R.J.F. Jenkins, pers. comm., 1997) interbedded with sandstones, along with the presence of meandering canyon systems (e.g. Eickhoff, 1988) casts doubt upon the submarine model. Evidence for shallow-marine sedimentary structures, tidal palaeocurrent distributions and a non-marine limestone mantling canyon walls (Eickhoff, 1988; Eickhoff *et al.*, 1988; Von der Borch *et al.*, 1989; this study) serves to shift the focus of attention towards subaerial incision.

This model requires sealevel fluctuations of approximately 1000 m during early Wonoka time (Von der Borch *et al.*, 1982.) in order to account for fluvial incision and the prograding marine sediments forming the canyon fill (Eickhoff *et al.*, 1988). This drawdown cannot be accounted for by eustasy alone (Miall, 1984) and implies either an unusual mechanism of drawdown or a tectonic influence.

Jenkins & Gostin (1988) reported that canyon incision may have been triggered by a warping phase near the termination of the Bunyeroo Formation and initiation of flyschoid type sedimentation of the Wonoka Formation. Von der Borch *et al.* (1982) agreed that canyon incision was related to a major tectono-sedimentary cycle, but stated that canyons were not obviously fault controlled. This was repudiated by Jansyn (1990) who mapped thickness variations in the Wilpena Trough in the central Flinders Ranges and suggested that canyon formation may be fault related. Binks (1971) suggested a period of pre-Delamerian uplift that could correspond to syn-depositional basin-floor warping elaborated by DiBona (1989) to account for thickness variations in the Bunyeroo Formation.

2.2.2a Messinian Event Style Formation.

Von der Borch *et al.* (1989) and Christie-Blick *et al.* (1990) suggested a subaerial model for canyon incision along similar lines to the Messinian event that drained the Mediterranean. River gorges were incised into the shelf-edge following the isolation of the Adelaide Geosyncline from the open sea. A reopening of links to the sea then

deposited shallow-marine sediments, thus ably overcoming the apparent inability of global eustasy to explain fluctuations in sealevel of the required magnitude.

2.2.2b Diapirism.

Yet another proposed mechanism (Scotford, 1984; Von der Borch *et al.*, 1989; Sukanta *et al.*, 1991; Dyson, 1996b) is the production of uplift by diapirism, leading to locally focussed erosive processes upon palaeotopographic highs. Clear evidence of widespread emergent diapirism during Wonoka time exists (DiBona, 1989; Scotford, 1984; Haines, 1986, 1987, 1988.) However, diapiric uplift, is essentially localised in its effects whilst the distribution of the Wonoka Formation canyons requires large scale regional uplift. Sukanta *et al.* (1991) hypothesise that a phase of diapirism was triggered by tectonism.

Chapter 3 - The Stratigraphy Of The Wilpena Group.

The study area comprises late Proterozoic sediments of the Umberatana and Wilpena Groups.

3.1 Umberatana Group.

The upper boundary of the Umberatana Group is used as an arbitrary frame of reference for the study area. The uppermost unit of this comprises either the grey-green siltstones and shales of the Enorama Shale, or the granulose sandstones of the Marinoan Elatina Formation.

3.2 Wilpena Group.

This is the youngest subdivision of the Neoproterozoic succession and records two apparent major transgressive-regressive cycles (Haines, 1987). Dyson (1996a) devised the most recent stratigraphic framework (Fig. 5.3).

3.2.1. The Sandison Subgroup.

Within the study area the Sandison Subgroup (Dyson, 1996a) comprises the distal facies of the Brachina Subgroup (Plummer, 1978a): the Ulupa Siltstone, and the ABC Range Quartzite. It records the development of a delta complex in response to an influx of coarse detritus from the Gawler Craton. Tectonic instability resulted in its partial erosion and reworking to form the western intertidal sandflat represented by the ABC Range Quartzite.(Plummer, 1990.)

3.2.1.1. The Ulupa Siltstone.

Comprising red-brown weathering, khaki-green to grey siltstones with local intercalations of slumped mudstones, fine sandstones and conglomerates, it represents the basinal deposit of a transgressive systems tract.

A prominent red-brown to black, ferruginous interval [Plate 1A-D], displaying small-scale HCS, abundant cross-bedding and symmetrical ripples, lies approximately 700 m below its upper boundary. This interval (Moorillah Siltstone Member equivalent) contains evidence of tuffaceous contributions [Plate 1B,C] (Plummer, 1978b). Evidence for diagenetic alteration of the sediments, probably in response to metasomatism associated with a pre-Delamerian tectonic event (R.J.F. Jenkins pers. comm., 1997), can be found in the form of authigenic pyrite [Plate 1D] and recrystallised silica nodules.

A coarse-grained sandstone interval, containing localised areas of lithic arkoses, lies 250 m below the same boundary. Above this interval the Ulupa Siltstone is composed characteristically of khaki mudstones displaying abundant synaeresis cracks (Plummer & Gostin, 1981). This facies shoals upwards into dirty, immature khaki sandstones and

quartzites.

3.2.1.2 ABC Range Quartzite.

The ABC Range Quartzite conformably succeeds the Ulupa Siltstone and records a sea-level transgression. It becomes finer-grained and lenses out towards the north and east, by interfingering [Plate 1E] with the underlying Brachina Subgroup (Plummer, 1978a; Eickhoff *et al.*, 1988; Christie-Blick *et al.*,1990). Such interfingering was observed within the field area.

Consisting of generally coarse to fine-grained, greyish-red to white to pale-orange felsarenites, it characteristically displays heavy mineral banding and micaceous lamination. Sedimentary structures include planar and herringbone crossbedding, mudcracks and rainspots, suggestive of a tidal-flat to deltaic environment.

3.2.3 The Aruhna Subgroup.

Defined by Dyson (1996a) as an overall transgressive third order cycle deposited during one eustatic fall and rise of relative sealevel.

3.2.3.1 Wilcolo Sandstone.

Overlies the ABC Range Quartzite with local unconformity and consists of a thin (2-5m) fluvial to shallow-marine channel-filling facies. It comprises interbedded coarse-grained, pebbly, crossbedded sandstones and pebble to cobble conglomerates and shales.

Dyson (1996a) reports fluvially incised valley-fills within this unit, their base being interpreted as a sequence boundary cut during a lowstand of relative sealevel. The unit is a transgressive systems tract with the transgression eroding and reworking the former beach sediments (Dalrymple *et al.*, 1994).

3.2.3.2 Bunyeroo Formation.

Deposited, for the most part, below storm wavebase in a middle- to outer-shelf setting, Dyson (1992) placed the Bunyeroo Formation in a transgressive systems tract, capped by Wearing Dolomite.

It consists of finely-laminated red to purple (with minor green intervals) siltstones and shales of an average 400m thickness (Haines, 1987). It sharply overlies the ABC Range Quartzite and represents a period of abrupt transgression and/or subsidence (Gostin & Jenkins, 1983.) Haines (1987) and Von der Borch (1988) indicate that its relatively monotonous nature is suggestive of suspension settling of sediment under low energy, oxidative conditions. Lonestones, interpreted to be of glacial origin occur within the formation [Plate 1F].

Considerable thickness variations have been noted by various authors (Scotford, 1984; Haines, 1987; Preiss, 1987; DiBona, 1989; Christie-Blick *et al.*, 1990) and are thought to relate to salt build up at depth preventing basin subsidence (Christie-Blick, 1990) or to syn-depositional tectonism warping the basin floor (DiBona, 1989).

3.2.4 Depot Springs Subgroup.

The Wearing Dolomite and Wonoka Formation embrace a transgressive-regressive cycle constituting an unconformity bounded depositional sequence.

3.2.4.1 Wearing Dolomite.

Equivalent to HU1, it constitutes a thin, cream dolostone or dolomitic siltstone that developed in a shallow-marine environment above SWB (Jansyn, 1990; Urlwin, 1992). Often sharply overlying the Bunyeroo Formation with apparent conformity, it corresponds to a combined sequence boundary and major flooding surface (Dyson, 1995). It marks a regionally significant,basin-wide lithostrome (Dyson, 1996a).

3.2.4.1a Burr Well Member.

The Wearing Dolomite can be traced into the Burr Well Member (DiBona, 1989) and is interpreted to be coeval with deposition of the wallplaster [Plate 3A]. It was deposited in a shoreface to lagoonal environment, with its sharp erosional base marking a combined sequence boundary and transgressive surface. It passes laterally into slumped conglomerates on the canyon shoulders; an observation supported, in part, by Dyson (1995, 1996a).

3.2.4.2 Wonoka Formation.

This formation is a mainly regressive mixed carbonate/siliciclastic sequence of marine origin. The Wearing Dolomite is overlain by the overall transgressive HU2 and grades up into HU3. The colour change from dominantly red to green within HU3 marks the base of regressive sedimentation within the Wonoka Formation and corresponds with the canyon unconformity. HU3-7 display an overall shoaling upwards trend, reflecting the gradual development, progradation and eventual destruction of a storm-dominated carbonate ramp (Haines, 1987.) Regressive sedimentation culminated with the deposition of lagoonal, tidal and supratidal carbonates and siliciclastics (HU8-11) which intertongue with the overlying Bonney Sandstone (Haines, 1987; DiBona, 1989.)

The stratigraphy of the lower Wonoka Formation is interrupted by the incision of large-scale valleys into the underlying sequence. Excavated and filled during early Wonoka Formation (HU3) time, their genesis is quite controversial. Later erosional incisions of more modest vertical amplitude are linked to the transition of HU8-9 to HU10. The overall style of canyon incision appears very similar to that described in the Seacliff Sandstone by Dyson & Von der Borch (1994).

Chapter 4 - Canyon Geometry.

The Wonoka Formation within the keel of the tightly folded, doubly-plunging, White Valley Syncline preserves evidence for two phases of canyon development (Fig. 5.4, Discussed in Chapter 5).

4.1 K1 Geometry.

A remnant of a primary phase of incision is preserved on the western wall of K2 [Plate 2A,B]. Incision of a minimum of 425m into the Ulupa Siltstone was most likely related to a time between Wearing Dolomite deposition and K2 incision. This implies a minimum of 640 m of Bunyeroo Formation was also eroded, giving a total depth of 1065 m.

4.2 K2 Geometry.

Unconformably overlying K1 is a second incision, 8800 m in length and 2000 m in width from west to east. It is asymmetrical in regional section. Its elongated outcrop and the axial trend of the canyon itself suggests the Wonoka Formation exposed within the study area represents a two-kilometre wide cross-section of an eastwards flowing canyon nearly 9000m in width.

The planing off and erosion of the pre-existing units [Plate 3C,D], rather than their slumping, suggests progressive erosion downslope. Greater amounts of erosion are observed on the eastern side of the canyon. The Ulupa Siltstone-ABC Range Quartzite is eroded 340m in the west and 480m in the east. Considering a minimum of 640 m of Bunyeroo Formation the incision depth varies from 980 m to 1120 m. In addition, an unknown thickness of HU1-3 was also eroded. Both incisions exhibit a terraced profile [Plate 3B,C] with overhanging walls. Measurement of wall angles is problematical because it is not possible to assume horizontal deposition. The presence of olistoliths within the canyon succession suggests relatively steep wall-profiles. Canyon fill units were observed to drape down the canyon walls.

Palaeocurrent analysis reveals that canyon morphology has been slightly altered by post-depositional folding, with deformation partially obscuring the canyon axis. Axial trends were calculated by aligning the two points of maximum incision trend towards 105°. Examination of the geological map (Appendix A) reveals the apparent axial trend concurs with the trends observed within the palaeocurrent profile (towards 120°).

4.3 Palaeogeographic Reconstructions.

Reconstructions of the study area prior to canyon incision can be made on the basis of two assumptions. Either:

Reconstruction 1) Pre-Wonoka Formation units were flat-lying and

undeformed.

or Reconstruction 2) Wearing Dolomite deposition occurred on what was essentially a horizontal basin floor.

The distribution of the Bunyeroo Formation within the syncline is of vital importance. It outcrops in the northern part of the study area as two synclines with axial trends that do not follow the regional axis. The western syncline, 6200 m long has a maximum limb thickness of 270 m, and is observed to be partially in line with the regional trends. The eastern syncline (4600 m long) attains a maximum limb thickness of 280 m. This morphology is mirrored by the southern outcrops that bifurcate out into two slivers that thin down the canyon walls. The western portion is 1200 m long, the eastern portion is 4000 m long.

Reconstruction 1: assumes that units deposited prior to Wearing Dolomite time are flat lying. Erosion of these strata left behind the particular outcrops of Bunyeroo Formation as two parallel ridges, separated by a valley eroded through the ABC Range Quartzite and into the Ulupa Siltstone and flanked on either side by similar, deeper valleys. The Bunyeroo Formation outcrop is bounded by Ulupa Siltstone at a deeper stratigraphic level implying it represents the preserved caps of palaeohighs.

This reconstruction envisages two relatively narrow, parallel ridges attaining maximum heights of well over 200 m. Temporal constraints require these sediments to be poorly lithified and thus, very susceptible to erosion. The steep topography inferred by this model would be unable to be sustained by these partially indurated sediments, especially in the light of the modest outcrop of modern-day, lithified, Bunyeroo Formation. Further evidence repudiating this model comes from the canyon itself: the palaeotopography requires a N-S drainage system. Since the Bunyeroo Formation represents palaeohighs, why then should canyon incision progress against the palaeoslope and bisect such a range of hills perpendicular to the localised depressions?

Reconstruction 2: assumes horizontal deposition of the Wearing Dolomite unconformably overlying the Bunyeroo Formation. This model accounts for Bunyeroo Formation outcrop (limb thicknesses: west syncline= 270 m thick, east syncline= 280 m thick) as having been deposited in a bifurcating 'Y-shaped' depression within the ABC Range Quartzite sheet. Although regional in nature, deposition was therefore focussed on these depressions. Such depressions/synclines are strongly suggestive of a pre-Delamerian phase of deformation. Later canyon incision bisected these outcrops leading to the a remarkably progressive thinning of the remnant Bunyeroo Formation down-plunge. The style of folding suggests that the rheology at the time of this initial phase of deformation allowed a compressibility of the strata that was very similar to that affecting Delamerian shortening.

Reconstruction 1- *Undeformed ABC Range Quartzite.*

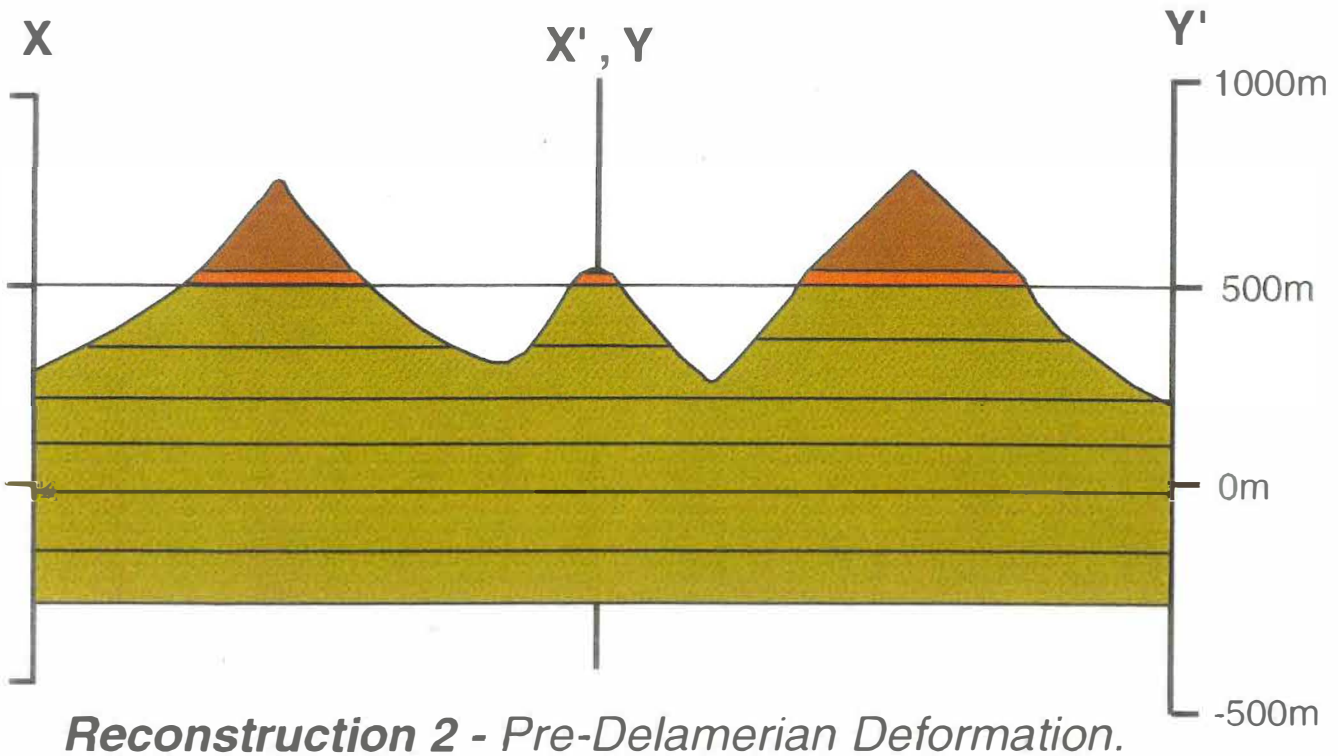

Reconstruction 2 - *Pre-Delamerian Deformation.*

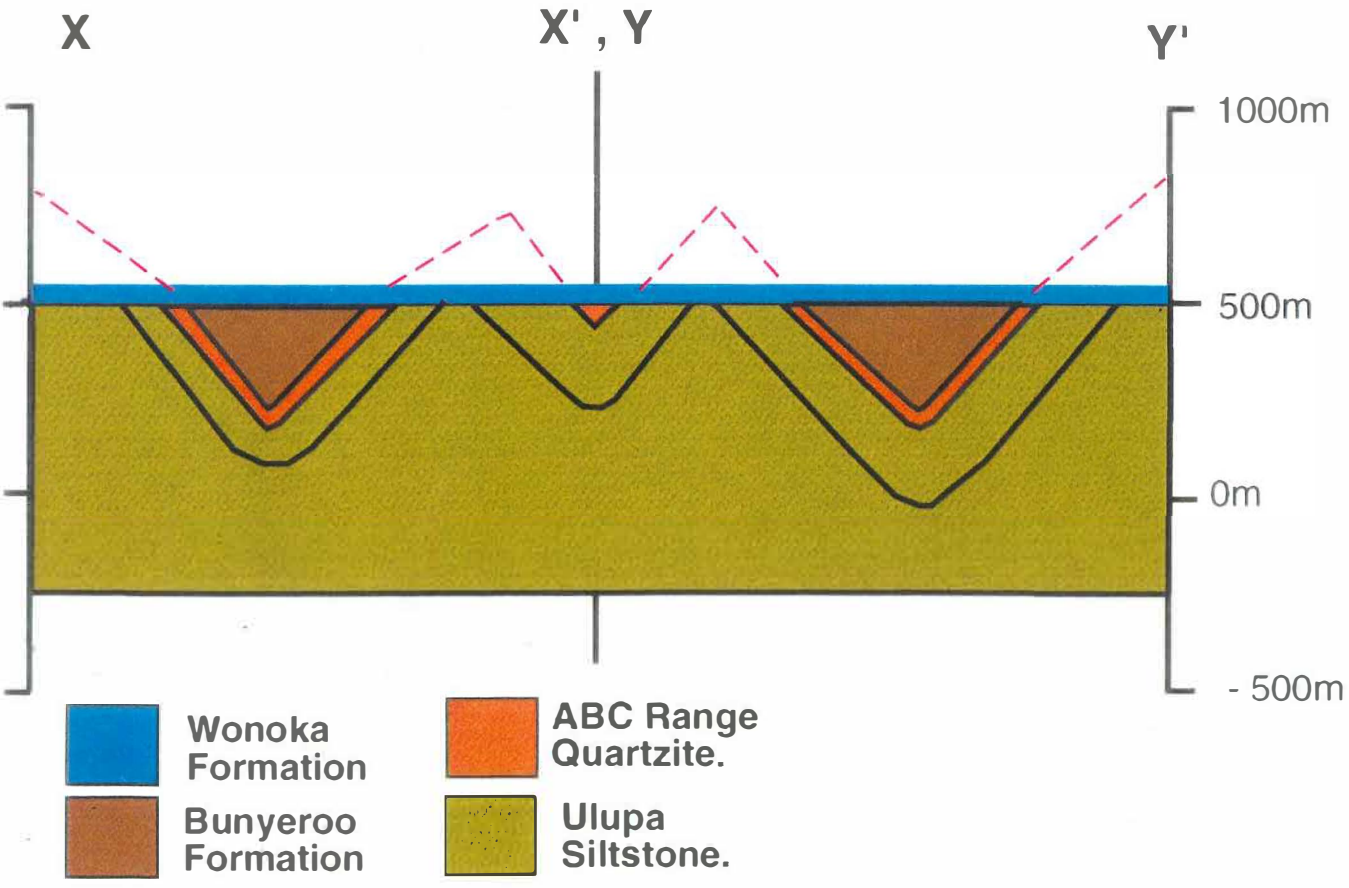

Figure 4.1. Reconstructions of two possible models for the palaeotopography

LIBRARY

4.4 Linked Canyon Systems.

The Pamatta Pass Canyon belongs to the easterly trending Southern Flinders Canyon Series (SFCS) of Haines (1987). This series is interpreted as extending eastwards for over 170 km, from the proximal Waukarie Creek and Yarra Vale Canyon Complexes, through the Pamatta Pass Canyon Complex to the distal Yunta Canyon Complex.

Von der Borch *et al.* (1985), Haines (1987) and DiBona (1989) suggest a genetic linking within the Northern Flinders Canyon Series (Haines, 1987). Geographical relationships within this canyon series and the inference of an easterly facing palaeoslope (Haines, 1987) suggests such a link is possible for the SFCS. Canyon morphologies imply that feeder channels drained into deeper canyons to the east. Eastwards deepening erosion and close comparisons between canyon successions throughout the region corroborate this connection. (DiBona, 1989).

Chapter 5 - Canyon Fill Stratigraphy.

5.1 Introduction.

Various lithostratigraphic units have been described in the Wonoka Formation canyons by previous authors (Von der Borch *et al.*, 1982, 1985, 1989); Eickhoff *et al.*, 1988); Haines, 1986, 1987; DiBona, 1989; DiBona *et al.*, 1990; Ayliffe, 1992). The described sequence corresponds to HU4-5 although P.W. Haines (pers. comm., 1997) stated that canyon facies are not expected to correspond to this classification. HU1-3 has been removed by canyon erosion with the canyon unconformity being mantled by the wallplaster veneer (Eickhoff, 1988).

The stratigraphic succession lies within the Neoproterozoic Wilpena Group (Fig. 5.1, 5.2) and records two successive and overlapping events of canyon incision. Each is startlingly distinctive and is characterised by sequential channel fills.

5.2 K1 Wonoka Formation.

This unit represents a primary phase of canyon incision and filling and is represented in Fig.5.3. The exact timing and nature of this incision is discussed Chapter 6.

5.2.1 K1 Unit.

This unit unconformably overlies the Ulupa Siltstone. It was deposited within a large-scale erosional channel of comparable magnitude and geometry to K2 [Plate 2A,B].

This unit is laterally variable, consisting of channel deposits of gritty, silty, micaceous and feldspathic coarse-grained sandstones/psammites and basal cobble to boulder conglomerates [Plate 2C,D]. The conglomerates contain rounded clasts of blue cherts, brown and pink limestones, sandstone, quartz and ironstone, and occasionally exhibit an imbrication towards 210°. The stratigraphy fines upwards into a laterally variable succession of medium-grained, feldspathic and micaceous calcareous sandstones interbedded with finely-laminated, grey to dark-purple siltstones [Plate 2E] and green shales. These silts and shales become dominant towards the upper part of the remaining K1 succession.

Interspersed amongst this facies are randomly oriented megaclasts of Ulupa Siltstone [Plate 7B,C,D] (up to 27 m X 8 m in size). Isolated 'pods' up to 1m in size, of pink limestone [Plate 2F] (closely resembling the limestones developed adjacent to the K2 wallplasters) and yellow, cryptalgal laminated dolomites [Plate 7A] are also present.

Small-scale crossbedding, parallel and ripple laminations and climbing ripples are present along with evidence of sunrises cracks. Palaeocurrent directions are towards 295°. This facies is unusual in its dark colour and metamorphosed appearance.

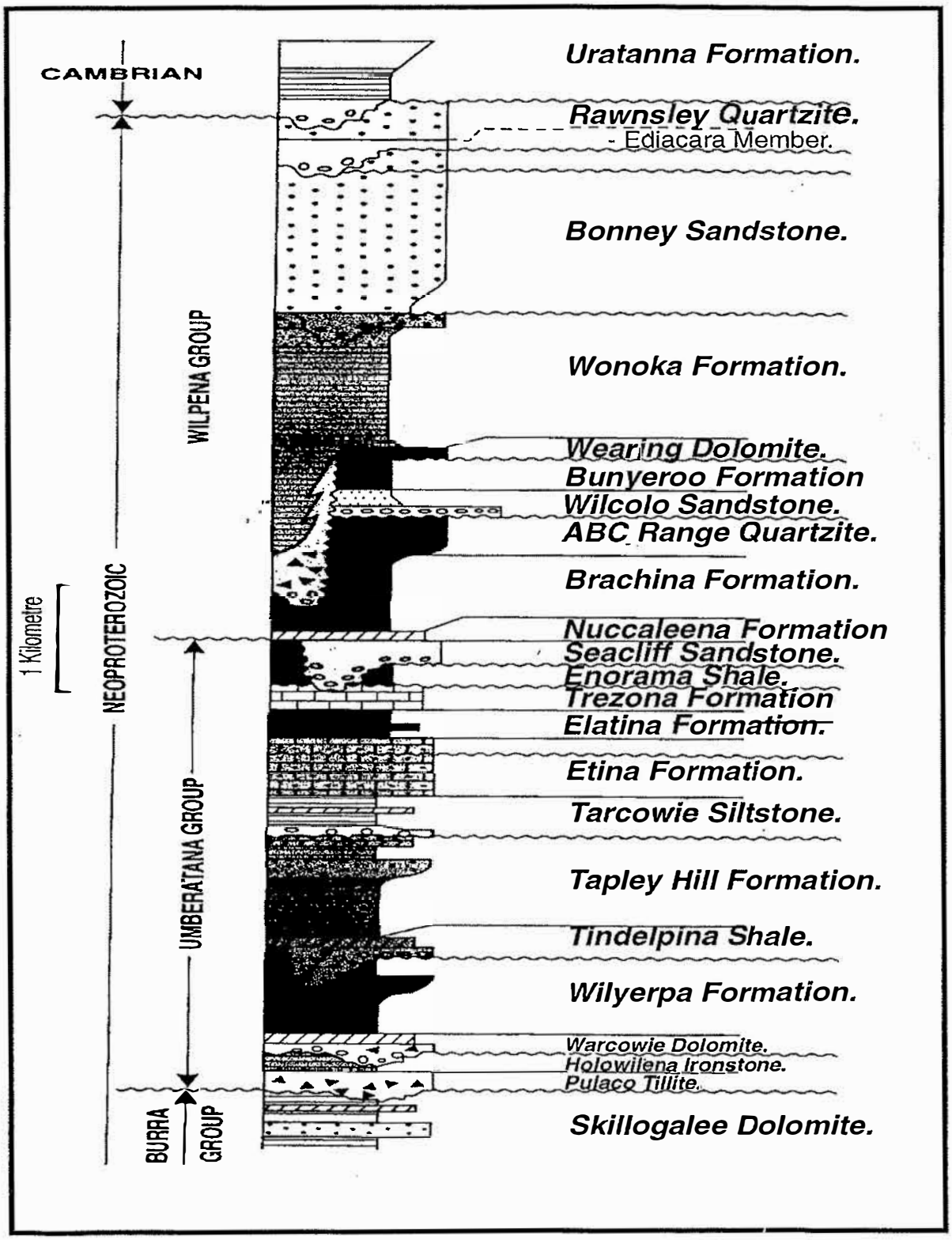

Figure 5.1 The sequence stratigraphy of the Heysen Supergroup within the Adelaide System (modified after Dyson, 1996a).

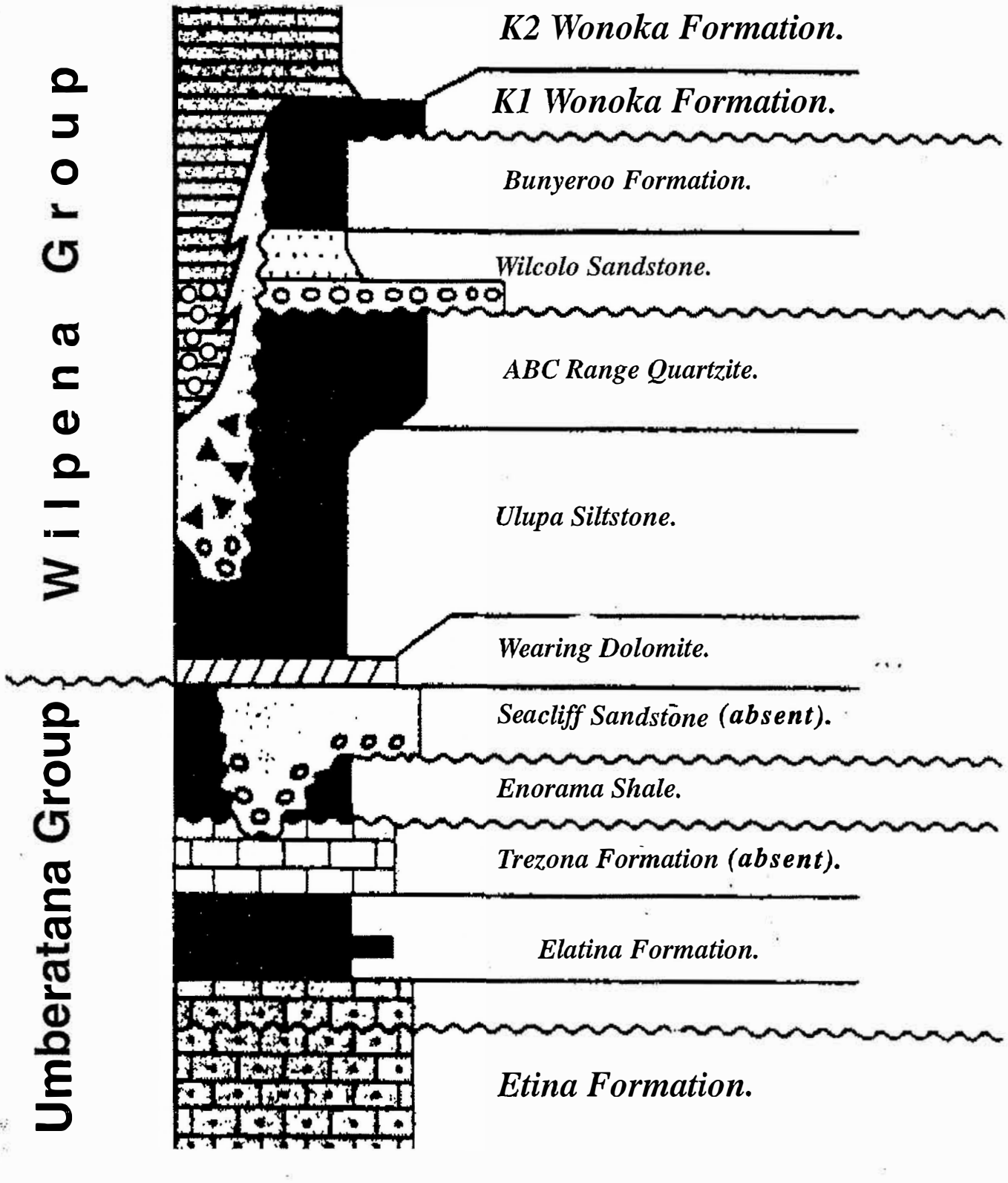

Figure 5.2 The stratigraphy of the Pamatta Pass Canyon Complex (modified from Dyson, 1996a).

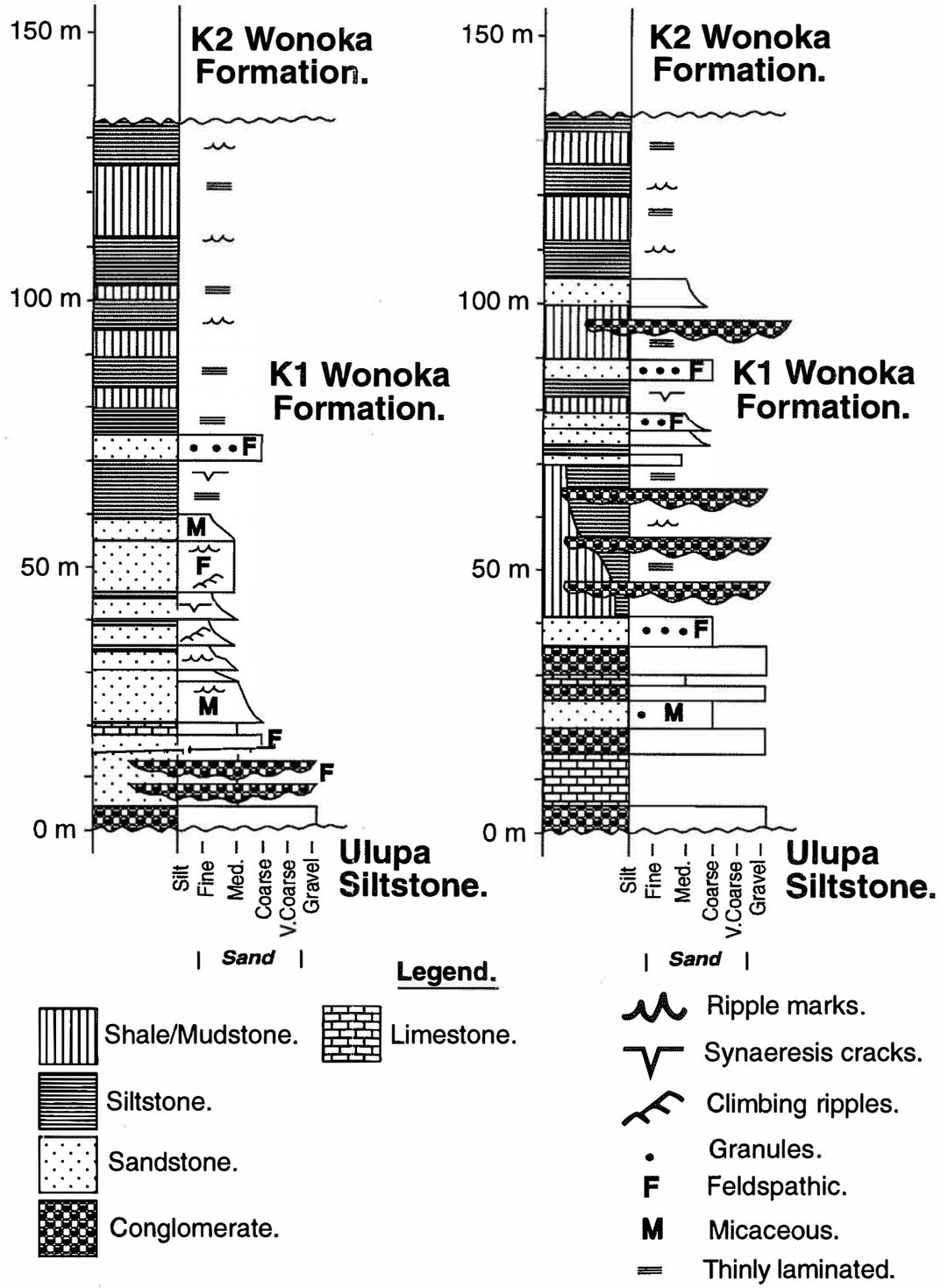

Figure 5.3 Stratigraphic representation of the K1 Unit. Note its fining upwards succession and the micaceous and feldspathic nature of the unit. This unit is characteristically very dark in colour and highly cleaved.

5.3. K2 Wonoka Formation.

This sequence unconformably overlies the older K1 succession and represents the typical canyon successions observed within the Flinders Ranges by various authors (e.g. Eickhoff, 1988; Von der Borch *et al.*, 1989). It is described in Fig. 5.4.

5.3.1 Basal Conglomerates/Olistostrome Unit.

Facies 1 Equivalent - Von der Borch *et al.* (1989).

This facies consists of thick, massively bedded lenticular granule to boulder conglomerates of mixed provenance. Clasts up to 5m in size of wallplaster [Plate 3E, 4E], Burr Well Member, early Wonoka Formation [Plate 3E,F] Bunyeroo Formation [Plate 4A], ABC Range Quartzite, Ulupa Siltstone [Plate 4B], cherts, quartzites, sandstones and ironstones are present. Basement derived clasts comprise granules, pebbles and cobbles of acid volcanics [Plate 4F], granules of Gawler Range Porphyry and basic volcanics derived from nearby diapiric intrusions.This unit occurs along the deepest part of the incision on the eastern side of the canyon.

Thin section and hand specimen examination reveals that the interbedded granule rich, coarse sandstones [Plate 4D] are bimodal in grainsize with coarse, well rounded frosted quartz grains set in a finer-grained, multimineralic matrix.

5.3.2 Basal Sands Unit.

Facies 2 Equivalent of Von der Borch *et al.* (1989).

Overlying the canyon unconformity are massive- to parallel-laminated, medium to thickly bedded, coarse-grained calcareous sandstones [Plate 4C], often interbedded with the basal conglomerates and wall slumps. The sands are well-sorted, with medium to fine sub-angular quartz grains, rare feldspars and micas. They occur in discrete sets and commonly display abrupt bases with load casts and other sole marks [Plate 4C]. Bed-tops are capped by symmetrical, interference, and combined flow ripples.

5.3.3 Wallplaster Unit.

Facies 3 Equivalent - Von der Borch *et al.* (1989).

The wallplaster is a characteristic calcareous to weakly dolomitic facies up to 1.5m thick, specifically veneering the eroded surface of the Ulupa Siltstone or Bunyeroo Formation. It comprises a massive, white to grey layer that often displays a diffuse parallel lamination. Its occurrence can be traced laterally for hundreds of metres [Plate 3B] from almost the top of each of the interfluves, plastering the canyon walls and thinning down towards the base of the incisions. Erosion has displaced fragments of the wallplaster into the lenticular breccias within the canyon fill, some of which

show evidence for soft sediment deformation [Plate 4E].

Interbedding of discrete conglomerate bodies with the canyon fill [Plate 6A-D] implies several stages of wallplaster genesis and dislocation during the filling of the incision. Haines (1987) and Jansyn (1990) observe that the base of HU4 is notably cupriferous. Wallplaster specimens often contain abundant visible malachite and weathered pyrite and this supports the observation that canyon infilling occurred largely during HU4 time.

Directly overlying the wallplaster is a limestone unit of variable thickness. It comprises massively bedded, well cemented, featureless pink micritic limestone that can be best observed on the southeastern wall of the canyon immediately south of the deepest part of the incision.

5.3.4 Burr Well Member Equivalent.

The wallplaster can be traced into the Burr Well Member in the southern portions of the canyon. Unlike the relatively featureless, whitish wallplaster, the Burr Well Member consists of a thin (<50 cm) yellow to brown dolostone, often displaying a cryptalgal lamination [Plate 3A]. Commonly interbedded with the wallplaster, it constitutes a prominent component of the clastics within the wallplaster and canyon fill. This suggests that canyon erosion was not confined to the base of the incision and proceeded partially via stripping of the canyon walls. It is generally poorly exposed, often being dramatically thinned or removed in places.

5.3.5 Wall Slumps.

Facies 6 equivalent of Von der Borch *et al.* (1989).

In places clast and matrix supported diamictites form elongate bodies that mantle the canyon walls and are occasionally interbedded with other canyon filling sediments within the canyon [Plate 3B-F]. Isolated clasts of Bunyeroo Formation, ABC Range Quartzite and Ulupa Siltstone occur in addition to angular to subrounded, poorly-sorted limestone and dolostone clasts within a matrix similar to their antecedent facies. DiBona (1989) reports similar breccias within Oodnapanicken Canyon, associated with offsets in the canyon walls that preserve evidence for syn-depositional faulting.

5.3.6. HU4 Equivalent Unit.

Facies 7, 8 & 9 of Von der Borch *et al.* (1989).

This unit is largely identical to that observed in the Waukarie Creek Canyon Complex (Ayliffe, 1992; Meredith, 1997). It either directly overlies the Ulupa Siltstone, the wallplaster or the basal conglomerates. This sequence emulates that described by Eickhoff (1988) within the Fortress Hill Canyon Complex.

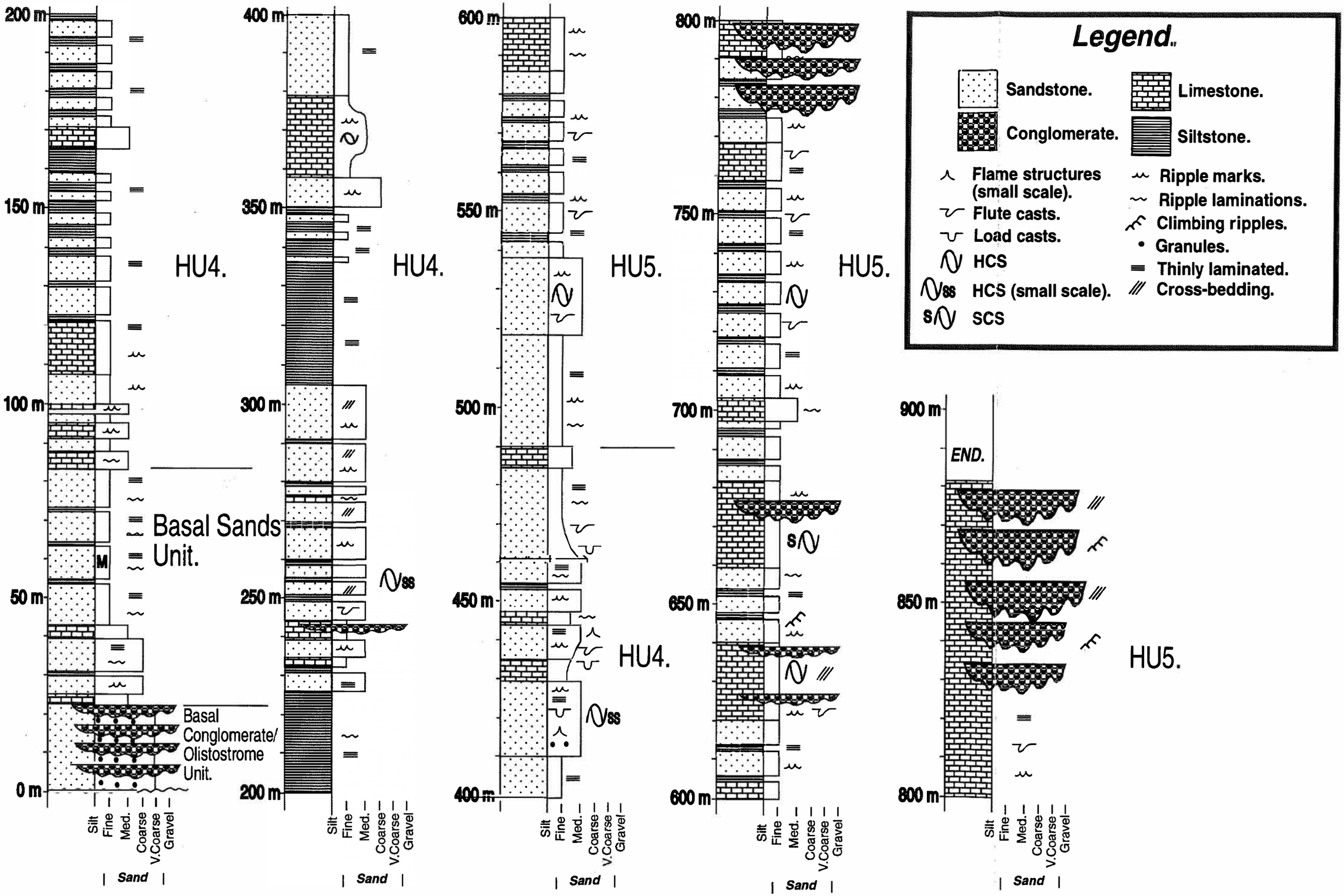

Figure 5.4 Composite stratigraphic column of the K2 Wonoka Formation units.

It is characterised by cyclical alteration of packets of thin-bedded, green, silty to fine sandy limestones interbedded with greenish silts and white fine- to medium-grained calcareous sandstones [Plate 5B-D]. Thinly laminated (on a millimetric to centimetric scale), chlorite- and muscovite-rich, green shale layers are common [Plate 6E,F]. Interspersed amongst these sediment packages are packets of yellow-brown calcareous siltstone and occasional pink limestones. A distinct rhythmical nature is noted to this unit [Plate 5D]. Rare maroon shales and sandy limestones (displaying stylolites) are found towards the margins of the canyon.

Intraformational conglomerates of shallow-marine origin [Plate 6A,B], are common within the canyon fill, sometimes exhibiting a southerly imbrication in addition to a ubiquitous compaction fabric. They are interpreted as slump or debris flows derived up-slope from the canyon walls. The similarity between clast types [compare Plates 3E,F with Plates 6A-D] within the wall slumps and the axial conglomerates substantiates this premise.

Small scale HCS/SCS is common in this unit [Plate 5A] and conform to the idealised HCS association proposed by Dott & Bourgeois (1982) and reported by Eickhoff (1988) within the Fortress Hill Canyon Complex.

Sedimentary structures include flute marks, scours, load casts, ball and pillow structures and sole marks. Erosional scours are common at the base of debris flow units. Ripple, parallel and wavy laminae [Plate 5D] are observed and double-crested, symmetrical, interference, oscillation and mono-directional current ripples are represented. Climbing ripples are observed associated with sandstones overlying conglomerate lenses.

5.3.7 HU5 Equivalent Unit.

Facies 7,8 & 9 Equivalents - Von der Borch *et al.* (1989).

This unit shows a distinct affinity to the previous unit, being composed of essentially the same sediments. It continues the overall upwards fining succession of small scale depositional cycles, gradually increasing in carbonate percentage upsection. Mapping of the unit boundary is impracticable due to its highly gradational nature. The unit is characterised by an increase in the outcrop of well-cemented equivalents of the rhythmical calcareous silts and sands of the HU4 equivalent unit.

Encompassing a succession of cycles of dominantly green silts, silty to fine sandy limestones and interbedded shales, Unit 5 displays a distal tempestite affinity [Plate 5B,E,F] (Haines, 1987) and corresponds to the idealised succession described by Eickhoff (1988). Depositional sequences are often incomplete.

Intraclast horizons (Facies 4 equivalents - Von der Borch *et al.*, 1989), composed of pebble to boulder sized, angular to subrounded carbonate clasts [Plate 6D], are prominent. Individual lenses (up to 5 m thick) may be traced for tens to hundreds of metres. They typically exhibit an erosive base with a fining upwards succession [Plate 6C] being capped by megaripples/sandwaves [Plate 6A,B] (up to 40 cm long) and/or finely laminated silty limestones (see photos.) These lenses show an imbrication towards the south and are dominated by tabular limestone and wallplaster/Burr Well Member clasts [Plate 6A-C].

5.4 Palaeocurrent Analysis.

5.4.1 K1 Facies.

The dearth of suitable sedimentary structures within this facies means that palaeocurrent data is limited to only 2 measurements, both trending towards 295°. (Fig. 5.5a). This suggests the K1 fluvial system flowed in essentially the opposite direction to the K2 system. Alternatively it reflects a tidal influence upon sedimentation analogous to K2. More data are necessary to ascertain the validity of this tentative conclusion.

5.4.2 K2 Facies.

Palaeocurrent analysis reveals a distinctly bimodal trend for the canyon (Fig. 5.5b). The dominant currents alternate by 180°, suggesting tidal currents played a major role in sediment deposition and reworking. The dominant trend is towards 165° with a lesser trend towards 130° being observed. This reflects the interplay between axial and tidal currents. Current directions roughly perpendicular to the canyon axis are interpreted to be the result of slumping down the canyon walls. Canyon filling conglomerates/lenticular breccia units show a predominant imbrication towards approximately 200° (± 30°).

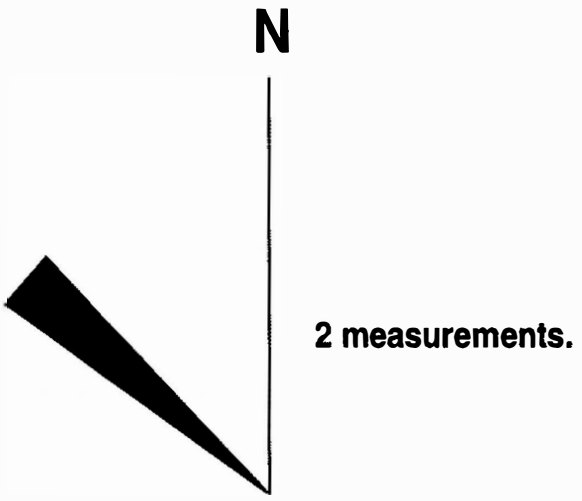

Figure 5.5a Palaeocurrent analysis of the K1 Unit.

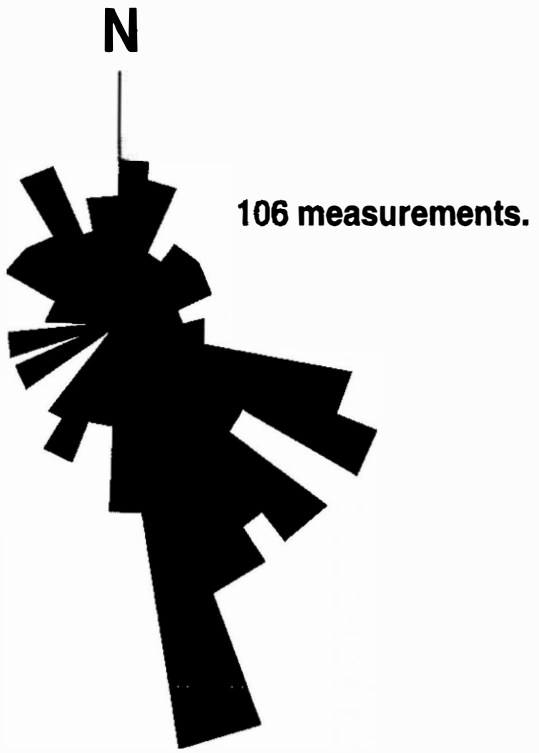

Figure 5.5b Palaeocurrent analysis of the K2 Wonoka Formation.

Chapter 6 - Canyon Fill Discussion.

The canyon fill facies are interpreted to have been deposited in a fluvial, deltaic to shallow marine environment on the basis of their mineralogy, lithology, sedimentary structures and isotopic ratios.

6.1 K1 Wonoka Formation.

The K1 unit is interpreted to be a terrestrially influenced deltaic facies on the basis of:

i) shallow-water sedimentary structures within the canyon fill,
ii) sedimentological characteristics,
iii) evidence for gradual canyon inundation,
iv) the absence of evidence for flyschoid turbiditic deposition,
v) incision into lithified sediments; and
vi) geochemical & isotopic analysis (discussed later).

This conclusion is based upon the occurrence of climbing and symmetrical ripples and the immature and dirty nature of this unit. Facies associations reflect initially rapid deposition that gave way to deposition of thinly-laminated monotonous silts and shales. The overall fining upwards trend, coupled with such silts and the units overall calcareous nature indicates an increasing shallow-marine influence upsection. K1 Incision occurred following ABC Range Quartzite time and eroded well lithified sedminents (as evidenced by rounded quartzite and Ulupa Siltstone clasts within the basal conglomerates [Plate 2C,D]).

A wallplaster unit mantling the K1 unconformity is conspicuous by its absence. Conditions were either unsuitable for its formation or the depositional environment precluded its preservation. The 'pods' of limestone [Plate 2F] and dolostone [Plate 7A] may reflect boudinaging of an incompetent facies in response to block rotation and cleavage development. Alternatively, they represent megaclasts of a K1 wallplaster emplaced into the unit via slumping. Certainly, identical clasts are present within the basal K1 conglomerates and bear a great resemblance to those associated with K2 wallplaster (i.e. pink limestone and cryptalgal laminated, yellow, Burr Well Member [compare plate 7A with Plate 3A] look-alike dolostone.) The absence of *in situ* wallplaster can therefore be attributed to its removal as erosion progressed via basal scouring and lateral wasting of the canyon walls.

If these carbonates do represent wallplaster facies then they record the development of a prior phase of wallplaster coeval with the K1 canyon unconformity and provide further evidence for subaerial canyon genesis. Observations of synaeresis cracks (Plummer & Gostin, 1981) affirm increasing marine flooding upsection.

6.2 K2 Wonoka Formation.

K2 is interpreted to have been eroded in a subaerial environment and later infilled by coastal onlap.

The wallplaster is interpreted to have formed in accordance with the model developed by Von der Borch *et al.* (1989), with precipitation influenced by groundwater discharge from canyon walls in response to a distinct hydraulic gradient. The release of lithostatic pressure would enable CO_2 degassing and $CaCO_3$ precipitation from discharging groundwaters, with microbial mats and stromatalites (DiBona, 1989; Von der Borch *et al.*, 1989) leaving their mark. Several phases of wallplaster development and disruption would then be associated with phases in canyon development, a fact supported by the observation of wallplaster and plastically deformed [Plate 4E] clasts interbedded with canyon infilling sediments.

Best developed on the canyon shoulders, the wallplaster progressively thins down the canyon walls. The relative sea-level rise responsible for infilling the canyons would have gradually inundated the canyon walls, halting wallplaster development. Logically, those areas remaining emergent for the longest period of time will display the optimum wallplaster profile. Unlike the Waukarie Creek Canyon Complex (Meredith, 1997), there is no unequivocal evidence that the base of the incision ever became emergent. Thus the lowest occurrence of the wallplaster may delineate the minimum sea-level within the canyon.

Oxidised pyrite cubes within the wallplaster (derived from erosion of the Ulupa Siltstone) and rounded ironstones pebbles within the basal conglomerates suggest palaeosol development resulting from the subaerial exposure of the landscape.

The plethora of wave modified and/or generated sedimentary structures and ripple types within the canyon fill suggest infilling was via shallow-marine backfilling from the basin. These include HCS and SCS (produced by fair-weather wave reworking of HCS), along with combined flow, symmetrical, double crested and interference ripples and point to a dominant wave influence upon sedimentation.

The association of ambiguous sedimentary structures previously cited in support of a submarine model (e.g. Haines, 1987; Ayliffe, 1992), such as HCS [Plate 5B], SCS [Plate 5A] (Prave, 1985; Allen, 1985) and symmetrical crested ripples (e.g. Ewing, 1973; Allen, 1984) and alternating palaeocurrent directions, with convincing evidence of shallow marine to subaerial deposition serves to highlight serious flaws with the submarine model. Further evidence for shallow water deposition comes in the form of sedimentary structures reminiscent of algal mats (Gerdes *et al.*, 1991). These structures are found adjacent to the canyon walls in the study area and are common within the Waukarie Creek Canyon Complex (Meredith, 1997), although their nature

is too indistinct to draw any valid conclusions. A gradual increase in water-depth, in accordance with filling via coastal onlap, within the canyon is suggested by the overall fining upwards succession. Thickness variations in the wallplaster, coupled with the increasing size and profusion of storm-generated sedimentary structures, and a decreasing abundance of shallow-water sedimentary structures upwards substantiates this premise. The increasingly well cemented limestones [Plate 5E,F] of HU5 indicate lower energy regimes and increasing carbonate production upsection.

Palaeocurrent distributions within the canyon suggests that tidal currents had a significant influence upon deposition. Climbing ripples indicating rapid sedimentation (Ashley *et al.*, 1982), a fact corroborated by Ayliffe (1992) and the episodic nature of portions of the canyon fill. Reworking of these event deposits by possible tidal currents is evident from the bimodal distribution of palaeocurrents and sedimentary structures interpreted by Klein (1985) as typical for the intertidal to shallow subtidal environment.

Von der Borch *et al.* (1982, 1985) describe the canyon fill deposits as turbiditic in origin, but Eickhoff (1988) and Von der Borch *et al.* (1989) report a lack of classical characteristics as summarised by Walker (1984.) Flysch-like turbidites should form a significant proportion of a submarine canyon fill, yet their absence is conspicuous. The 'rhythmical' U4/5 limestones (displaying $T_{C,E}$ & $T_{B,C,E}$ Bouma sets), of distal tempestite affinity, reinforce the shallow-marine assessment.

Canyon incision was undoubtedly into lithified sediments (Von der Borch *et al.*, 1985). The presence of megaclasts (showing a randomly oriented cleavage) of Bunyeroo Formation, Ulupa Siltstone and ABC Range Quartzite within the olistostrome unit [Plate 4A,B] along with rounded pebbles of the same lithologies in the basal and axial conglomerates [Plate 6D] indicate this to be the case. The sheer size of the megaclasts requires their mechanical strength to exceed the shear stresses resulting from mass-wasting events. Lithification implies a break in sedimentation consistent with subaerial incision.

Chapter 7 - Sedimentological Analysis.

7.1 XRD Mineralogical Analysis.

Wonoka Formation Calcite Mineralogy.

Samples comprise low Mg calcite (LMC). There is a gradual trend towards lower magnesian calcite upsection:-

K1 Facies Calcite Composition:- 1.3 to 2.7 mol% Mg. (mean = 1.94 mol% Mg [LMC]).These sediments are the most variable in their calcite mineralogy.
Wallplaster Unit Calcite Composition:- 1.0 to 2.4 mol% Mg (mean= 1.56 mol% Mg [LMC]).
K2 Facies Calcite Composition:- 0.4 to 2.1 mol% Mg (mean = 1.28 mol% Mg [LMC]). These sediments begin with a basal elevated value (2.1 mol% Mg) before falling to 1.6 mol% Mg. These sediments are the least variable in their calcite mineralogy.

Mineralogy.

K1 Facies: The dominant mineralogy comprises either calcite or quartz. Minor amounts of plagioclase, muscovite and chlorite are present along with trace amounts of biotite and orthoclase. Dolomite only occurs in trace amounts at the basal K1-XX sample.

Wallplaster Unit: The mineralogy is calcite in conjunction with minor quartz and with trace amounts of feldspars (plagioclase largely) and chlorite.

K2 Facies: The typical Wonoka Formation canyon fill sediments are composed of mainly calcite with minor feldspar and quartz and trace amounts of muscovite, chlorite and plagioclase. The basal section shows trace amounts of dolomite.

7.2 XRF Major And Trace Element Analysis.

The results of geochemical analysis are summarised in the table 1.

K1 Wonoka Formation.

Unlike the relatively homogeneous wallplaster the K1 unit displays a marked variability in its analytical results, reflecting varying depositional environments and effects of marine influence. This unit is interpreted to possess a subaerial component on the basis of the following data:

1) Sr concentrations (av. - 2903 ppm), although variable, record a high value typical of deposition in a terrestrially influenced subaerial environment. Y.Bone (pers. comm., 1997) suggests they may even be indicative of an evaporitic to lacustrine environment. The low Rb values (av. - 13.24 ppm) indicate that Sr was not derived

from the decay of volcanic Rb.

Wallplaster Data.			***K1 Unit Data.***		
Element	**Range.**	**Average.**	**Element**	**Range**	**Average**
Ca	42.29 - 46.72%	42.59 %	Ca	2.4 - 43.93%	0.235
Fe	0.57 - 1.01%	0.92 %	Fe	0.91 - 6.57%	0.0264
Mg	1.68 - 1.92%	1.71 %	Mg	1.29 - 3.25%	1.88 %
Mn	0.05 - 0.28%	0.13 %	Mn	0.05 - 0.37%	0.17 %
Sr	315 - 1615ppm	682.11ppm	Sr	36.8 - 8044ppm	2903.4ppm
Rb	6.3 - 22ppm	13.24ppm	Rb	10.9 - 166.9	89.34ppm

Table 1. Geochemical Analytical Results.

2) Fe concentrations are high and suggest oxidative soil development was probably occurring at the time of incision. Values range from a low of 0.91% in a limestone block to 6.57% within a siltstone (av. = 2.63%) and point to considerable weathering of a landsurface at the time of K1 deposition. R.J.F. Jenkins (pers.comm., 1997) has reported the existence of palaeosol horizons within Central Australia at this particular stratigraphic level. Again this suggests close similarities between the two phases of canyon cutting.

3) Mn concentrations are variable but generally high (av. = 0.17%.) and suggestive of a derivation from surficial weathering of an exposed landsurface.

4) Mg values are only slightly higher than those of the wallplaster (av. = 1.83%), suggests a similar environment.

5) Na values are relatively nominal (av. = 1.65%) and indicative of a non-marine source.

6) Ca values are variable reflecting the lateral variability of the sediments.

Interpretation.

The K1 unit is interpreted to have been deposited in a terrestrially influenced, deltaic environment, deepening upsection to a marine environment. The anomalously high Sr values are interpreted to reflect temporary lacustrine conditions within the subaerial river-gorge as the result of damming of the river by large-scale slumping. When compared to the essentially homogeneous wallplaster, the geochemical signature of the K1 reflects its lateral variability and a shallow-marine to estuarine influence upon deposition .

Wallplaster Unit.

The wallplaster is similarly interpreted to be a non-marine precipitate on the basis of

the following geochemical analyses:

1) Relatively high Sr concentrations (av. = 682.1 ppm) coupled with low Rb concentrations (av. = 13.24 ppm). The values recorded are indicative of a non-marine environment of deposition (values around 400 ppm would be expected if the sediments were marine in origin.).

2) Moderately high Fe concentrations (av. 0.92% - 9200 ppm) - A stable trend.

3) Mn concentrations were moderately high (av. = .13%) - Again, a very stable trend reflecting subaerial weathering.

4) Mg concentrations were also typically stable (av. = 1.71%.)

5) Na concentrations were very low (av. = 0.82%) and extremely unlike the expected values if the wallplaster was a marine precipitate.

6) The Ca concentration reflects the loss on ignition (LOI) values with a very consistent trend throughout all the samples. Indeed, the homogeneous composition of this unit is quite marked.

Interpretation.

The geochemical results strengthen the notion that the wallplaster was deposited in a subaerial environment. The isotopic measurements and the presence of weathered, rounded pyrite crystals and ironstone pebbles as clastic fragments within the wallplaster support this premise.

Diagenetic Alteration.

The canyon strata show elevated Sr, Fe and Mn values and low Mg values. Similar results were reported within the canyon sequence at the Waukarie Creek Canyon Complex by Ayliffe (1992) who noted that elevated Mn and Fe values were indicative of diagenetic alteration. Tucker (1992) reports that elevated Sr values are indicative of neomorphism, from an aragonitic precursor to the low Mg calcite that dominates the mineralogy.

7.3 Cathodoluminescence Analysis.

Instead of the suppressed or non-existent luminescence expected from samples containing high Fe and Mn concentrations (Paeche, 1995), the samples luminesce moderately to very strongly. The slides record a minimum of three diagenetic events, the last of which was responsible for precipitating ferroan dolomite in the wallplaster. This luminescence indicates that post-depositional alteration of the samples has occurred although the extent is uncertain.

7.4 Stable Isotope Analysis.

Proterozoic isotope geochemistry has been hampered by the assumption that their age and associated likelihood of metamorphism makes them poor candidates for analysis. Nevertheless, careful sample selection when used in conjunction with petrographic, sedimentological and geochemical observations, means that isotopic resolution is

comparable to that of the Phanerozoic.

Results.

The isotopic composition of the K1 Unit, the wallplaster Unit and the K2 facies were examined using the techniques outlined in Appendix C and the results displayed in Figures 7.1-3.

i) K1 Wonoka Formation.

$\delta^{13}C$ Range = -7.45‰ to -9.86‰. Mean = -8.14‰.
$\delta^{18}O$ Range = -13.35‰ to -15.67‰. Mean = -15.37‰.

The K1 succession begins with the most depleted carbon isotopic signal observed within the study area (-9.86‰). Following this negative excursion the signal reverts to a less depleted signal and remains relatively constant until to the top of the unit. Oxygen values are relatively consistent throughout the unit and are the most depleted within the canyon succession. The K1 Unit isotopic signal (Fig. 7.1) is consistent with deposition in a subaerial environment and exhibits very little range in its values.

One point of concern is raised by the inference that a small proportion of the limestones within the K1 unit may be displaced blocks of wallplaster. This obviously then complicates chemostratigraphy and offers two possibilities: firstly, the consistent signal within the K1 reflects a diagenetic overprinting event; secondly, it reflects non-marine conditions throughout the entire canyon.

ii) Wallplaster Unit.

$\delta^{13}C$ Range = -7.85‰ to -8.86‰. Mean = -8.54‰.
$\delta^{18}O$ Range = -10.22‰ to -17.36‰. Mean = -12.66‰.

Numerous authors have proposed that K2 incision occurred sometime during deposition of HU3 (e.g. Von der Borch *et al.,* 1990; Haines, 1987; this study). Isotopic similarities between K2 facies, and their carbonate platform equivalents (Urlwin, 1992), in addition to other lines of evidence, corroborate this suggestion.

The wallplaster shows rather consistent highly depleted carbon and oxygen isotope signals (Fig. 7.2). They are suggestive of relatively constant non-marine conditions throughout its precipitation on the walls of the canyon. The highly negative carbon values are considered also to imply a microbial origin. (Eickhoff *et al.*, 1988) and aspects of the canyon-fill facies support this idea.

iii) K2 Filling Units.

$\delta^{13}C$ Range = -6.102‰ to -7.606‰ Mean = -7.304‰
$\delta^{18}O$ Range = -5.673‰ to -14.155‰. Mean = -12.241‰.

The canyon fill is somewhat less negative at its base (within the basal sands unit) before quickly reverting back to the typical negative values of the Wonoka Formation units (Urlwin, 1992.) Oxygen isotope values are consistently depleted with the exception of one anomalously heavy signal (Fig. 7.3).

Interpretation.

Due to the limited nature of the canyon succession, large-scale, global correlations lie outside the boundaries of this study. The data obtained are consistent with that reported earlier by Singh (1986), Eickhoff *et al.* (1988), Pell, (1989), Ayliffe (1992) & Urlwin (1992).

1) Carbon Isotopic Signal.

The lower portions of the Wonoka Formation are characteristically highly depleted in $\delta^{13}C$. Contrastingly, Proterozoic marine carbonates are relatively conservative, varying relatively little outside ± 3‰ (Degens, 1971; Vezier & Hoefs, 1976, Knoll *et al.*, 1986; Margaritz *et al.*, 1986; Tucker, 1986; Lambert *et al.*, 1987; Brasier *et al.*, 1990; Brasier, 1992, Kaufman *et al.*, 1991, 1993; Narbonne *et al.*, 1994; Kaufman & Knoll, 1995). The extreme consistency of these values within the Adelaide Geosyncline is obviously not the product of localised primary or diagenetic influences and implies either regionally consistent alteration processes or deposition within a basin in a unique geological setting. Recent work in North America reveals values as low as -10‰, interpreted to be of primary origin, (R.F.J. Jenkins - pers. comm., 1997) and thus suggestive of inter-regional correlation. Nevertheless, the regionally invariant $\delta^{13}C$ trends of the Wonoka Formation suggests a signal of regional, rather than global, importance.

McKirdy *et al.* (1975) and Haines (1987) report that the Wonoka Formation has undergone relatively little thermal metamorphism (chlorite grade - lower greenschist facies.) The low organic carbon content (Pell, 1989; Jansyn, 1990). of the Wonoka Formation suggests that deviations resulting from thermal decarboxylation processes are negligible.

Ayliffe (1992) invoked a primary model for highly depleted carbon isotopic values in response to a post-Marinoan glaciation. This extremely negative signal is thought to have been produced by basin stratification and bacterial recycling of organic matter, following the departure of the late Proterozoic climate from an ice-house state. The effects of this glaciation are not represented in the AFB sediments but are inferred to be present.

2) Oxygen Isotopic Signal.

The highly depleted aspect of all units, and their less well constrained ranges indicate

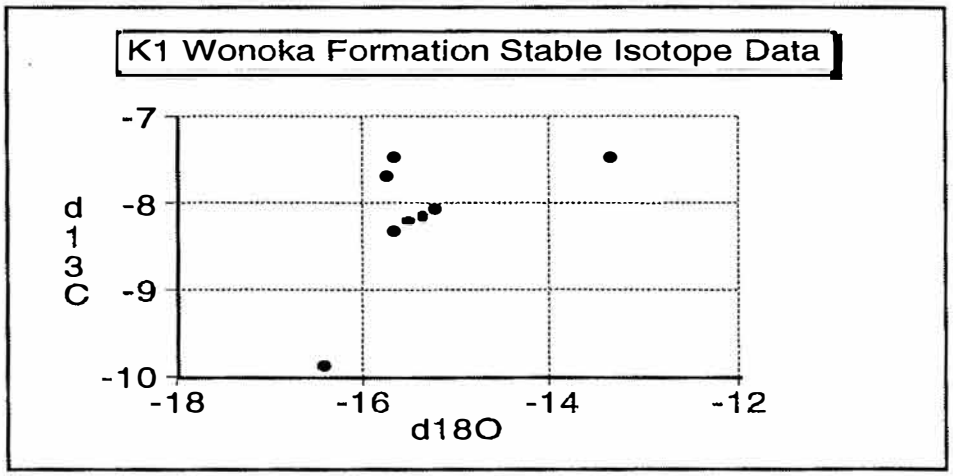

Figure 7.1 This graph illustrates the relatively consistent isotopic trends within the K1 unit. The lateral variability of the unit leads to a somewhat inconstant isotopic signal that is partly dependent upon the carbonate content of the sample.

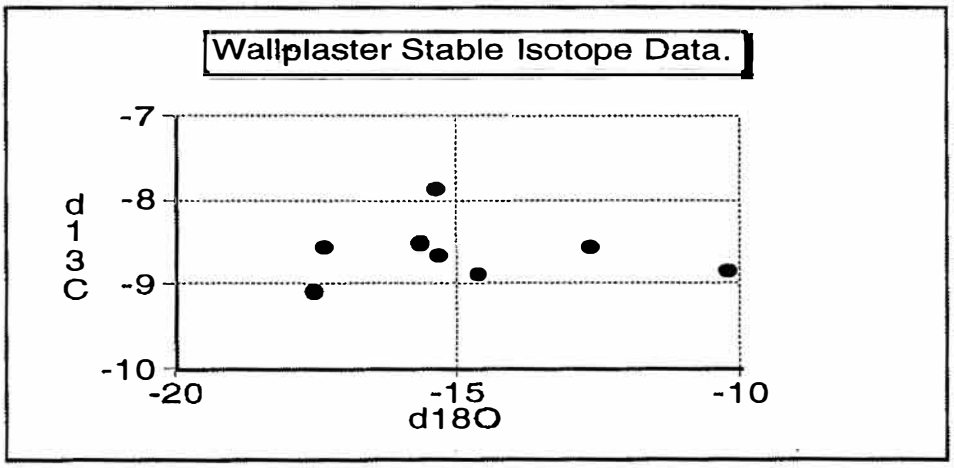

Figure 7.2 The wallplaster unit stable isotope trend is characteristically varied along its X-axis whilst remaining constant on its Y-axis. Such a pattern suggests a primary carbon isotope signal in addition to an oxygen isotope signal that has been reset.

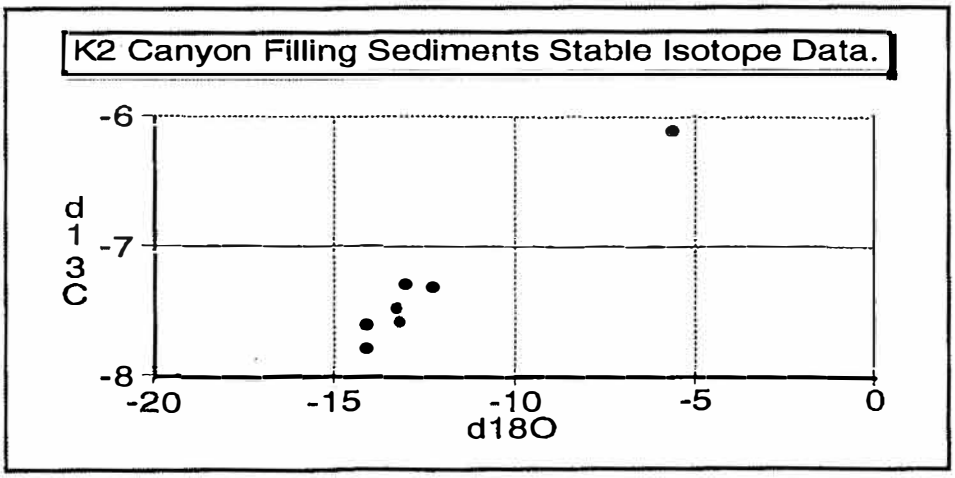

Figure 7.3 Isotopic analysis of the K2 units displays a very stable trend. This succession is the least negative of all the facies analysed and most probably represents a decrease in the role of meteoric waters during diagenesis. The isolated outlier displays a carbon isotope signal consistent with published results throughout the Adelaide Geosyncline (e.g. Eickhoff, 1988) whilst its oxygen isotope signal reflects the effects of diagenesis.

that $\delta^{18}O$ values have probably been reset. Burial temperatures (Ayliffe, 1992) and consistencies between the shallow-marine and subaerial facies support this conclusion. Similarly, the lack of dolomite within the canyon successions implies an innate susceptibility to alteration (Margaritz & Holser, 1986). Nevertheless, recent work in America (R.J.F. Jenkins, pers.comm., 1997) reveals that signals up to -12‰ may be reliable primary isotopic indicators. If the oxygen isotopic composition is indeed a primary signature, then it represents the influence of meteoric waters, thus providing strong evidence for subaerial canyon incision.

Chapter 8 - Depositional Model.

8.1 Introduction.

The Pamatta Pass Canyon Complex is inferred to have been eroded and infilled in a subaerial to shallow marine setting in accordance with the drowned river model. The simple model of erosional incision and infill put at question by the existence of a unique canyon facies: the K1 Unit. Two recognisable episodes of canyon erosion and infilling produced the canyon system with prior or syn-depositional tectonism influencing sedimentation as suggested by Binks (1971), Eickhoff (1988), DiBona (1989) and Jansyn (1990).

8.2 K1 Canyon Model.

The K1 Unit is deltaic to shallow-marine in origin and its correct interpretation has important ramifications for the development of the Adelaide Geosyncline.

8.2.1 Model 1 - Wilcolo Sandstone Time Deposition.

Deposition within a type 1 transgressive systems tract saw the development of fluvial channels infilled by the Wilcolo Sandstone. This model interprets the K1 Unit as the fluvial fill to one of these channels, incised a minimum 425 m into the already indurated underlying Ulupa Siltstone.

1) This model requires a tectonic and/or glacio-eustatic drawdown to expose the indurated sediments of the lower Wilpena Group into which K1 was subsequently incised.

2) Extensive reworking of previously deposited sediments culminated in the development of incised fluvial valleys (Dyson, 1996a) within the Adelaide Geosyncline, within which the Wilcolo Sandstone was deposited. This model interprets K1 genesis as related to the subaerial exposure of the region and the incision of the regionally significant Wilcolo Sandstone valleys.

3) Canyon infilling was by riverine sediments with the addition of a terrigenous component. Infilling is interpreted to have then progressed from this fluvial phase, through a deltaic phase to shallow-marine siliciclastic stage.

4) A marine transgression terminated deposition of the primary fluvial phase of the Wonoka Formation and continued into Bunyeroo time. Deposition of the Bunyeroo Formation then infilled the remaining topographic depressions.

5) Syn-depositional basin floor warping occurred in response to a new phase of compressional tectonism throughout the Adelaide Geosyncline. Bunyeroo Formation deposition was concentrated in troughs.

6) Regressive sedimentation then led to the deposition of the marine Wearing Dolomite and the shelfal facies of the succeeding Wonoka Formation (HU2-3).

8) The regression reached its zenith with the deposition of the supratidal Burr Well Member which provides evidence for a regional unconformity (DiBona, 1989).

9) Renewed tectonism, responsible for the development of the syn-depositional tectonic cleavages entailed further uplift of the region. This orogenic event generated uplift >1065 m and resulted in the initiation of the second phase of canyon incision following the template laid down by K1. Subaerial exposure is recorded by the angular unconformity between K1 and K2 lithologies.

8.2.2 Model 2 - Late Bunyeroo Time Incision.

1) K1 incision (700-800 m in depth) commenced in late Bunyeroo time, with the subaerial development of a low gradient river valley system in response to a relative sea-level drawdown.

2) The K1 facies were then deposited within the base of this incision, representing a canyon-filling facies of the Bunyeroo Formation. Deposition persisted outside the canyon systems, possibly extending down the canyon shoulders and into the incisions, as sea-level continued to rise (Eickhoff, 1988)

3) Syn-depositional basin floor warping occurred in response to a new phase of compressional tectonism throughout the geosyncline with Bunyeroo Formation deposition localised in troughs.

4) Bunyeroo deposition was terminated by this persistent regression that deposited the Wearing Dolomite and shoaling upwards HU2-3.

5) Continued uplift and shoaling eventually concluded marine sedimentation and led to the second phase of canyon development. This phase resulted in the removal of almost all the K1 facies as the canyon system further developed along the template provided by the K1. The continued history of the study area is summarised in the K2 Wonoka Formation depositional model.

8.2.3 Model 3 - Wearing Dolomite Time Incision.

This model attributes K1 incision to erosive downcutting associated with deposition of the shallow marine Wearing Dolomite, interpreting it as recording continued regression resulting in subaerial, fluvial canyon entrenchment.

1) Subaerial incision of K1 by fluvial means progressed to a minimum depth of 1050 m (incision depth + Bunyeroo thickness) during Wearing Dolomite time and may have

continued into HU2/3 time.

2) A cessation of uplift resulted in a relative sealevel rise. Fluvial processes were supplanted by shallow-marine deposition as the canyons were drowned and eventually buried in a manner analogous to K2.

3) Renewed tectonism again exposed the landscape and produced the second phase (K2) of canyon development.

8.2.4 Model 4 - Wonoka Time incision (post-HU1.)

This model requires two, closely related, stages of relative sealevel fall (>1km) within lower Wilpena Group time. Such regressive phases are interpreted to be primarily of tectonic origin.

1) A post-Wearing Dolomite phase of compressive tectonism produced rapid uplift (>1 km) within the Adelaide Geosyncline.

2) The palaeodrainage system then acted to rapidly incise the K1 into the underlying Wilpena Group sediments, as is evidenced by the inferred steepness of the canyon walls.

3) Cessation of uplift allowed at least partial infilling of the canyon with the unique K1 facies. By analogy with K2 this was followed by a rapid sealevel transgression which infilled the remaining topographic depression with a succession of shallow marine sediments.

4) Renewed tectonism, responsible for the development of the pre-K2 cleavages observed, entailed further uplift (>1065 m) and is recorded by the angular unconformity between K1 and K2 sediments. The second phase of canyon development then occurred in accordance with the K2 model.

8.3 K2 Wonoka Formation.

The K2 Wonoka Formation units are interpreted to have been deposited according to the classical drowned river model where a subaerially incised valley was progressively filled by coastal onlap associated with a relative sea-level rise based on wider regional relationships (DiBona, 1989; Sukanta *et al.*, 1991; Dyson, 1995, 1996a). K2 development occurred subsequent to deposition of the Burr Well Member Equivalent/HU3 with erosion stripping HU1-3.

1) A relative sea-level fall (>1 km) allowed the subaerial incision of the fluvial Wonoka Canyon systems. These canyon systems became entrenched into bedrock as incision progressed through the lateral erosion and mass-wasting of the canyon walls.

2) Development of the wallplaster was coeval with canyon incision, beginning once the incision was deep enough to create a sufficient hydraulic gradient.

3) An ensuing relative sea-level rise, probably in response to tectonism, then gradually infilled the river gorge by coastal onlap. The gorge remained the main sediment conduit and it is inferred that the basal fluvial facies were removed by the abrasive action of sediment transport.

4) Sea-level rise continued, progressively drowning K2. This is substantiated by the fining upwards succession within the canyon filling strata. The canyon shoulders remained emergent for the longest period of time and logically the subaerial wallplaster is best developed in these locations.

5) The subsequent canyon history can be ascertained by analogy with other canyon systems. It saw the complete infilling of the remnant canyon depressions by deposition of overlying sands and silts (HU6-11) as observed by Haines (1987), Eickhoff (1988) and Ayliffe (1992).

Chapter 9 - Depositional Model Discussion.

The subaerial model for canyon incision implies that the tectono-stratigraphic history of the Wilpena Group is considerably more complex than previously assumed. Judicious application of Occam's razor to depositional models is required in order to adequately elucidate the tectonic profile of the region.

9.1 K1 Wonoka Formation.

9.1.1 Model 1

The recognition of a regional unconformity corresponding to the Wilcolo Sandstone (Dyson, 1996a.) provides ample evidence for subaerial exposure at this time. The shallow depth of K1 incision does not necessitate a large scale relative sealevel downdraw and is inkeeping with the notion of proto-canyon development prior to the K2 incision. Whilst adequately explaining mechanisms for fluvial channel incision, this model fails to account for the the large discrepancy between the scale of the fluvial channels and the inferred depth for K1 incision.

The Wilcolo Sandstone is poorly developed within the study area and implies that reworking was not extensive. Hence, the conditions necessary for canyon development were not in place at this time. This model necessitates the K1 Unit to be a canyon-filling facies of the siliceous Wilcolo Sandstone, yet its substance does not reflect the observable relationships expected.

9.1.2 Model 2.

This model is eminently plausible in its simplicity yet several serious flaws pose questions concerning its validity.

This subaerial model demands a regional unconformity with parallel evidence for shallow water deposition within the Bunyeroo Formation. Eickhoff (1988) reports a cherty carbonate within the Bunyeroo Formation interpreted as corresponding to such an event. Nevertheless, the paucity of evidence testifying to this model contradicts Eickhoff's interpretation. Throughout the Flinders Ranges the Bunyeroo Formation shows no evidence for shoaling of any degree, especially during late Bunyeroo time when the transgression was nearing its zenith. Further discrediting this model is the requirement for the K1 Unit to be a hitherto undiscovered facies of the Bunyeroo Formation, a situation that is not supported by the calcareous nature of the unit and the regionally invariant characteristics of the Bunyeroo Formation.

9.1.3 Models 3 & 4.

These models are essentially identical, being differentiated by the timing of the first phase of incision.
The K1 Unit is interpreted as part of the Wonoka Formation on the grounds that it

superficially resembles HU2: a succession of siltstones and mudstones with lesser calcareous sandstone intervals. Remarkable similarities are observed between K1 and K2 facies (wallplaster blocks, basal conglomerates, and calcareous sandstones) and for these reasons K1 incision must be attributed to early Wonoka time. By analogy with K2, K1 also truncates the Bunyeroo Formation (this cannot be confirmed due to limited outcrop), providing further indication that this unit constitutes a facies of the Wonoka Formation. The apparent lack of Bunyeroo Formation megaclasts in K1 disputes this premise, although such clasts may exist in its northern extremity.

Another major problem with these models is that the sheer size of these canyons defies any comparison with localised erosion. R.J.F. Jenkins (pers. comm., 1997) reports that the Wearing Dolomite, at Donkey Creek and Bathtub Gorge, is locally erosive (<20 cm erosion) upon the underlying Bunyeroo Formation. Similarly, erosional channels several metres deep are commonly incised into the lower Wonoka Formation. Such erosion is very dissimilar to the incision of channels near Grand Canyon-depth and it requires a large leap of faith to link the two.

Close morphological links imply a similarly close temporal tie between the two phases. Model 4 attributes K1 genesis to just prior to K2 incision (**late** HU3 time). However, the superficial similarity between HU2 and the K1 Unit suggests this is not the case, instead favouring Model 3. Model 4 seems unlikely considering that subaerial incision should be associated with a regionally important facies. The Wearing Dolomite is of such significance and it was for this reason that Dyson (1996a) raised it to formation status. Model 4 implies two large-scale relative sealevel falls within a relatively short space of time - too short a space of time unless glacial eustasy is involved, in which instance sea-level fall would be implausibly great. The lack of a significant regionally equivalent facies at this time additionally shifts the focus of attention towards Model 3. DiBona (1989) associated a prior phase of incision (i.e. at around the K1 level) with the Burr Well Member and HU3. This poses a problem for Model 4 because the Burr Well Member is apparently coeval with the wallplaster unit, a paradox that Model 3 adequately acknowledges.

9.2 K2 Wonoka Formation.

The controversy over the Wonoka Formation canyon systems is in part due to the ambiguity of some of the canyon-related characteristics. The lack of known analogues to these canyons, for comparison of either facies or setting, further compounds this problem. Canyon development followed the progression displayed in Figure 9.1 and is summarised in Figure 9.2.

Of crucial importance is the interpretation of the wallplaster as a subaerial precipitate. This is based upon the non-marine isotopic and geochemical signatures and their observed characteristics. DiBona's (1989) observation of a possible regional

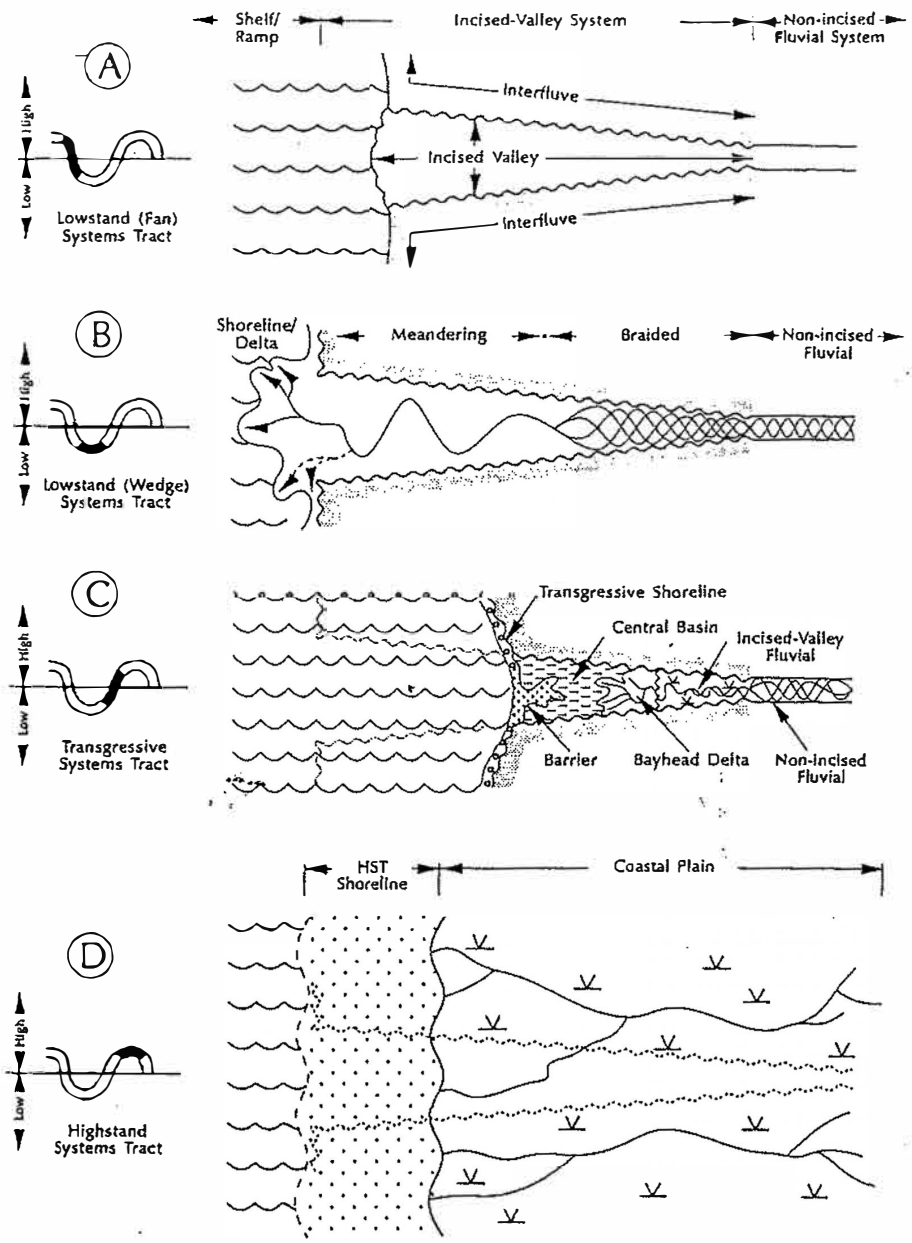

Figure 9.1 Hypothetical depositional model for the development of one phase of canyon incision during one cycle of eustatic sea-level rise and fall. (**A**) Regional uplift initiates the incision of a prototype river valley. (**B**) Continued uplift widens and deepens the river valley allowing the development of several types of river valley morphologies along its length. (**C**) The beginnings of a sea-level transgression begin to inundate the canyon allowing the development of deltaic to shallow-marine facies. (**D**) Further transgression gradually inundates the canyon system, eventually culminating in the complete drowning of the canyon and its burial by shallow marine sediments (modified from Zaitlin *et al.*, 1994).

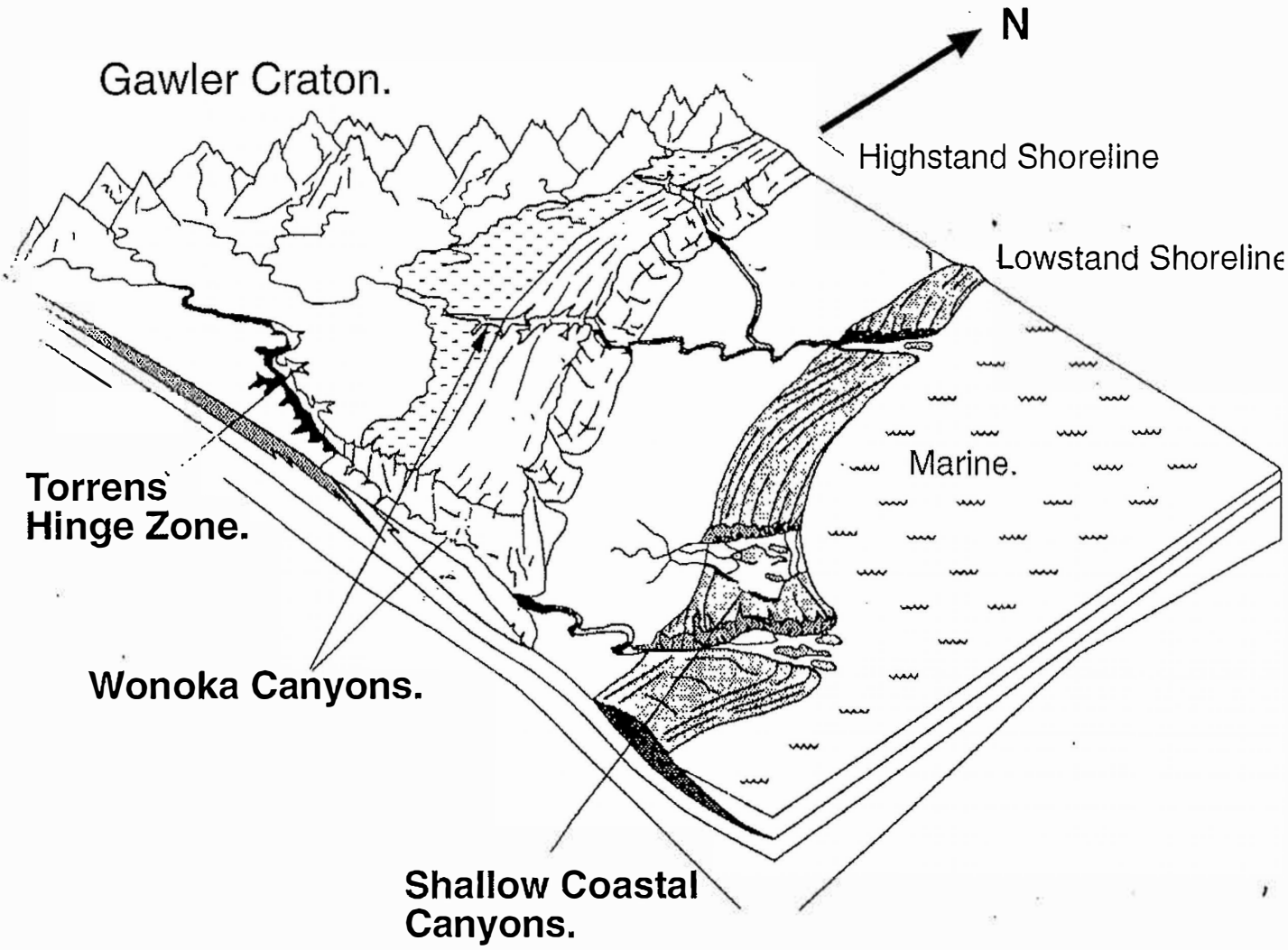

Figure 9.2 Palaeogeographical reconstruction of the region during Wonoka Formation time. Drainage systems extending eastwards from the Gawler Craton incised large-scale river gorges into the exposed shelf. A wide variety of valley morphologies thus developed ranging from simple, shallow incisions to multiple valleys and meandering canyon complexes (modified from Zaitlin *et al.*, 1994).

unconformity corresponding to subaerial exposure at the coeval Burr Well Member level associated with canyon cutting, vicariously supports such a model. Weathered and rounded ironstone pebbles present within the basal conglomerates serve to illustrate ironstone development within the region. Comparably, oxidised authigenic pyrite cubes, are preserved within the wallplaster. Such ferricretes are best observed in the more proximal areas of the basin (where exposure is interpreted to have been more extensive) where massive ironstones are developed above the canyon unconformity.

The shallow-marine origin of the canyon fill is based upon previously described sedimentary characteristics the facies associations they provide. When coupled with the observed relationships between the unconformity and the wallplaster, and the nature of the canyon fill, a submarine model for incision seems improbable. Following canyon erosion, a sea-level rise is postulated to have deposited the observed shallow marine sediments. The upwards deepening facies succession, as noted by Jansyn (1990), purports that canyon filling was via progressive inundation.

This model infers a major break in sedimentation, during which the Wilpena Group was exposed and eroded. The subaerial model has previously been severely hampered by the inability of eustatic fluctuations to account for this exposure and shallow water infilling. With evidence for a pre-existing phase of deformation then a viable mechanism for large-scale uplift exists.

9.2.1 Messinian Style Event.

One model that deserves particular attention is the Messinian model as proposed by Von der Borch *et al.* (1989) and Christie-Blick *et al.* (1990) who imply that such an event would explain subaerial erosion, canyon distribution, regional palaeocurrent patterns, the sudden appearance of widespread calcareous lithofacies within the Adelaide Geosyncline and the equivalent thin stratigraphic succession in regions remote from canyon incision. This model implies a single evaporitic downdraw that is not inkeeping with the multiple phases of canyon development observed. This model is not seriously considered because of the inference of a previous phase of deformation and is further contradicted by a probable tidal influence upon canyon sediments and the absence of a correlative major evaporite unit.

Chapter 10 - Structural Geology.

10.1 Folding.

Folding styles throughout the region consist of a series of tight, steep-limbed NNE-SSW trending folds generated in response to westwards verging Delamerian compression. They may reflect refolding of previous folds. Supporting this premise is the extremely tight nature of the chevron folds in the northern outcrop of Ulupa Siltstone. Such a relationship is also corroborated by warping of the axis of the northwestern Bunyeroo Formation syncline and the presence of an angular unconformity between the K1 and K2 facies.

10.2 Cleavages.

Delamerian compression has produced a pervasive, NNE-SSW (generally trending to 040°) cleavage throughout the study area. It varies from poorly to very well developed, depending on the particular lithology.

A prominent feature of the sediments pre-dating the K2 Wonoka Formation is the development of multiple cleavages. This older succession shows evidence of at least 2 phases of deformation and cleavage development, being dominated by the regional Delamerian cleavage, but also exhibiting a noticeable secondary cleavage (striking approximately 010°) These cleavages further substantiate Binks' (1971) suggestion of a pre-Delamerian tectonic event largely along the same regional axes. Optimum cleavage development is observed within the K1 unit (and some areas of the Bunyeroo Formation). This unit displays a slaty cleavage overprinted by a pair of conjugate cleavages and the regional cleavage [Plate 10A & B]. Orientated 'prisms', formed by cleavage intersections, were sampled for thin section analysis and substantiate the notion of two phases of cleavage development [Plate 9A-F].

The presence of slaty cleavages within the K1 poses a problem for a regional model of tectonic uplift as such cleavages indicate burial depths in excess of five kilometres. (M.Hand, pers. comm., 1997). This implies considerable post-depositional burial and erosion of the K1 (related to the formation of an orogenic belt) prior to incision of K2. Care must be taken when drawing such conclusions from one location. Further work needs to be concentrated upon finding evidence for such erosion within this jurisdiction.

10.3 Tectonic History Of The Region.

10.3.1 Pre-Depositional Tectonism.

Evidence for deformation of the ABC Range Quartzite prior to the commencement of the Wonoka Formation sedimentation can be found within the region (Chapter 5.) This supposition is confirmed by other workers (DiBona, 1989, Meredith, 1997).

Examination of cleavages within K1 Unit megaclasts indicate they do not correspond to either the regional or pre- K1 cleavage. Most likely they are randomly oriented slumped blocks that illustrate a deformation event prior to the incision of K1, or jointing in response to subaerial exposure and erosion.

10.3.2 Syn-depositional Tectonism.

The close similarities between the styles of canyon infilling and incision along with the canyon geometry suggest that the cutting of the canyons had a tectono-physiographic control. Jansyn (1990) suggests canyon incision may have begun in extensionally controlled tectonic lineaments that would have acted to focus fluvial erosion. The slaty cleavage within the K1 unit implies deep burial of the entire K1 system and begs the question of why did K2 evolve in exactly the same manner with exactly the same morphology? This tectonic control suggests a solution.

Eickhoff (1988) and DiBona (1989) both describe syn-depositional faulting within the Fortress Hill and Oodnapanicken Canyons, respectively. Haines (1987) and Jansyn (1990) report similar observations related to subsiding faults probably relating to cycles of thermal subsidence and lithospheric extension (Jenkins, 1990).

Cleavage development within the K1 Unit provides substantial evidence for a syn-depositional period of tectonism closely liked to the uplift responsible for K2 incision. Randomly oriented cleaved olistoliths of Bunyeroo Formation and Ulupa Siltstone occur within the wall conglomerates and olistostrome unit of both K2 and the Waukarie Creek Canyon Complex (Meredith, 1997).

Moores (1991), Drexel *et al.* (1993) and Royer & Rollet (1997) cite similarities between the Neoproterozoic regional structures, sediments and stratigraphy of Antarctica and Australia (Fig. 10.1). Analogously, Jenkins (1990) proposed a linking of the Adelaide Geosyncline with western Tasmania via the 'Dundas-Flinders Shear'. (Fig.10.2.)

These affiliations suggest two possible candidates for tectonism within the study area: the Penguin Orogeny and the Beardmore Orogeny. The multi-phase Penguin Orogeny has been dated at 750 - 650 Ma (Turner, 1989; Burret & Martin, 1989; Adams *et al.*, 1985) and was responsible for widespread deformation within northwestern Tasmania. Comparably, the Beardmore Orogeny of Antarctica has been dated 680 - 620 Ma (Thomson *et al.*, 1991) and is considered to have generated considerable Neoproterozoic deformation and igneous activity within the Transantarctic Mountains, where a folded Neoproterozoic sequence is unconformably overlain by lower Cambrian marine sediments (Thomson *et al.*, 1991).

10.3.3 Post Depositional Tectonism.

a) The Cambro-Ordovician Delamerian Orogeny.

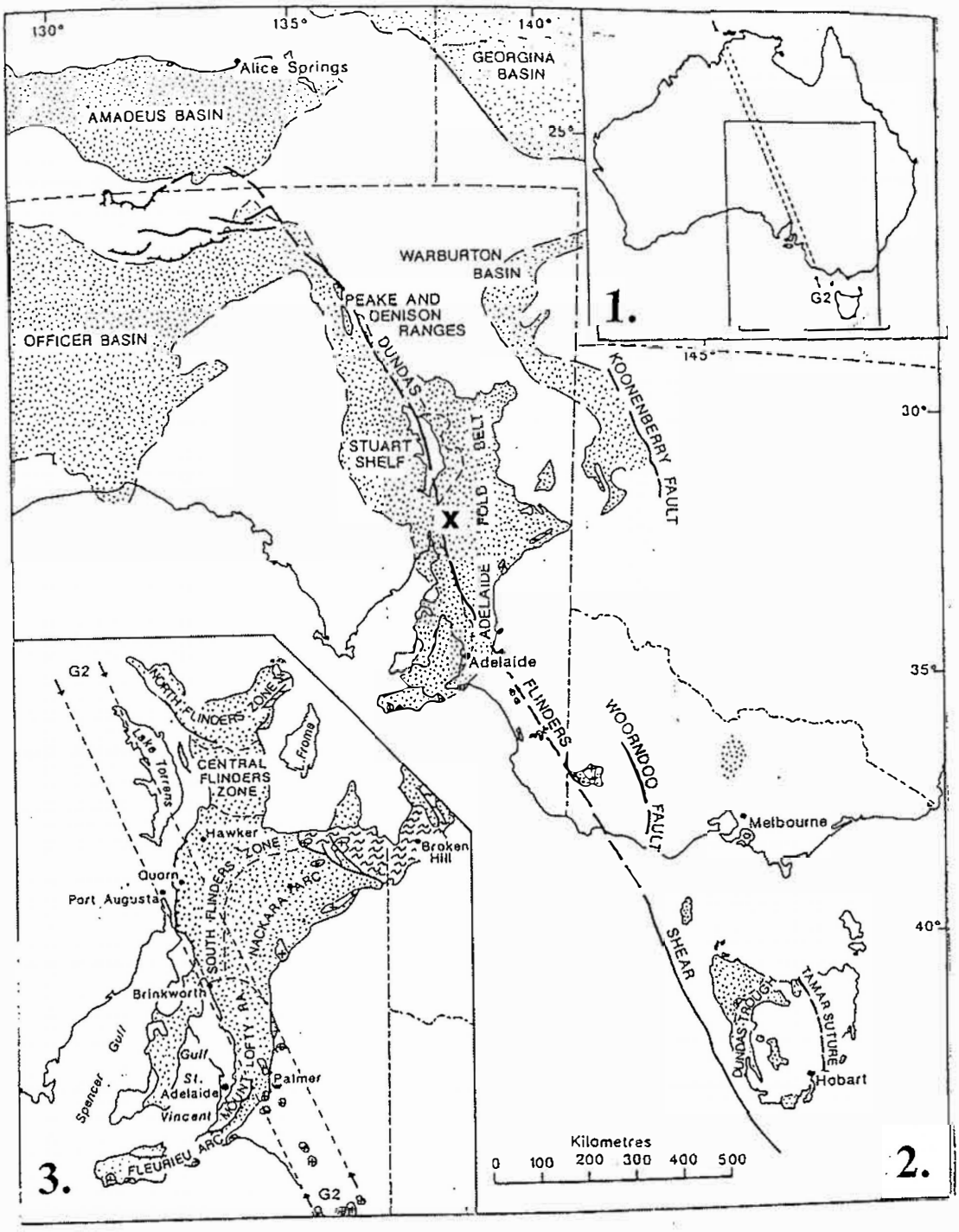

Figure 10.1 (1) Locality map of the Adelaide Geosyncline in relation to major crustal lineaments. (2) It is suggested that the 'G2 gravity corridor' allows the interlinking of Late Proterozoic basins of Adelaidean age via the Dundas Flinders Shear. The study area lies in the South Flinders Zone at 'X' (modified from Jenkins, 1990). (3) Tectono-stratigraphic divisions of the Adelaide Fold-Belt (after Rutland *et al.*, 1981).

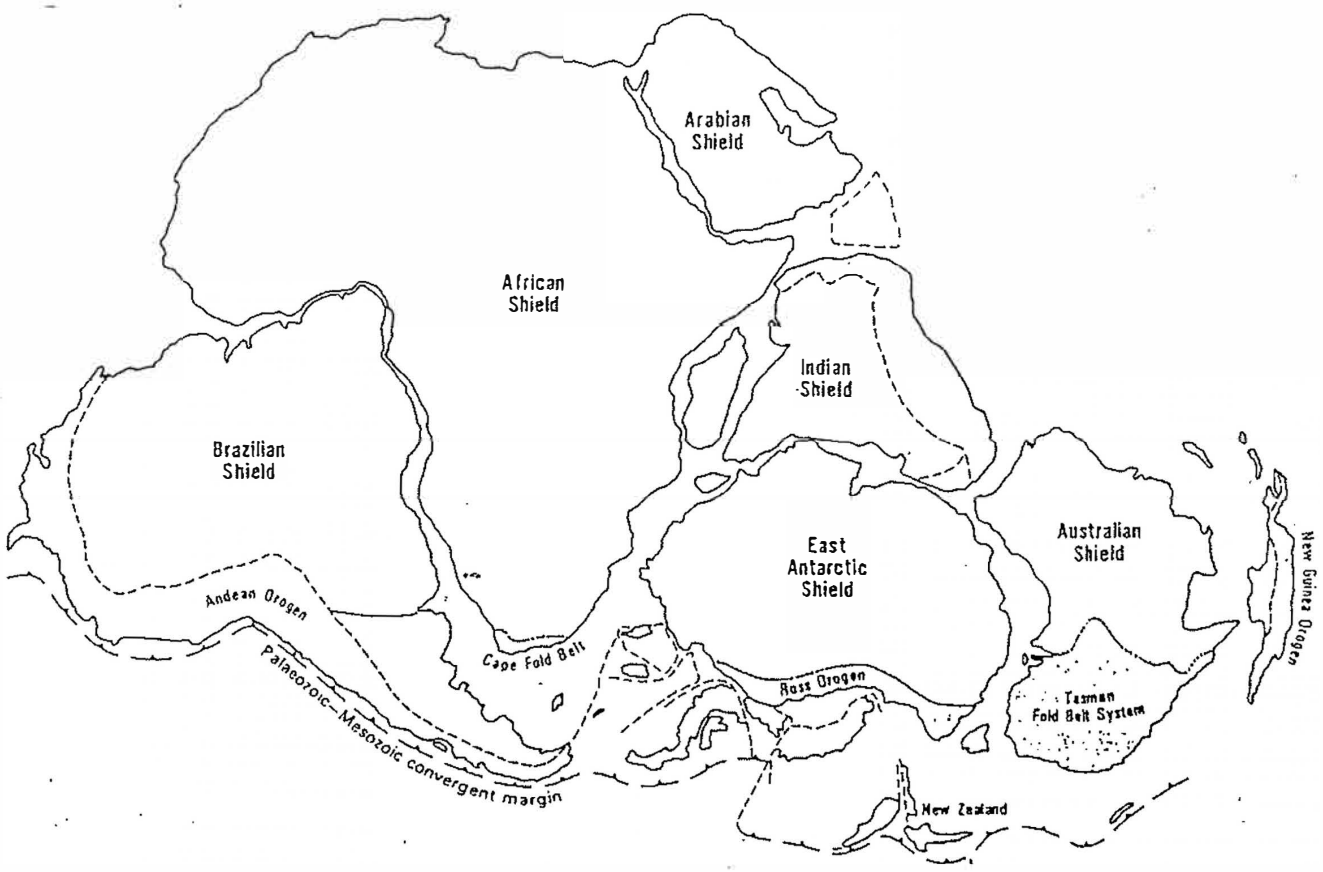

Figure 10.2 Illustration of the palaeogeographic relationships of Gondwana. Note the close affiliation between mainland Australia, Tasmania and Antarctica and the extent of the Ross-Delamerian Orogeny throughout the region. It is postulated that prior phases of deformation occurred throughout the same area along similar lines (after Moores *et al.*, 1990).

Deformation associated with the Delamerian orogeny (515-490Ma; Thomson, 1969) terminated Adelaidean deposition. Two separate compressional events which produced folding and deformation are observed (Preiss, 1987; Jenkins, 1990). The first, in response to E-W compression, formed relatively tight linear N-S folds, whilst the second, north-south compressional phase, produced NNE-SSW trending folds in the Nackara arc.

b) Other Phanerozoic Movements.

Reactivation of Proterozoic and Delamerian age faults occurred throughout the Mezozoic and Tertiary in response to spasmodic compressional events, culminating with the sequential uplift of the Adelaide Fold Belt to its present physiographic position.

Chapter 11 - Conclusions.

1) Canyon development occurred in two recognisable phases. The K1 Unit is interpreted to be a terrestrially-influenced, deltaic to shallow-marine facies. The K2 units are interpreted to have been deposited in a shallow marine environment .

2) Erosion occurred via fluvial incision and mass-wasting of canyon walls. This is substantiated by possible palaeosol development within the region and cleaved megaclasts within the basal units of both K1 and K2.

3) K1 incision occurred just after Wearing Dolomite deposition. K2 incision occurred during HU3 time with infilling by sediments ascribed to HU4-5.

4) A regional unconformity exists for both phases of canyon incision. The Wearing Dolomite corresponds to the K1 canyon unconformity, the Burr Well Member corresponds to the K2 canyon unconformity.

5) Both canyon facies record the subaerial precipitation of a wallplaster unit in response to the model proposed by Von der Borch *et al.* (1990). Canyon filling was by sediments largely corresponding to the classifications proposed by Haines (1987) and Von der Borch *et al.* (1989)

6) Both phases of canyon development followed the drowned river model. Minimum depth of erosion for both phases is of the order of 1065 m. Rising water-levels within the canyons are indicated by the wallplaster profile, rising carbonate contents and the upwards deepening facies succession.

7) Canyon infilling occurred progressively via backfilling from the basin in response to sea-level rise. This is corroborated by the lack of an obviously turbiditic pile and deepwater facies. The abundance of shallow-marine sedimentary structures further substantiate this proposition and requires a lowering of base level >1 km.

8) Geochemical and stable isotope data support the drowned river model.

9) A pre-Wonoka Formation phase of folding is suggested by folding styles and reconstructions of the region in addition to cleaved megaclasts within the K1 Unit.

10) Syn-depositional tectonism was active between the two phases of canyon incision. Cleavage development within the K1 Unit is of great importance.

11) Tectonism affecting Wilpena Group sedimentation may be related to the multi-phase Penguin Orogeny and/or Beardmore Orogeny.

Acknowledgements.

I am indebted to numerous people without whom this project would not have been possible.

My sincerest thanks are extended to Dr Richard Jenkins for accepting my application and suggesting such a fascinating research topic. His assistance, co-operation and advice throughout the year was of inestimable value, whilst his expertise in this particular field was something to be marvelled at. I can only hope to fulfil the high expectations and standards he exemplifies.

I wish to express my appreciation to Mr Gordon Jones and Mr John Smith for their hospitality and detailed insights into the history and geography of the environs surrounding Carrieton.

In addition I would like to applaud the efforts of the academic staff of the Geology Department. Discussions held with Dr's Vic Gostin, Yvonne Bone, Chris Nedin and Martin Hand were extremely fruitful and their assistance is greatly appreciated.

The efforts of the technical staff of the department are also to be congratulated: Dr Keith Turnbull, for his assistance with carbon and oxygen isotope work, Mr John Stanley for geochemical preparation and analysis, Mr Wayne Mussared for his work in the preparation of thin and polished sections, and Mr David Bruce for assistance with the CL equipment.

I would also like to commend my fellow students in the Honours class of 1997, in particular my field work partner, Kirsten Meredith for her constantly challenging ideas that always seemed to be correct!

Finally I wish to thank my good friend Emily Downes, for all her support and encouragement throughout the past years. Without her counsel this Honours project would never even have begun.

References.

- Adams, C.J., Black, L.P., Corbett, K.D. & Green, G.R. 1985. Reconnaissance isotopic studies bearing on the tectonothermal history of Early Palaeozoic and Late Proterozoic sequences in western Tasmania. *Aust. J. Earth Sci.,* Vol.32, pp7-36.

- Allen, P.A. 1985. HCS is not produced purely under progressive gravity waves. *Nature*, 313: pp562-564.

- Ashley, G.M., Southard, J.B. & Boothroyd, J.C. 1982. Deposition of climbing ripple beds: a flume simulation. *Sedimentology*, 29: pp67-79.

- Ayliffe, D. 1992. *Geological setting of the Late Proterozoic Wonoka Formation at Pichi Richi Pass, Southern Flinders Ranges, South Australia: geochemical, stable isotope and diagenetic analysis.* B.Sc. Honours Thesis, University of Adelaide, Unpublished.

- Binks, P.J. 1968. Orroroo map sheet, geological atlas of South Australia, 1:250,000 Series. *Geol. Surv. of S.A.*

- Binks, P.J. 1971. The geology of the Orroroo 1:250,000 Map Area. Report on investigations. Department Of Mines, South Australia, No. 36.

- Bouma, A.H. 1962. *Sedimentology of some flysch deposits.* Amsterdam: 168pp.

- Brasier, M.D. 1992. Global ocean-atmosphere change across the Precambrian-Cambrian transition. *Geological Magazine*, 129(2): pp61-168.

- Brasier, M.D., Margaritz, M., Cornfield, R.M., Huilin, L., Xiche, W., Lin, O., Zhiwen, J., Hamdi, B., Tinggui, H. & Fraser, A.G. 1990. The carbon and oxygen-isotope record of the Precambrian-Cambrian boundary interval in China and Iran and their correlation. *Geological Magazine,* 4: pp319-332.

- Burrett, C.F. & Martin, E.L. [Eds.] 1989. The geology & mineral resources of Tasmania. *Geol. Soc. of Aust. Special Publication* 15, 574p.

- Christie-Blick, N., Von der Borch, C.C., & DiBona,P.A. 1990. Working

hypotheses for the origin of the Wonoka canyons (Neoproterozoic), South Australia. *Amer. J. of Sci.*, V290-A, pp295-332.

- Cloud, P. & Glaessner, M.F. 1982. The Ediacaran Period and System: metazoa inherit the Earth. *Science*, V271, pp783-792.

- Coats, R.P. 1964. Large-scale Precambrian slump structures, Flinders Ranges. *Quarterly Geological Notes, Geol. Surv. of S.A.*, 11:1-2.

- Dalgarno, C.R. & Johnson, J.E. 1964. The Wilpena Group. In; Thomson *et al.*, Precambrian rock groups in the Adelaide Geosyncline: a new subdivision. *Quarterly Geological Notes, Geol. Surv. of S.A.*, 9: pp7-12.

- Dalrymple, R.W., Boyd, R & Zaitlin, B.A. (1994.) History of research, types and internal organisation of incised valley systems: introduction to the volume. In; Incised valley systems: origin & sedimentary sequences. *SEPM Special Publication No.51*: pp3-10.

- Degens, E.T. 1971. *Stable isotope distribution in carbonates.* In; Chilingar, G.V., Bissel, H.J. & Fairchild, R.W. [Eds.] Carbonate rocks. Developments in Sedimentology 9B, pp193-208.

- DiBona, P.A. 1989. *Geologic history and sequence stratigraphy of Lower Proterozoic Wonoka Formation, Northern Flinders Ranges, South Australia.* Ph.D. Thesis, Flinders University.

- DiBona, P.A., Von der Borch, C.C., & Christie-Blick, N. 1990. Sequence stratigraphy and evolution of a basin slope succession - the Late Proterozoic Wonoka Formation, Flinders Ranges, South Australia. *Aust. J. of Earth Sci.*, V37, pp135-145.

- Dott, R.H.Jr & Bourgeois, J. 1982. Hummocky Cross-Stratification: significance of its variable bedding sequences. *Geol. Soc. of Amer. Bull.* 93; pp168-194.

- Drexel, J.F., Preiss, W.V. & Parker, A.J. [Eds.] 1993. *The geology of South Australia, Volume 1: the Precambrian.* State Print: Adelaide.

- Dyson, I.A. 1992. Stratigraphic nomenclature and sequence stratigraphy of the lower Wilpena Group, Adelaide Geosyncline: the Sandison Subgroup. *Quarterly Geological Notes, Geol. Surv. of S.A.*, V122, pp2-13.

- Dyson, I.A. 1996a. Stratigraphy of the Neoproterozoic Aruhna and Depot Springs Subgroups, Adelaide Geosyncline. *Trans. R.Soc. of S.A.*, 120(3),

pp101-115.

- Dyson, I.A. 1996b. A new model for diapirism in the Adelaide Geosyncline. *MESA Journal,* Vol.3, October, 1996.

- Dyson, I.A., Christopher, C. & Von der Borch, C.C. 1994. Sequence stratigraphy of an incised valley fill: the Seacliff Sandstone, Adelaide Geosyncline, South Australia. In; R.W. Dalrymple, R.Boyd & B.A. Zaitlin (Eds.) "Incised valley systems: origin and sedimentary sequences." *SEPM Special Publication* No.51, pp209-222.

- Eickhoff, K.H. 1988. The Wonoka Formation in the Fortress Hill area, Northern Flinders Ranges. 8th Australian Geological Convention, Adelaide. *Geol. Soc. of Aust. Abstr.*, 15, pp61-62.

- Eickhoff, K.-H., Von der Borch, C.C., & Grady, A.E. 1988. Proterozoic canyons of the Flinders Ranges (South Australia): Submarine Canyons or Drowned River Valleys? *Sed. Geol.*, V58, pp217-235.

- Ewing, J.A. 1973. Wave-induced bottom currents on the outer shelf. *Marine Geology* 15, pp31-35.

- Farre, J.A., McGregor, B.A., Ryan, W.B.F., & Robb, J.M. 1983. Breaching the shelfbreak: passage from youthful to mature phase in submarine canyon evolution. In; Stanley & Moore (Eds.) The shelfbreak: critical interface on continental margins. *SEPM Spec. Pub.* No.33, pp25-39.

- Gerdes, G., Krumbein, W.E. & Reineck, H.E. 1991. *Biolaminations - ecological versus depositional dynamics.* in; Einsele et al. [Eds.] Cycles & events in stratigraphy. Springer-Verlag: Berlin, pp592-607.

- Gostin, V.A. & Jenkins, R.J.F. 1983. Sedimentation of the early Ediacaran, Flinders Range, South Australia. Sixth Australian geological convention, Canberra, 1983. *Geol. Soc. of Aust. Abstr.* Series 9, pp196-197.

- Gunn, P.J. 1984. Recognition of ancient rift systems: examples from the Proterozoic of South Australia. *Exploration Geophysics*, V15, pp85-97.

- Haines, P.W. 1986. Late Precambrian carbonate shelf to shale basin transition, Wonoka Formation, Flinders Ranges, S.A. *Geol. Soc. Aust. Abstr.* 15: pp92-93.

- Haines, P.W. 1987. *Carbonate shelf and basin sedimentation, Late Proterozoic Wonoka Formation, South Australia.* Ph.D. Thesis, University Of Adelaide,

Adelaide, 152p.

- Haines, P.W. 1988. Storm-dominated mixed carbonate/siliciclastic shelf sequence displaying cycles of hummocky cross-stratification, Late Proterozoic Wonoka Formation, South Australia. *Sedimentary Geology,* V58, pp237-254.

- Haines, P.W. 1990. A Late Proterozoic storm-dominated shelf sequence: the Wonoka Formation in the Central and Southern Flinders Ranges, South Australia. In; B. Jago & P.S. Moore (Eds.) The evolution of a Late Precambrian-Early Palaeozoic rift complex: The Adelaide Geosyncline. *Geol. Soc. Aust. Spec.Pub.* No.16, pp177-198.

- Hesse, R. & Rakofsky, A. 1992. Deep-sea channel/submarine -Yazoo System of the Labrador Sea: a new deep-water facies model. *AAPG Bulletin,* V76, No.5, pp680-707.

- Jackson, M.P.A. & Talbot, C.J. 1986. External shapes, strain rates, and dynamics of salt structures. *Geol. Soc. Amer. Bull.*, 97: pp305-323.

- Jansyn, J. 1990. *Strato-tectonic evolution of a large subsidence structure associated with the Late Proterozoic Wonoka Formation at Wilpena Pound, Central Flinders Ranges, South Australia.* B.Sc. Honours Thesis, University Of Adelaide, Unpub.

- Jenkins, R.J.F. 1981. The Concept of an 'Ediacaran Period' and its stratigraphic significance in Australia. *Trans. R. Soc. S.A.*, 105: pp179-194.

- Jenkins, R.J.F. 1990. The Adelaide Fold-Belt: A tectonic reappraisal. In; B. Jago & P.S. Moore (Eds.) The evolution of a Late Precambrian-Early Palaeozoic rift complex: The Adelaide Geosyncline. *Geol. Soc. Aust. Spec. Pub.* No.16, pp396-420.

- Kaufman. A.J., Hayes, J.M., Knoll, A.H. & Germs, G.J.B. 1991. Isotopic compositions of carbonates and organic carbon from Upper Proterozoic successions in Namibia: stratigraphic variation and the effects of diagenesis and metamorphism. *Precamb. Res.*, 49: pp301-327.

- Kaufman. A.J., Jacobsen S.B. & Knoll, A.H. 1993. The Vendian record of Sr & C isotopic variations in seawater: implications for tectonics and palaeoclimate. *Earth & Planetary Science Letters*, 120: pp409-430.

- Kaufman. A.J., & Knoll, A.H. 1995. Neoproterozoic Variations in the C-isotopic composition of seawater: stratigraphic and biogeochemical implications.

Precamb. Res. 73: pp27-49.

- Knoll, A.H., Hayes, J.M., Kaufman, A.J., Swett, K. & Lambert, I.B. 1986. Secular variation in carbon isotope ratios from Upper Proterozoic successions of Svalbard and East Greenland. *Nature*, 321: pp832-838.

- Lambert, I.B., Walter, M.R., Wenlong, Z., Sangian, L. & Guogan, M. 1987. Paleoenvironmental carbon isotope stratigraphy of Upper Proterozoic carbonates of the Yangtze Platform. *Nature*, 325: pp140-142.

- Margaritz, M., Holser, W.T. & Kirschvink, J.L. 1986. Carbon-isotope events across the Precambrian/Cambrian boundary on the Siberian Platform. *Nature*, 320: pp258-259.

- Meredith, K. R. 1997. *Geological history of the Waukarie Creek Canyon Complex, Southern Flinders Ranges, South Australia.* University of Adelaide, B.Sc. Honours thesis, in submission.

- Miall, A.D. 1984. *Principles of sedimentary basin analysis.* Springer Verlag: New York. 490pp.

- Narbonne, G.M., Kaufman, A.J. & Knoll, A.H. 1994. Integrated chemostratigraphy and biostratigraphy of the Windermere Supergroup, Northwestern Canada: implications for Neoproterozoic correlations and the early evolution of animals. *Geol. Soc. Amer. Bull.*, V106, pp1281-1292.

- Paeche, H. 1995. *Cathodoluminescence signature of selected minerals of South Australia.* University of Adelaide, B.Sc. Honours Thesis, Unpub.

- Pell, S. 1989. *Stable isotope composition of organic matter and coexisting carbonate in the Late Precambrian of the Officer Basin. stratigraphic relationships with neighbouring basins and environmental significance.* B.Sc. Honours Thesis, University of Adelaide, Unpub.

- Piper D.J.W. [Ed.] 1989. Submersible observations off the east-coast of Canada. *Geol. Surv. Canada*, Paper 88-20.

- Plummer, P.S. 1978a. Stratigraphy of the lower Wilpena Group (Late Precambrian), Flinders Ranges, South Australia. *Trans. R. Soc. S.A.*, V102, pp25-38.

- Plummer, P.S. 1978b. *The Upper Brachina Subgroup: a Late Precambrian Intertidal deltaic and sandflat sequence in the Flinders Ranges, South Australia.*

Ph.D. Dissertation, University of Adelaide, Adelaide, 170p.

- Plummer, P.S. & Gostin, V.A. 1981. Shrinkage cracks: dessication or synaeresis? *J. Sed Petr.*, 51(4), pp1147-1156.

- Plummer, P.S. 1990. Late Precambrian wave- to tide-dominated delta evolution in the west-central Adelaide Geosyncline, South Australia. In; Jago, J.B. & Moore, P.S.: The evolution of a Late Precambrian-Early Palaeozoic rift complex; The Adelaide Geosyncline. *Geol. Soc. Aust. Spec. Pub.* 16., pp164-176.

- Prave, A.R. 1985. Can hummocky cross-stratification be formed below effective storm wave base? *Geol. Soc. Amer. Abstr.*, V17, pp693.

- Preiss, W.V. (1987.) *The geology of South Australia: Volume 1, The Precambrian.* MESA, 347p.

- Preiss, W.V. 1990. A stratigraphic and tectonic overview of the Adelaide Geosyncline, South Australia. In; B. Jago & P.S. Moore (Eds.) The evolution of a Late Precambrian-Early Palaeozoic rift complex: The Adelaide Geosyncline." *Geol. Soc. Aust. Spec Pub.* No.16, pp1-33.

- Royer, J.Y. & Rollet, N. 1997. Plate tectonic setting of the Tasmania region. *Aust.J. Earth Sci.*, 44, pp543-560.

- Rutland, R.W.R, Parker, A.J., Pitt, G.M., Preiss, W.V. & Murrell, B. 1981. *The Precambrian in South Australia.* In; D.R. Hunter [Ed.] Precambrian of the Southern Hemisphere. Elsevier: Amsterdam, pp309-360.

- Scotford, G.L. 1984. *Sedimentation of late Proterozoic sediments with syn-depositional diapirism, and Delamerian thrust faulting, Warraweena, North Flinders Ranges, South Australia.* B.Sc. Honours Thesis, University of Adelaide, Unpub.

- Shephard, F.P. & Marshall, N.F. 1973. Currents along floors of submarine canyons. *AAPG Bulletin*, 57: pp244-264.

- Singh, U. 1986. *Late-Precambrian carbonates of the Adelaidean in the Flinders Ranges, South Australia: a petrographic, electron microprobe and stable isotope study.* Ph.D. Thesis; University of Adelaide, Unpub.

- Sprigg, R.C. 1952. *Sedimentation in the Adelaide Geosyncline and the Formation of the continental terrace.* In Glaessner, M.F. & Sprigg, R.C. [Eds.],

Sir Douglas Mawson Anniversary Volume. University of Adelaide, Adelaide, pp153-159.

- Sukanta, U., Thomas, B., Von der Borch, C.C. & Gatehouse, C.G. 1991. Sequence stratigraphic studies and canyon formation, South Australia. *PESA Journal,* No.19, pp68-73.

- Thomson, B.P. 1969. Precambrian basement cover in the Adelaide System. In; L.W. Parkin [Ed.] Handbook of South Australian geology. *Geol. Surv. S.A.*: Adelaide, pp49-83.

- Thomson, M.R.A., Crame, J.A. & Thomson, J.W. 1991. *Geological evolution of Antarctica - world and regional geology.* Cambridge University Press, pp143-147.

- Tucker, M.E. 1986. Carbon isotope excursions in Precambrian/Cambrian boundary beds, Morocco. *Nature*, Vol.319, pp48-50.

- Tucker, M.E. 1992. The Precambrian-Cambrian boundary: seawater chemistry, ocean circulation and nutrient supply in metazoan evolution, extinction and biomineralisation. *J. Geol. Soc. London*, Vol.149, pp655-688.

- Urlwin, B. 1992. *Carbon isotope stratigraphy of the Late Proterozoic Wonoka Formation of the Adelaide Fold Belt: diagenetic assessment and interpretation of isotopic signature and correlation with previously measured isotopic curves.* B.Sc. Honours Thesis, University of Adelaide, Unpub.

- Vezier, J & Hoefs, J. 1976. The nature of $^{18}O/^{16}O$ and $^{13}C/^{12}C$ secular trends in sedimentary carbonate rocks. *Geochemica Et Cosmochimica Acta,* 40: pp1387-1395.

- Von der Borch, C.C. 1980. Evolution of Late Proterozoic to Early Palaeozoic Adelaide Foldbelt, Australia: comparisons with post-Permian rifts and passive margins. *Tectonophysics*, V70, pp115-134.

- Von der Borch, C.C., Smit, R. & Grady, A.E. 1982. Late Proterozoic submarine canyons of Adelaide Geosyncline, South Australia. *AAPG Bull.*, V66, pp332-347.

- Von der Borch, C.C. & Grady, A.E. 1983. Submarine canyons. *Geol. Soc. Aust. Abst.*, 10: p55.

- Von der Borch, C.C., Grady, A.E., Aldam, A., Miller, R., Neumann, R.,

Rovira, A & Eickhoff, K.H. 1983. Submarine canyons - Wilpena Group, Adelaide Geosyncline. *Geol. Soc. Aust. Abstr.*, 9: p121.

- Von der Borch, C.C., Grady, A.E., Aldam, A., Miller, R., Neumann, R., Rovira, A & Eickhoff, K.H. 1985. A large-scale meandering submarine canyon outcrop example from the Late Proterozoic Adelaide Geosyncline, South Australia. *Sedimentology*, V32, pp507-518.

- Von der Borch, C.C., Christie-Blick, N. & Grady, A.E. 1988. Depositional sequence analysis applied to Upper Proterozoic Wilpena Group, Adelaide Geosyncline, South Australia. *Aust. J. Earth Sci.*, V35, pp59-71.

- Von der Borch, C.C., Grady, A.E., Eickhoff, K.H. & DiBona, P. 1989. Late Proterozoic Patsy Springs Canyon, Adelaide Geosyncline: submarine or subaerial in origin? *Sedimentology*, V36, pp777-792.

- Zaitlin, B.A., Dalrymple, R.W. & Boyd, R. 1994. The Stratigraphic organisation of incised-valley systems associated with relative sea-level change. *SEPM Spec. Pub.* 51, pp46-60.

Appendix A - Geological Cross Sections.

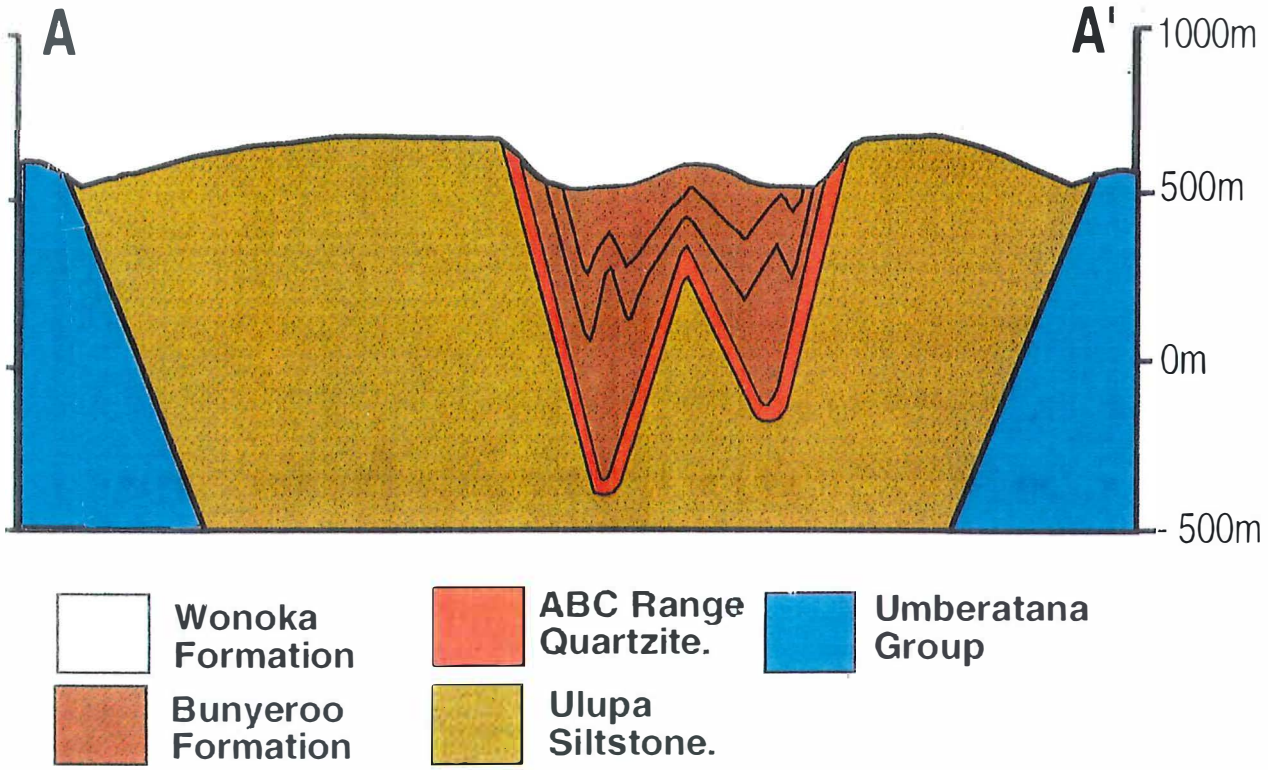

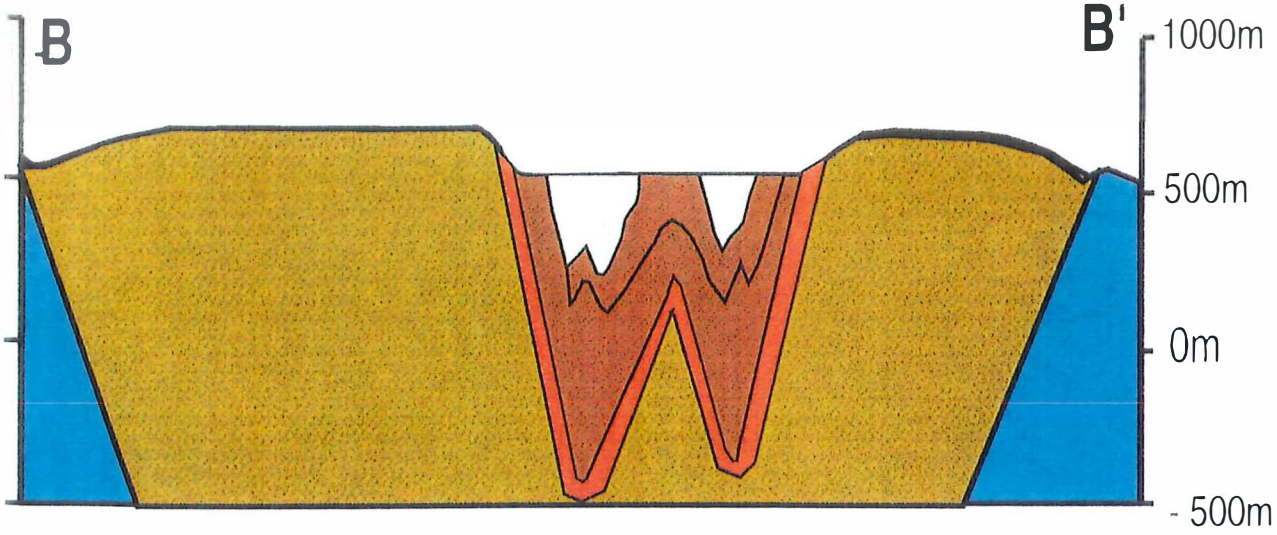

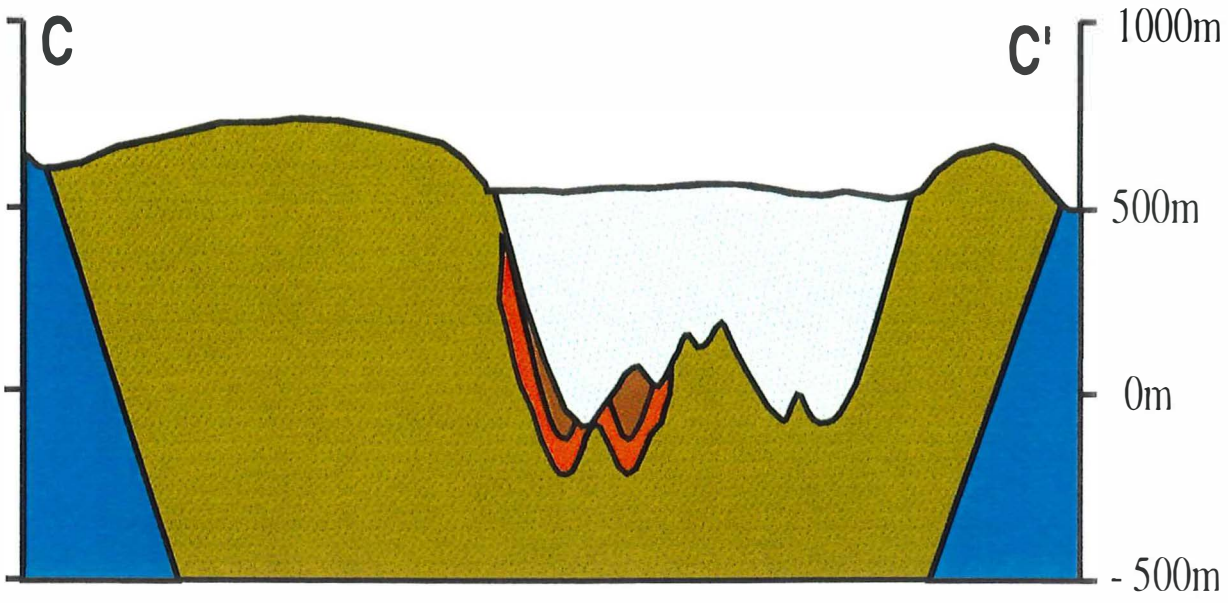
C
C'
1000m
500m
0m
- 500m


Wonoka Formation
ABC Range Quartzite.
Umberatana Group
Bunyeroo Formation
Ulupa Siltstone.

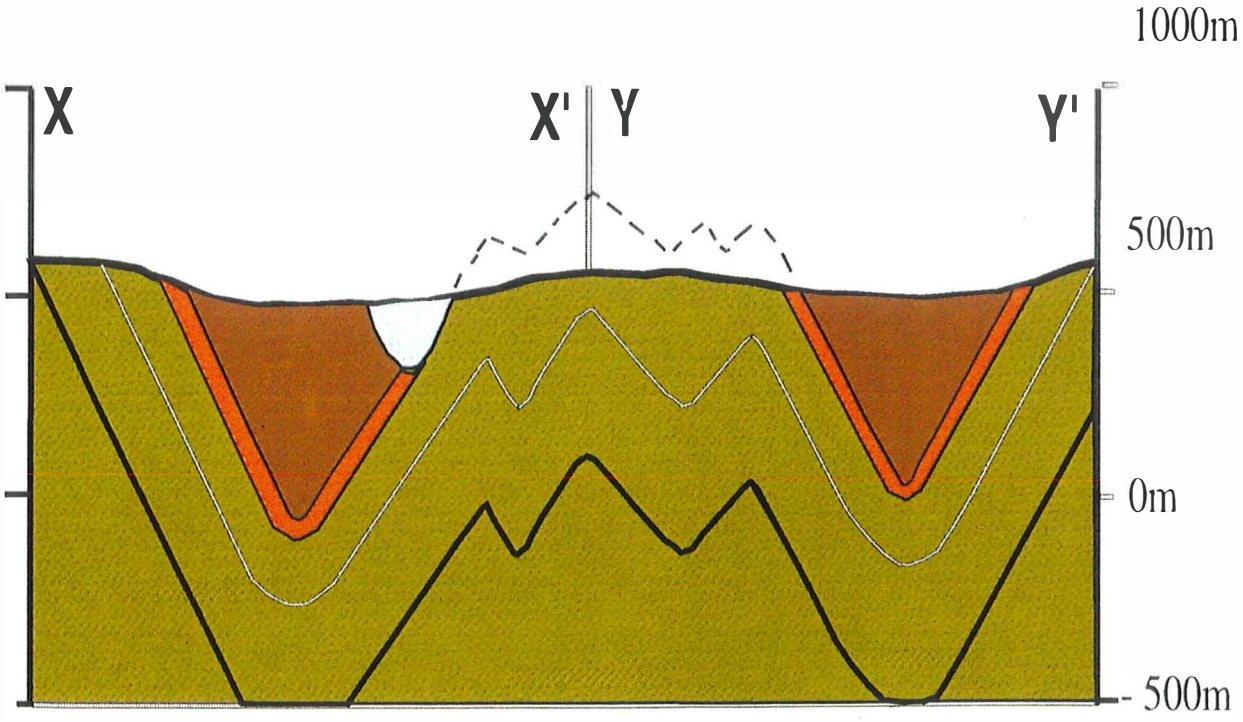
1000m
X
X'
Y
Y'
500m
0m
- 500m

Appendix B - Plates.

Plate 1.

A) Ferruginous medium to coarse-grained sandstones within Ulupa Siltstone (Moorillah Member equivalent) displaying soft sediment slumping. Compass is 8cm long.

B) Tuff layer within ferruginous sandstones of the Ulupa Siltstone. Pencil is 15cm long.

C) Ferruginous, medium to coarse-grained silty sandstones of the Ulupa Siltstone. Note the well developed cross-bedding and ripple laminations. This particular lithology is associated with tuff layers (Moorillah Member equivalent) and is characteristically medium to coarse-grained and red-brown to black. Interbedded with this lithology are khaki siltstones, displaying synaeresis cracks, that is typical of the Ulupa Siltstone. Hammer head is 17.5cm long.

D) Authigenic pyrite crystals ('Devils's dice') within the Ulupa Siltstone. Note the 'bleached' zone enclosing the crystals where crystal formation in response to metasomatism has depleted the rock of Fe.

E) Interfingering between the fine-grained sandy Ulupa Siltstone and ABC Range Quartzite. Hammer handle is 25cm long.

F) Typical outcrop of Bunyeroo Formation within the study area. The Bunyeroo Formation is characteristically highly cleaved and contains lonestones (of probable glacial origin) of finely bedded sandstones, as illustrated here. The pen is 13.5cm long.

Plate 1.


A


B

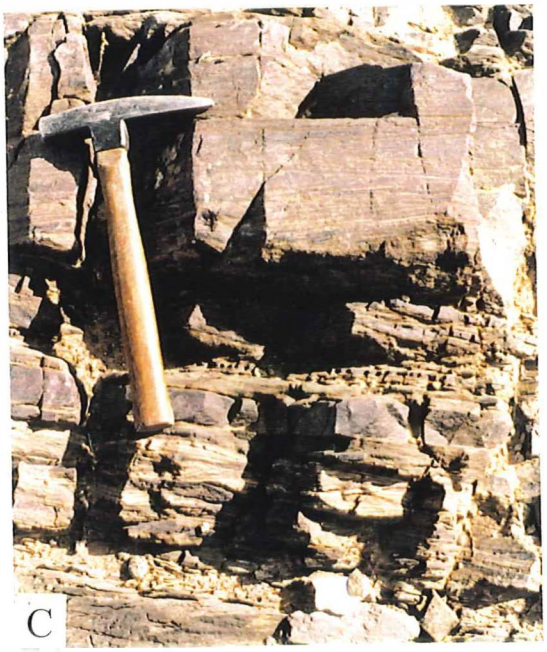
C

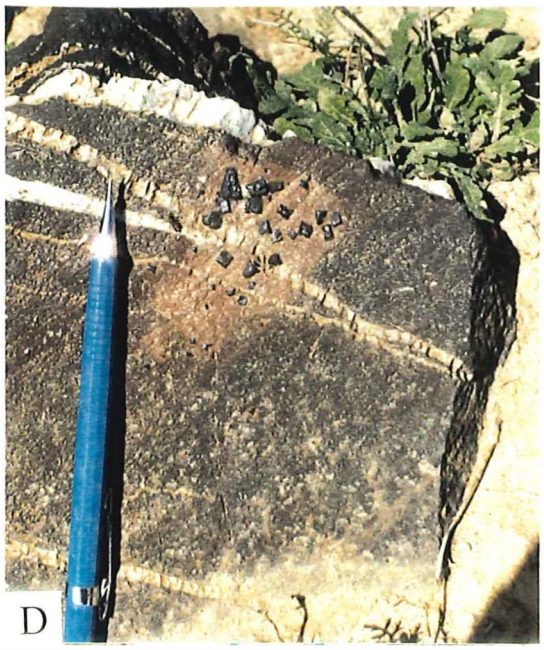
D

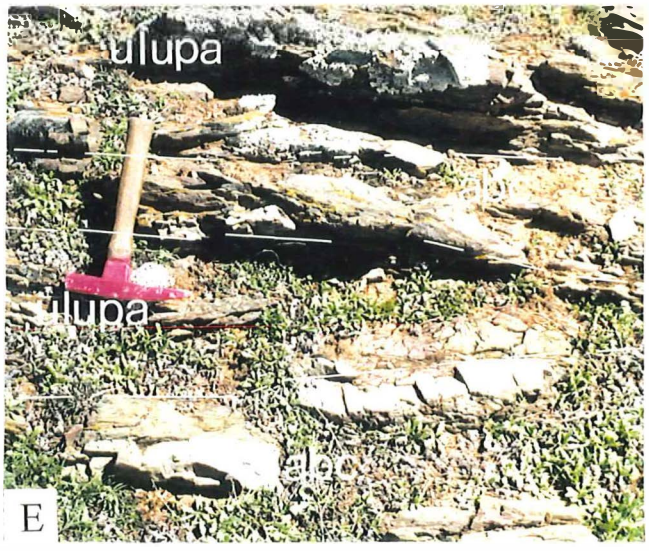

E


F

Plate 2.

A) Looking south along the K2 erosional unconformity towards the K1 Wonoka Formation. In the middle ground lie lenses of basal conglomerates very similar to those displayed in Plate 3B,E,F.

B) Diagrammatic representation of Plate 2A.

C) Conglomerate layer preserved within the K1 Unit containing rounded clasts and angular blocks of pink limestone and cryptalgal laminated yellow dolostone petrologically similar to the K2 wallplaster unit and Burr Well Member (Plate 3A.) Other clasts include rounded cobbles of blue chert, Ulupa Siltstone lithology, ABC Range Quartzite lithology, grey and purple limestones, and medium to coarse sandstones. Hammer handle is 25cm long.

D) Basal conglomerate layer immediately overlying the K1 erosional conformity. Occasional slight imbrications are observed within these conglomerates. These conglomerates occur as discrete lenses within the base of erosional channels in the Ulupa Siltstone. Hammer head is 17.5cm long.

E) Characteristic outcrop of K1 Wonoka Formation. The interplay between two cleavage planes has produced the long 'pencils' with a distinctive rhomboid cross section. Sampling of this unit and the Bunyeroo Formation for thin section analysis was concentrated upon such outcrops. Hammer head is 17.5cm long.

F) 'Pod' of pink limestone sharing distinct similarities with clasts within the basal K1 conglomerates and the pink limestones associated with the K2 wallplaster. The 'pod may represent boudinaging of an incompetent limestone facies or a block of K1 wallplaster emplaced into the unit by slumping. Hammer handle is 25cm long.

Plate 2.

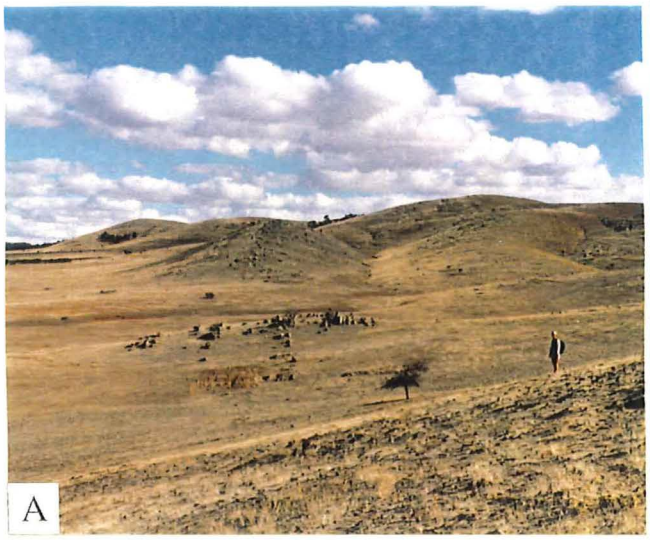
A

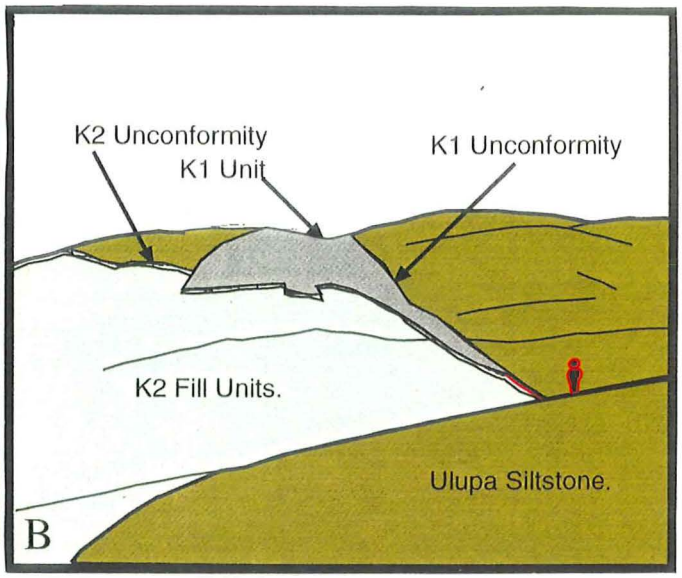

B


C


D

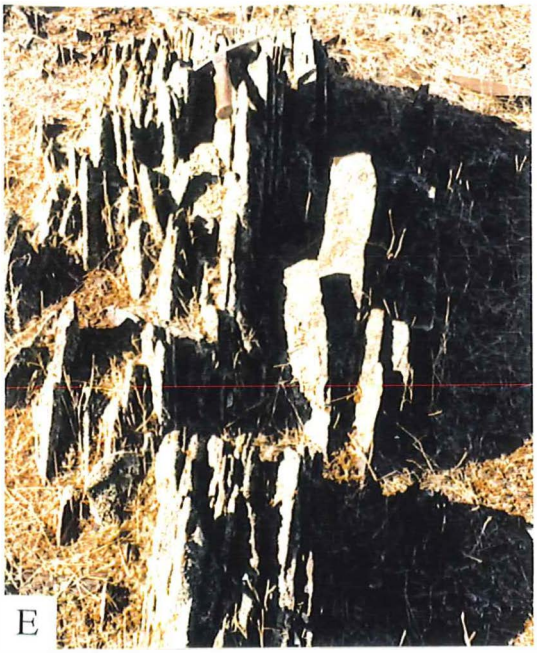
E


F

Plate 3.

A) Outcrop of yellow dolostone (Burr Well Member equivalent) within the K2 wallplaster unit. It disconformably overlies the green silts of the Ulupa Siltstone. Note the highly cleaved nature of the Ulupa siltstone and the cryptalgal laminations within the dolostone. Such clasts are prominent within the conglomerates interbedded with the K2 filling sediments (See also Plate 3A, 6A,B,C,D). Hammer head is 17.5cm long.

B) Characteristic outcrop of the wallplaster conglomerates towards the deepest part of the K2 incision. The canyon unconformity in the background incorporates the olistostrome unit. Note the irregular, terraced profile to the boundary reflecting successive episodes of channel cutting and canyon development.

C) Looking south upon the canyon unconformity in the deepest part of the incision. The unconformity here is marked by a series of thin-bedded pinkish -grey limestones that can be seen in the centre of the photograph. Left of the unconformity lies the Ulupa Siltstone. Dr Richard Jenkins stands at the site of Plate 3D.

D) Close up of the canyon unconformity shown in Plate 3C. Below the pencil lies the flat-bedded Ulupa Siltstone. It is unconformably overlain by a thin conglomerate (5-10cm) before passing into the pinkish-grey limestones and basal conglomerates present at this location. The pencil is 15cm long.

E) This photograph illustrates the nature of the basal conglomerates towards the deeper parts of the canyon. Clast types are characteristically tabular to sub-rounded. Note the similarity in size and shape of the large clast to that of the limestone 'pod' (Plate 2F.) This location displays an imbrication towards the south, reflecting the predominant currents within the canyon. The hammer handle is 25cm long.

F) Illustration of sub-rounded clasts of yellow dolostone (Burr Well Member Equivalent) within the basal and wall conglomerates within K2. These units are poorly sorted and exhibit a matrix of similar composition to the antecedent clast lithology's.

Plate 3.


A

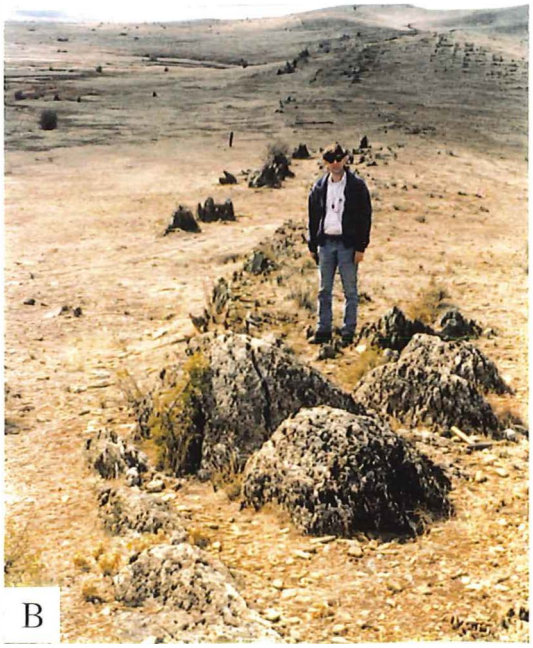
B

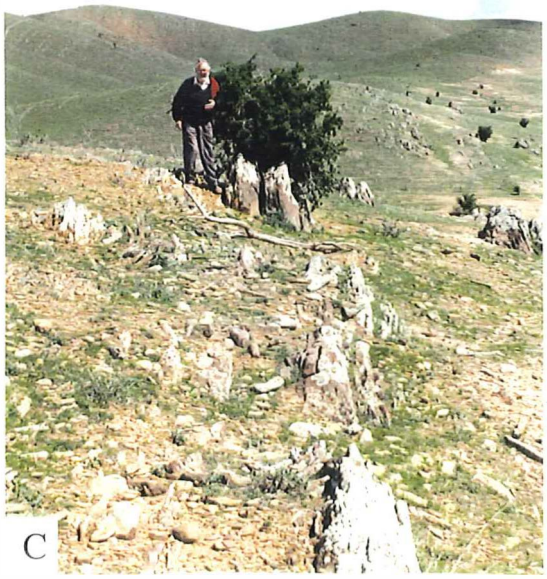
C


D


E


F

Plate 4.

A) Olistoliths of Bunyeroo Formation within the olistostrome unit. Note the randomly oriented, well developed cleavages.

B) Cleaved boulder of Ulupa Siltstone emplaced into the HU4 equivalent unit adjacent to the olistostrome unit.

C) Sole marks within the basal sands unit. Note the massive nature to the sandstone forming the base of the bed that becomes progressively finer laminated towards the top of the bed. The hammer handle is 17.5cm long.

D) Close up of granulose coarse sands interbedded within the basal conglomerate unit. The pen lid is 4cm long.

E) Photograph of a limestone boulder displaying evidence for soft sediment deformation. The boulder has essentially rolled up on itself as slumping progressed. The hammer handle is 25cm long.

F) Close up of a volcanic cobble present within the basal conglomerates unit. In addition to clasts of this lithology, rounded cobbles and pebbles of basic volcanics (hornfels) were also present in this unit and are suggestive of emergent diapirism during K2 incision. The pencil is 15cm long.

Plate 4.


A


B

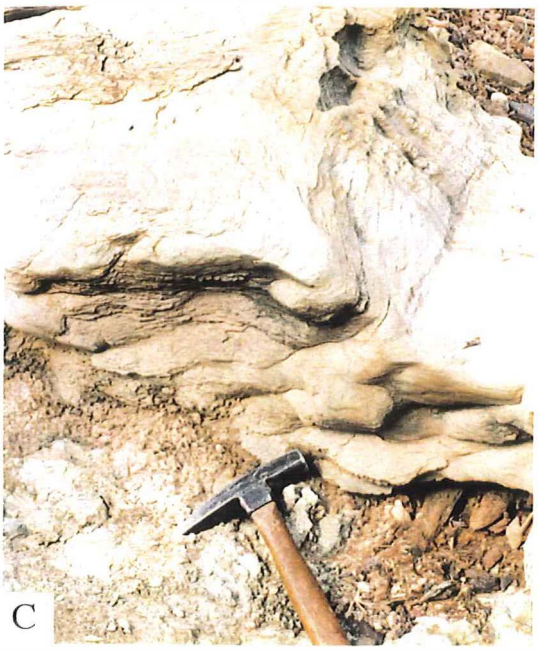
C


D


E


F

Plate 5.

A) Photograph of small scale SCS within sandy limestones of the HU4 equivalent unit. The hammer head is 17.5cm long.

B) Illustration of HCS within the upper portions of the HU4 equivalent unit. The dimensions of the hummock are 25cm high and in excess of 1m long. The hammer handle is 25cm long.

C) An example of the typical outcrop of the HU4 equivalent unit. It consists of the cyclical alternation of fine, white, calcareous sands and green shales that exhibit the regional cleavage. The hammer handle is 25cm long.

D) A close up of the rhythmically laminated green calcareous silts and very fine calcareous sands developed within the HU4 equivalent unit. This facies exhibits ripple laminations and occasional climbing ripples, with bedding occasionally being disturbed by the regional cleavage.

E) Typical outcrop of finely laminated and very well cemented HU5 equivalent limestones. Such outcrops become increasingly more predominant upsection and are often cyclically interbedded with the facies illustrated in Plate 5C, D and E. The hammer handle is 25cm long.

F) Thinly laminated, calcareous green silts and white very fine, silty sands of the upper portions of the HU5 equivalent unit and the upper portions of HU4. These facies record the increasing dominance of carbonate production upsection. The hammer handle is 25cm long.

Plate 5.


A


B

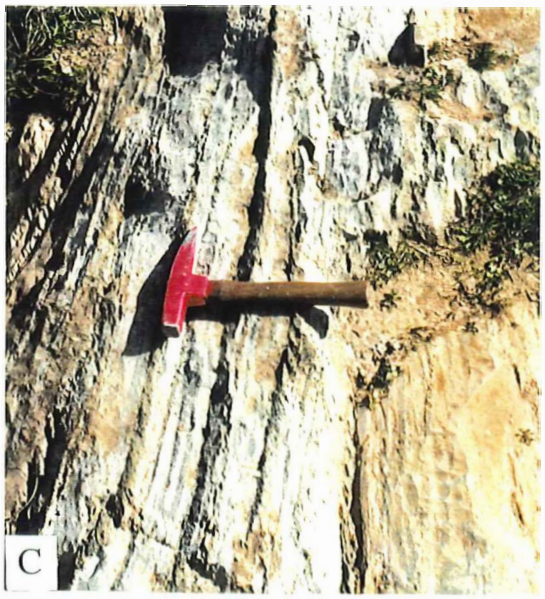
C

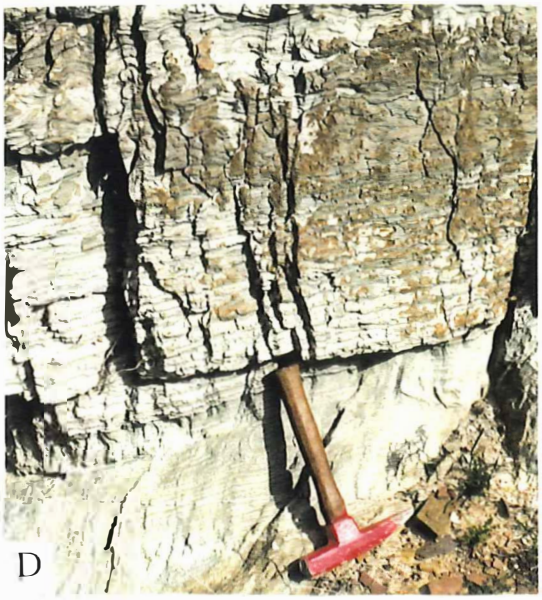
D

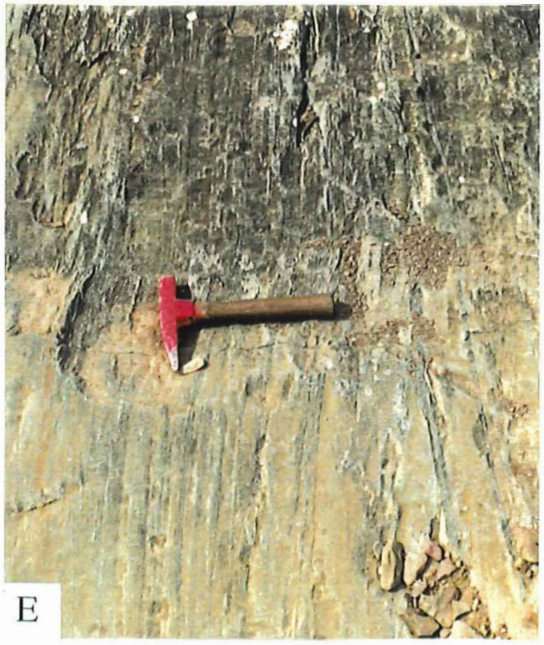
E

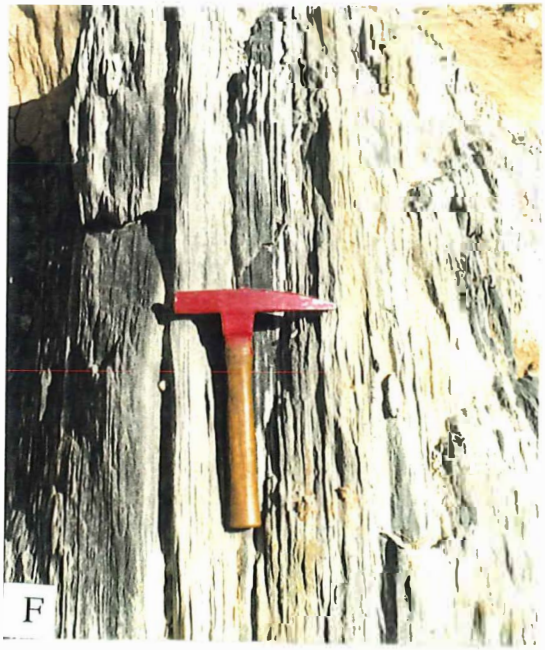
F

Plate 6.

A) Photograph of well developed conglomerates within the canyon axis towards the top of the stratigraphy. These conglomerates have a significant proportion of subrounded yellow dolostone (Burr Well Member equivalent) and pink limestone clasts of wallplaster affinity. These conglomerates exhibit a fining upwards succession (see Plate 6C) and a well-developed imbrication towards the south. Current direction is indicated by the arrow. The hammer handle is 25cm long.

B) Similar photograph of axial conglomerates displaying normal grading. Note the prominent sand-waves/megaripples at the top of the underlying bed which are also suggestive of considerable current velocities. The current direction is indicated by the arrow. The hammer handle is 25cm long.

C) Close up of normal grading within the axial conglomerates (HU5 equivalent unit). Note the yellow dolostone and pink limestone clasts. Their tabular nature indicates a proximal source (most probably the canyon walls). The basal bed fines upwards from coarse, poorly sorted conglomerate into a thinly laminated green limestone (that is well developed within the HU4&5 equivalent units) before being erosively truncated by the succeeding conglomeratic bed. Hammer handle is 25cm long.

D) Illustration of a clast derived from the ferruginous, coarse grained sandstone facies within the Ulupa Siltstone. The pen is 13.5cm long.

E & F) Photographs of the style of folding evident within the Wonoka Formation. Note the dominance of the Delamerian age cleavage (S3) and the absence of any other cleavage (S1 or S2). These photographs display the typical HU4 equivalent unit sediments. Bedding is clearly delineated by the thin green silts and/or green mud layers. The hammer handle is 25cm long.

Plate 6.

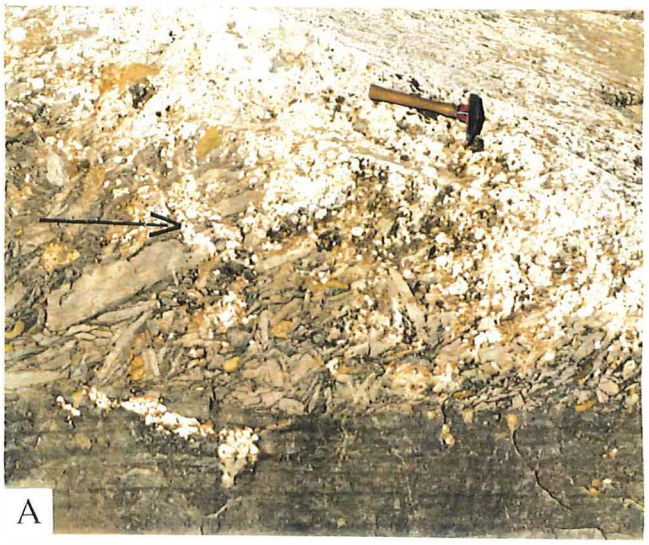
A


B


C

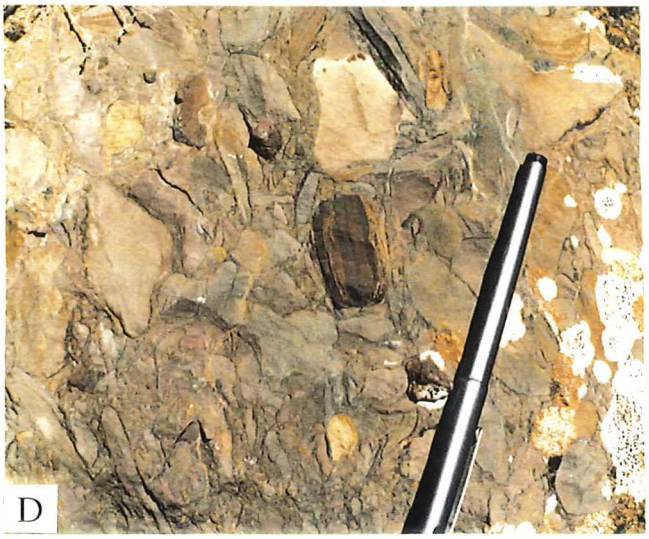
D

E

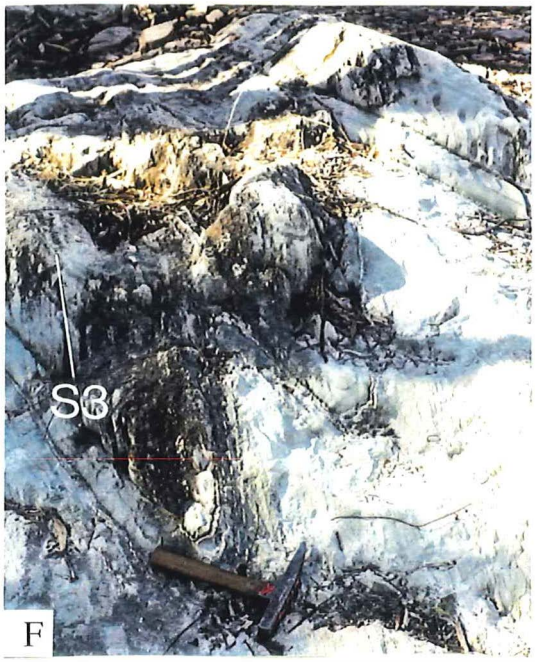

F

Plate 7.

A) Cryptalgal laminated yellow dolostone clast within the K1 Unit. Hammer handle is 30cm long.

B) Ulupa Siltstone boulder within the K1 Unit. Note that it has assumed a weak regional cleavage (S3). It is surrounded by the dark coloured silts characterising the upper portions of this succession. The hammer handle is 25cm long.

C) Photograph of a Ulupa Siltstone megaclast within the K1 Unit. The Ulupa siltstone moderately develops the regional cleavage (S3) and weakly assumes S2. Its bedding is proven by the presence of synaeresis cracks and ripple marks.

D) Close up of the cleavage development within the Ulupa Siltstone megaclast pictured in Plate 7C. Note that the regional cleavage dominates the rock, obscuring S2.

E) Illustration of the typically chaotically cleaved K1 Unit. The regional cleavage overprints the previous conjugate cleavage pair (S2i & S2ii). Further complicating this outcrop if the effects of creep as can be viewed in the centre right of this photograph.

F) Illustration of the primary slaty cleavage developed within the K1 unit. This cleavage is essentially parallel to bedding and almost always obscures it. This cleavage has been overprinted by the second cleavage phase (S2) and by the Delamerian cleavage (S3) in turn.

Plate 7.


A


B

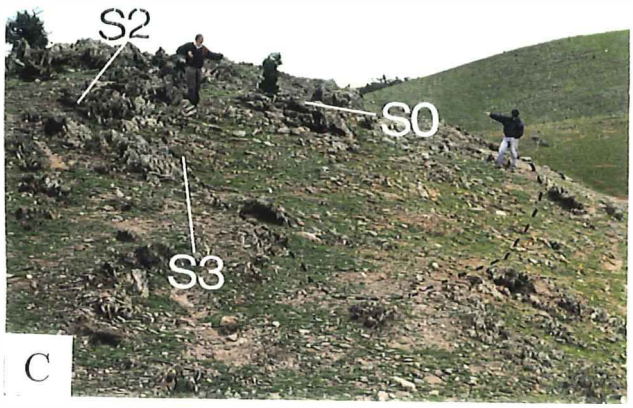

C

D

E

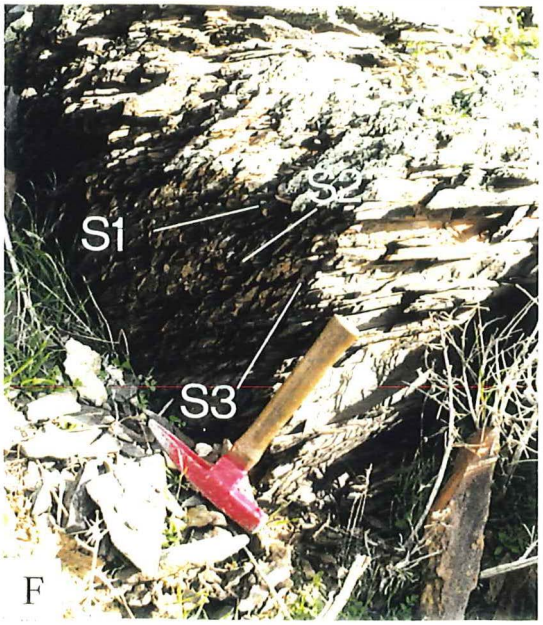

F

Plate 8.

High levels of luminescence observed reflect elevated concentrations of Mn.

A & B) Sample 2002-07B6. The plain light photomicrograph illustrates a calcite vein in this wall plaster sample. Two stages of diagenetic vein development (V1 & V2) are observed. This has then been overprinted by the dark euhedral crystals (c) seen in the cathodoluminescence photomicrograph. These crystals reflect a third stage of diagenesis responsible for the development of ferroan dolomite.

Cathodoluminescent photomicrograph (Plate 8A): Exposure time = 2.01s, Gun current = 236μA, Magnification = X4, Zoom = X8.
Plain light photomicrograph (Plate 8B): Exposure time = 1.18s, Gun current = 163μA, Magnification = X4, Zoom = X8.

C &D) Sample 2002-01V3. The plain light photomicrograph shows compositional variations within the wallplaster in addition to three stages of diagenetic veining (V1, V2, & V3). Cathodoluminescence confirms this and highlights a Ferroan dolomite (black euhedral crystals [c]) overprint in response to diagenesis.

Cathodoluminescent photomicrograph (Plate 8C): Exposure time = 6.60s, Gun current = 162μA, Magnification = X4, Zoom = X7.
Plain light photomicrograph (Plate 8D): Exposure time = 1.33s, Gun current = 180μA, Magnification = X4, Zoom = X7.

E & F) Sample 2002-01V3 displays two stages of veining (V1 & V2) intersecting the bedding. Cathodoluminescence confirms this but also highlights that diagenesis has produced a ferroan dolomite (black euhedral crystals [c]) overprint.

Cathodoluminescent photomicrograph (Plate 8A): Exposure time = 10.61s, Gun current = 168μA, Magnification = X4, Zoom = X8.

Plain light photomicrograph (Plate 8B): Exposure time = 0.99s, Gun current = 162μA, Magnification = X4, Zoom = X8.

Plate 8.

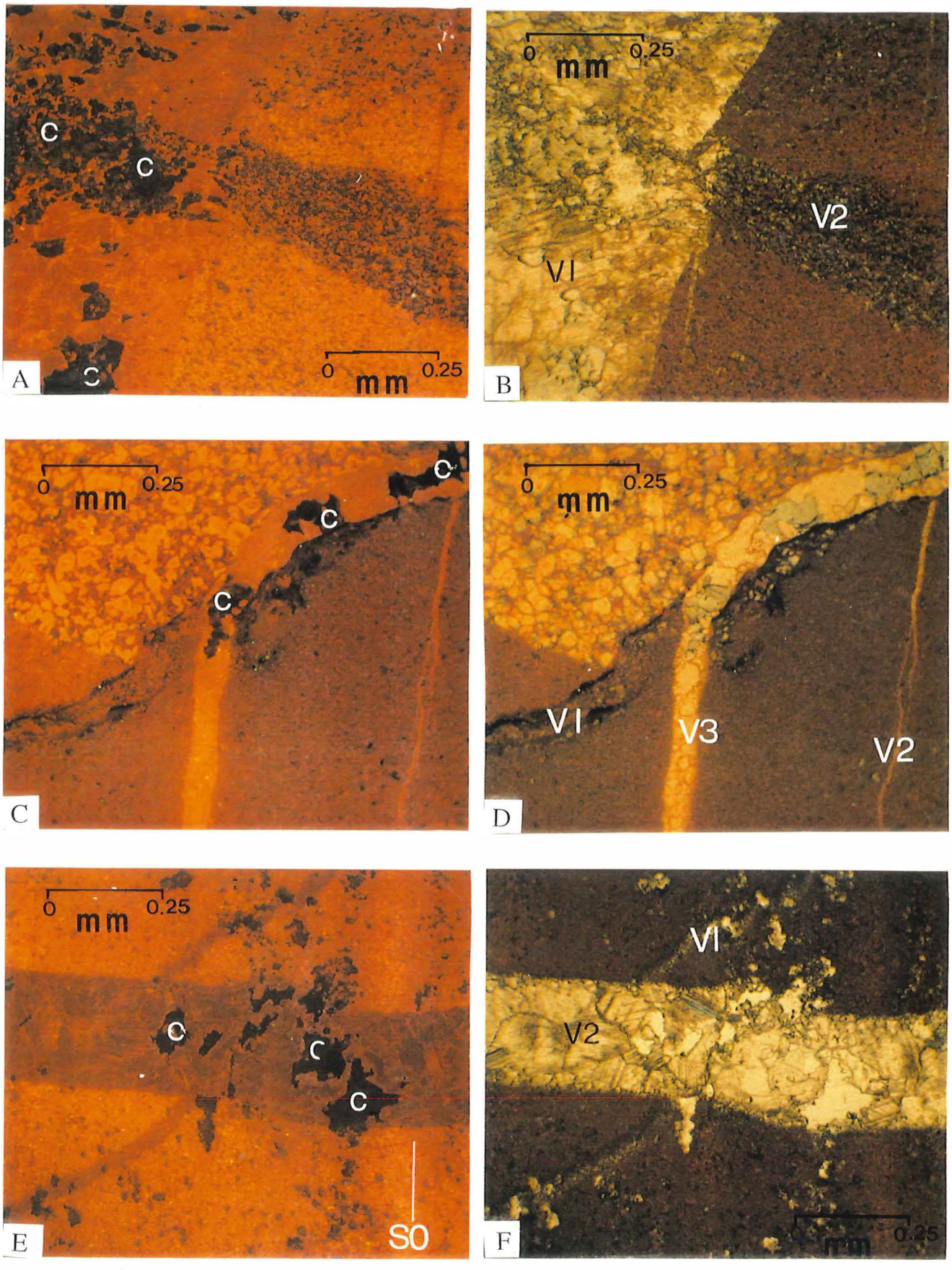
C
C
C
0 mm 0.25
A
0 mm 0.25
V2
V I
B
0 mm 0.25
C
C
C
C
0 mm 0.25
V I
V3
V2
D
0 mm 0.25
C
C
C
S0
E
V I
V2
0 mm 0.25
F

Plate 9.

The following plates illustrate the two major cleavages present within the region. S0 is the bedding plane, S2 is the pre-Delamerian cleavage and S3 is the regional, Delamerian age overprinted cleavage. In all photomicrographs S3 can be seen to kink S2 and bedding. S1 lies parallel to bedding and is obscured within these illustrations.

A) Sample 2002-04E5K1. Magnification = X10.
K1 Wonoka Formation

B) Sample 2002-04E5K1. Magnification = X10.
K1 Wonoka Formation

C) Sample 2002-13H6K1. Magnification = X10.
K1 Wonoka Formation

D) Sample 2002-17K1. Magnification = X5.
K1 Wonoka Formation

E) Sample 2002-16A13a. Magnification = X10.
Bunyeroo Formation

F) Sample 2002-16A13b. Magnification = X10.
Bunyeroo Formation

Plate 9.

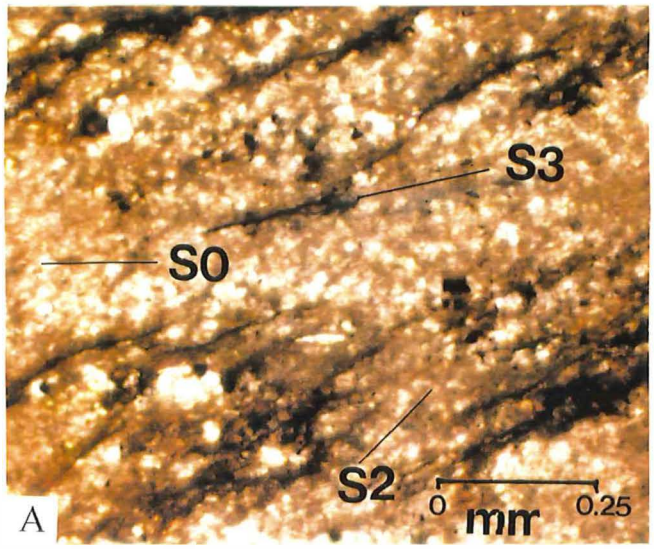

A

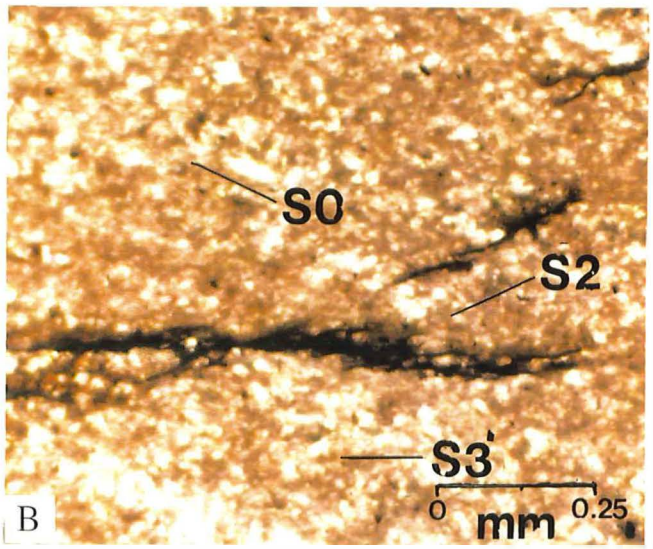

B

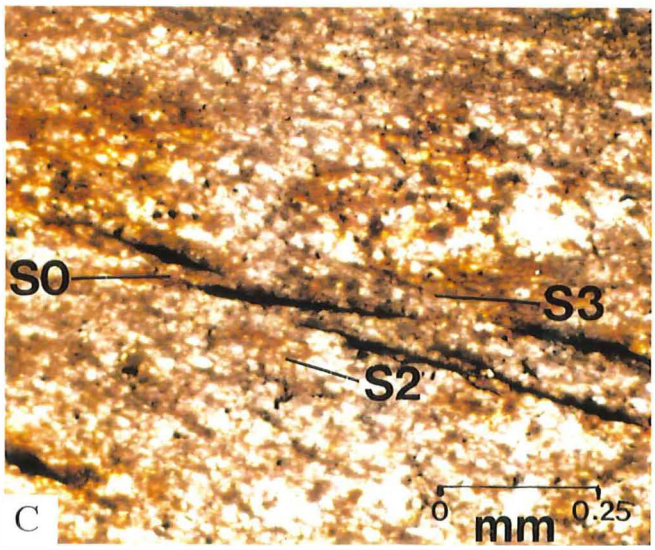

C

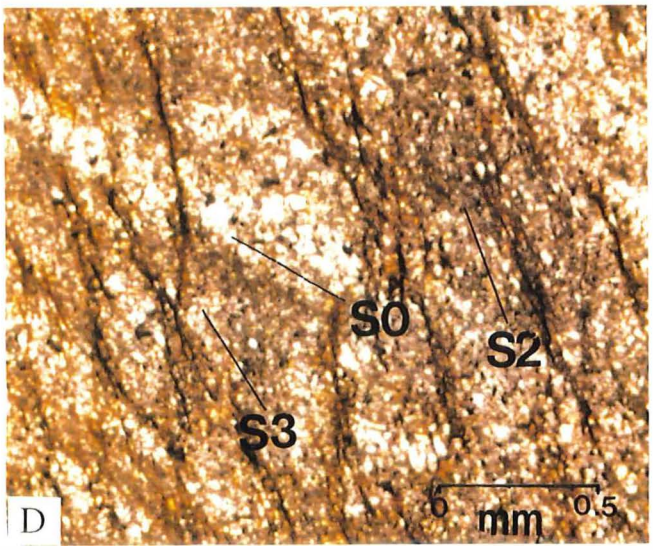

D

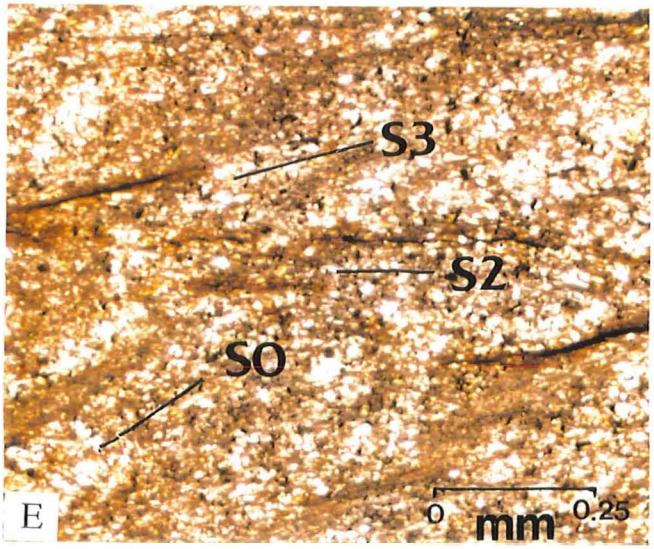

E

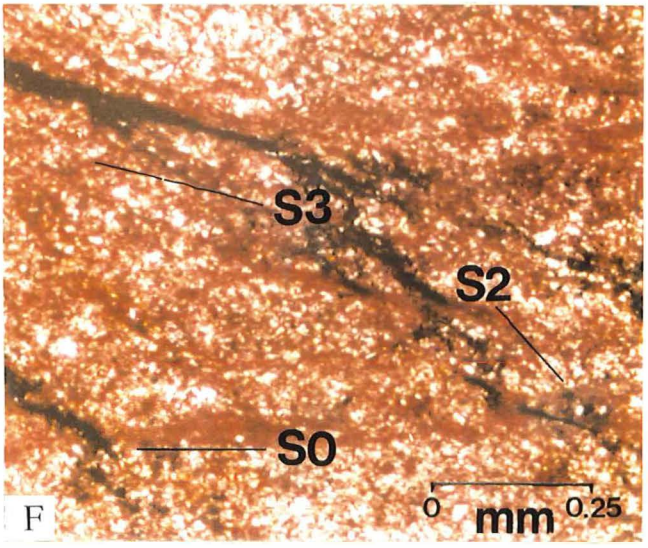

F

Plate 10.

1) Deformation prior to the Delamerian Orogeny that produced the regional cleavage (S3). A slaty cleavage (S1) is also present within this lithology although it has been obscured by subsequent deformation.

2) This particular sample exhibits all three cleavage types in addition to weakly displaying S3.

Plate 10.

Appendix C - Analytical Procedures.

1) X-ray Fluorescence (XRF) Analysis.

Preliminary Sample Preparation.

1) The samples were cut using an Allegro Supercut Model 63S rock saw to remove any weathered areas or veining.

2) Selected samples were crushed in a John Heine model 183A jaw crusher to produce gravel-sized pieces and milled for a short time in a Labtechnics W_2C (tungsten carbide) mill vessel to produce a fine powder suitable for analysis.

1) Major Element Analysis.

1) The samples were dried in an oven at 110°C for over 2 hours to remove any absorbed moisture.

2) Using a Sartorius R200D dual range electronic balance, the samples were weighed into alumina crucibles and the sample weight was logged into the SEDLOSS program being run on an Epson PC AX2 computer.

3) The samples were then placed into a muffle furnace and ignited overnight at 960°C.

4) The samples were removed from the furnace and allowed to cool in a dessicator.

5) The loss on ignition (LOI) was then calculated by reweighing the samples and logging the values into the computer This comprises organic material, CO_2 from carbonate minerals,water within crystal lattices and possibly S, Cl and other volatiles, depending on the mineralogy of the samples.

6) 1g of ignited sample was then weighed with 4g of flux (commercially available as type 12:22, comprising 35.3% lithium tetraborate and 64.7% lithium metaborate).

7) The sample-flux mixture was fused using a propane-oxygen flame, at a temperature of approximately 1150°C, using Pt-Au crucibles, and cast into a preheated mould to produce a glass disc suitable for analysis.

8) The samples were then analysed using a Philips PW 1480 X-Ray Fluorescence Spectrometer, using an analysis program calibrated against several international and local Standard Reference Materials (SRM's) A dual-anode (Sc-Mo) X-ray tube was used, operating at 40kV & 75mA.

Results.

Results were presented on a 'dry basis' in tabular form as oxides. The analyses are on the whole sample, including any residual organic material. The iron analysed is the total Fe, combining the ferrous and ferric forms, expressed as Fe_2O_3.

The oxides analysed are SiO_2, Al_2O_3, Fe_2O_3, MnO, MgO, CaO, Na_2O, K_2O, TiO_2, P_2O_5 & SO_3.

2) Trace Element Analysis.

1) About 5g of powdered sample was mixed with 1ml of PVA (Poly Vinyl Alcohol) binder solution.

2) This mixture was then pressed to form a pellet, using a Simplex 20HJ hydraulic press.

3) The was allowed to dry in air before being further heated for 2 hours in an oven at 60°C to ensure the pellet was completely dry before analysis.

4) The samples were analysed using a Philips PW 1480 XRF Spectrometer, using several analysis programs covering suites of from 1 to 7 trace elements, with conditions optimised for the elements being analysed. The programs were calibrated against many (30 or more in some cases) local and international SRM's. The dual anode Sc-Mo tube (operated at sufficient voltage to excite the Mo) and a Au tube were used for the analyses. Matrix corrections are made up using either the Compton scatter peak, or mass absorption coefficients calculated from the major element data.

Results.

The results are expressed in tabular form as ppm.The calibrations assume trace levels of the elements, usually p to one to several thousand ppm. Samples containing one or more of these trace elements in major proportions cannot be successfully analysed using the general trace element programs. In this case, special programs may need to be developed to permit satisfactory analysis.

Elements analysed include Sr (1.0), Rb (1.0), Zr (2.0), Y (1.0), U (1.5), Th (1.5) & Pb (2.5). The detection limits (DL) are in ppm in brackets with their accuracy being defined as +/- 5% at 100 X DL.

2) X-ray Diffraction (XRD) Analysis.

XRD analysis was used to assess the mineralogy of each particular sample prior to further geochemical and isotopic analysis.

1) A small amount of powdered sample was mixed with 3-4 drops of deionised water and ground up using a mortar and pestle.

2) The resultant slurry was then spread evenly over a glass slide.

3) The slide was then dried in an oven at 110°C to remove any water vapour before being analysed in a Philips-Siemens hybrid X-ray diffractometer.

Analysis was made using a Cobalt X-ray tube and a Philips PW1050 goniometer (employing a graphite monochrometer) under the following conditions:

- 50kV, 30mA.
- Divergence Slit Spacing = 1°.
- Receiving Slit Spacing = 1°.

A general scan was made from 3-75° at a rate of 2° per minute, which was then followed by a detailed scan of the calcite range, between 30-38°, at a rate of 1°/minute.

4) The resultant diffraction graphs were logged into the computer and examined, with the aid of reference peaks, in order to determine the relative abundances of the dominant, minor and trace minerals. The calcite and dolomite peaks were analysed in greater detail using the computer program 'mgcalc', to determine their exact characteristics. This facilitated the determination of the percentage of Magnesium Calcite present, along with the nature of any dolomite present.

3) Whole Rock $\delta^{13}C$ & $\delta^{18}O$ Determination.

Using the XRD analyses samples containing a suitable amount of calcite were selected for isotopic analysis. Due to the extremely low TOC values for the Wonoka Formation (Pell, 1989; Jansyn, 1990) and probable thermal alteration of organic carbon, C_{org} analysis was not attempted. The samples were analysed using the automated analytical procedures for the mass spectrometer. A lack of precision led to them being re-run individually on the mass spectrometer with the sample preparation being as follows.

Preliminary Sample Preparation.

1) The samples were cut using an Allegro Supercut Model 63S rock saw to remove any weathered areas or veining.

2) Selected samples were crushed in a John Heine model 183A jaw crusher to produce gravel-sized pieces and milled for a short time in a Labtechnics W_2C (tungsten carbide) mill vessel to produce a fine powder suitable for analysis.

3) Approximately 1g of sample was weighed on the Sartorius Sartorius R2007 dual range electronic balance before being placed in one half of a clean, dry glass sample tube.

4) 4ml of 100% phosphoric acid (H_3PO_3) was then added to the other arm of the sample tube.

5) The tube was the sealed and then attached to the vacuum line to be evacuated.

6) The samples were the placed in a water bath at 25°C and the temperatures were allowed to equalise for at least 20 minutes.

7) The sample tubes were then inverted and returned to the water bath. There they were left for a minimum of 16 hours (usually overnight) to enable the acid to react with the sample and liberated CO_2.

Collection Of CO_2.

1) The sample tubes were removed from the water bath and connected to the vacuum line.

2) Water and any other unwanted condensable volatiles were removed by the judicial application of near freezing ethanol.

3) The remaining CO_2 was then condensed using liquid nitrogen, into a glass tube which was then sealed using an oxygen/acetylene torch.

4) The sample gas volume was calculated along with the percentage yield of the sample using the following formulae:

a) Volume (cc) = 0.0795 X CO_2 pressure (at room temperature)

b) Yield % = Volume/sample weight X 415.

This value could be used to cross check with the percentage carbonate values obtained from the LOI analyses.

Measurement of $\delta^{13}C$ and $\delta^{18}O$.

1) The CO_2 distilled from the sample was then analysed using the OPTIMA dual inlet

stable isotope mass spectrometer (Fisons Instruments.) The isotopic signature of the sample CO_2 was then measured relative to a standard reference gas. The reference gas was calibrated against the international carbonate standard NBS-19.

2) Craig corrections for ^{14}C and ^{17}O were automatically applied by the computer to compensate for their contribution to the mass.

3) Isotopic ratios for $\delta^{13}C$ and $\delta^{18}O$ were then calculated using the following formulae:-

$$\delta^{13}C = (^{13}C/^{12}C_{sample} - {}^{13}C/^{12}C_{standard})/{}^{13}C/^{12}C_{standard} \text{ X } 1000.$$

$$\delta^{18}O = (^{18}O/^{16}O_{sample} - {}^{18}O/^{16}O_{standard})/{}^{18}O/^{16}O_{standard} \text{ X } 1000.$$

The values were reported using delta (δ) notation relative to both PDB and SMOW standards with the former being used for ease of reference.

4) Cathodoluminescence (CL.)

Polished thin sections were made of the samples of wallplaster and examined using a Leitz Ortholux PCL-X microscope in conjunction with a Technosyn cold-cathode, luminescence model 8200, Mk2.

Photomicrographs of slides of particular interest were made using the Leitz Orthomat 'E' photographic apparatus under the following conditions:

CL Conditions:-
- 10-15KV
- 200mA
- Reciprocity Failure Correction: 4
- Light/Dark Field Correction: D80%

Photographic Conditions:-
1-15 seconds exposure.
Ektapress 1600 film.

Appendix D - Analytical Results.

1. XRD Results.

K1 Unit.

Sample.	Dominant.	Minor.	Trace.	Calcite Composition.
K1-XX	Calcite	Quartz Chlorite Biotite Muscovite Plagioclase Orthoclase	Dolomite	2.4 mol% $MgCO^3$ LMC
K1-X	Calcite	Quartz Chlorite	Biotite	1.8 mol% $MgCO_3$ LMC
K1-AA	Quartz	Calcite Muscovite Chlorite Orthoclase	Biotite Plagioclase	2.4 mol% $MgCO_3$ LMC
K1-A	Quartz Calcite sub dominant	Muscovite Chlorite Plagioclase	Biotite Dolomite	1.3 mol% $MgCO_3$ LMC
K1-B	Quartz	Calcite Chlorite Muscovite Plagioclase	Biotite Dolomite Orthoclase	2.1 mol% $MgCO_3$ LMC
K1-D	Quartz	Calcite Orthoclase Plagioclase Muscovite	Biotite Chlorite	2.7 mol% $MgCO_3$ LMC
K1-E	Quartz	Chlorite Plagioclase	Calcite	Not measureable

		Muscovite Orthoclase		
K1-G	Quartz		Calcite	2.1 mol% $MgCO_3$ LMC
		Orthoclase Chlorite Plagioclase Muscovite		
K1-H	Calcite		Quartz Orthoclase Muscovite	2.7 mol% $MgCO_3$ LMC

Average Calcite Composition = 1.94 mol% $MgCO_3$ (LMC.)

Wallplaster.

Sample.	Dominant.	Minor.	Trace.	Calcite Composition.
B6WP	Calcite	Quartz	Orthoclase	1.8 mol% $MgCO_3$ LMC
D9WP	Calcite	Quartz	Chlorite	1.3 mol% $MgCO_3$ LMC
D12WP	Calcite	Quartz	Chlorite	2.4 mol% $MgCO_3$ LMC
F15WP	Calcite	Quartz	Chlorite Plagioclase	1.3 mol% $MgCO_3$ LMC
U5WP	Calcite	Quartz	Chlorite Plagioclase	1.3 mol% $MgCO_3$ LMC
V3WP	Calcite	Quartz	Chlorite	1.0 mol% $MgCO_3$ LMC
V21WP	Calcite	Quartz	Chlorite Plagioclase	1.0 mol% $MgCO_3$ LMC

WP1	Calcite	Quartz	Chlorite Plagioclase	2.4 mol% $MgCO_3$ LMC

Average Calcite Composition = 1.56 mol% $MgCO_3$ (LMC.)

K2 Sediments.

Sample.	Dominant.	Minor.	Trace.	Calcite Composition.
71.1m	Calcite	Quartz Muscovite Dolomite Plagioclase		2.1 mol% $MgCO_3$ LMC

Dolomite Composition - 45% $MgCO_3$
55% $CaCO_3$

223.5m	Calcite	Quartz Plagioclase	Muscovite Chlorite	0.4 mol% $MgCO_3$ LMC
299.0m	Calcite	Quartz	Orthoclase Muscovite Chlorite	1.3 mol% $MgCO_3$ LMC
400.0m	Calcite	Quartz	Muscovite Plagioclase Chlorite	1.6 mol% $MgCO_3$ LMC
488.6m	Calcite	Quartz	Muscovite Chlorite Orthoclase Plagioclase	1.3 mol% $MgCO_3$ LMC
922.0m	Calcite	Quartz Muscovite Plagioclase Chlorite		0.4 mol% $MgCO_3$ LMC
949.9m	Calcite	Quartz	Muscovite	1.6 mol% $MgCO_3$

			Chlorite Plagioclase	LMC
963.1m	Calcite	Quartz	Muscovite Chlorite Plagioclase	1.6 mol% $MgCO_3$ LMC

Average Calcite Composition = 1.28 mol% $MgCO_3$ (LMC.)

2. Sr/Rb Analyses (And Some Other Elements).

Sample	Zr ppm	Y ppm	Sr ppm	Rb ppm	U ppm	Th ppm	Pb ppm
Wallplaster.							
KMWP	52.9	11.6	484.7	12.2	1.1	6.3	3.5
A1WP	44.90	3.60	487.80	12.50	1.70	4.90	9.40
B6WP	62.80	13.80	660.60	16.60	2.20	5.20	18.30
B10WP	48.80	5.10	338.40	11.70	2.10	6.00	9.80
D12WP	126.20	19.60	1651.20	12.70	1.20	5.60	11.90
F15WP	60.90	10.00	488.00	6.30	2.40	8.40	141.40
V3WP	43.90	8.50	315.00	22.00	0.10	4.20	13.00
V21WP	87.20	3.80	833.80	10.90	0.40	5.10	18.10
Average	**67.81**	**9.20**	**682.11**	**13.24**	**1.44**	**5.63**	**31.70**
K1 Unit.							
K1-XX	209.30	22.20	659.50	54.80	4.10	12.80	7.60
K1-X	67.60	17.10	615.50	12.90	1.50	6.20	8.20
K1-AA	219.20	36.80	36.80	166.60	3.50	19.80	10.50
K1-A	670.20	16.30	8044.40	44.50	4.60	10.00	4.50
K1-B	732.70	26.30	6931.00	72.20	4.90	14.90	23.30
K1-D	201.20	24.10	91.40	150.20	11.00	18.00	68.60
K1-E	248.10	32.60	136.70	143.80	4.30	16.60	14.90
K1-G	268.40	35.20	85.60	148.20	5.20	18.60	43.40
K1-H	81.50	18.60	820.00	10.90	3.50	4.70	9.00
Average	**449.7**	**38.2**	**2903.4**	**89.34**	**7.1**	**20.27**	**31.67**

Major Element Data.

Sample Name	SiO2%	Al2O3%	Fe2O3%	MnO%	MgO%	CaO%	Na2O%	K2O%	TiO2%	P2O5%	SO3%	LOI%	Total%
Wallplaster.													
KMWP	8.91	1.92	0.6	0.45	2.07	44.67	0.98	0.24	0.12	0.11	0.08	37.84	97.99
A1WP	8.11	1.57	0.57	0.08	1.49	45.68	0.86	0.24	0.11	0.14	0.05	38.7	97.6
B6WP	8.56	1.45	0.71	0.05	1.85	45.43	0.64	0.31	0.12	0.17	0.07	38.61	97.95
D12WP	14.49	1.69	1.01	0.16	1.77	42.49	0.74	0.2	0.11	0.1	0.06	35.63	98.45
F15WP	10.51	2.35	0.46	0.38	1.92	43.18	1.4	0.11	0.15	0.12	0.06	37.17	97.81
V3WP	9.98	2.13	2.21	0.14	1.43	43.61	0.83	0.4	0.15	0.13	0.25	36.97	98.22
V21WP	9.28	1.57	0.72	0.06	1.83	45.03	0.71	0.19	0.13	0.1	0.1	38.16	97.88
WP1	6.38	1.59	0.73	0.06	1.68	46.72	0.57	0.4	0.12	0.14	0.05	39.44	97.88
Average	**9.62**	**1.76**	**0.92**	**0.13**	**1.71**	**44.59**	**0.82**	**0.26**	**0.13**	**0.13**	**0.09**	**37.81**	**97.97**
K1 Unit.													
K1-XX	41.99	7.81	3.13	0.23	1.91	22.23	2.09	1.09	0.49	0.16	0.02	18.85	100.02
K1-X	11.08	2.13	0.98	0.37	1.64	43.72	1.01	0.24	0.15	0.12	0.09	36.61	98.13
K1-AA	60.7	13.91	6.57	0.05	3.25	2.4	1.25	3.39	0.87	0.19	0.19	6.18	98.8
K1-A	52.44	7.23	2.39	0.07	1.51	15.51	2.57	0.74	0.39	0.12	0.12	13.44	97.43
K1-B	57.8	7.37	1.85	0.07	1.29	13.2	2.06	1.26	0.75	0.08	0.08	11.52	98.09
K1-H	10.86	1.81	0.91	0.25	1.7	43.93	0.89	0.19	0.13	0.15	0.15	37.01	97.94
Average	**39.15**	**6.71**	**2.64**	**0.17**	**1.88**	**23.50**	**1.64**	**1.15**	**0.46**	**0.14**	**0.11**	**20.60**	**98.40**

Major Element Data.

Sample Name	SiO2%	Al2O3%	Fe2O3%	MnO%	MgO%	CaO%	Na2O%	K2O%	TiO2%	P2O5%	SO3%	LOI%	Total%
Wallplaster.													
KMWP	8.91	1.92	0.6	0.45	2.07	44.67	0.98	0.24	0.12	0.11	0.08	37.84	97.99
A1WP	8.11	1.57	0.57	0.08	1.49	45.68	0.86	0.24	0.11	0.14	0.05	38.7	97.6
B6WP	8.56	1.45	0.71	0.05	1.85	45.43	0.64	0.31	0.12	0.17	0.07	38.61	97.95
D12WP	14.49	1.69	1.01	0.16	1.77	42.49	0.74	0.2	0.11	0.1	0.06	35.63	98.45
F15WP	10.51	2.35	0.46	0.38	1.92	43.18	1.4	0.11	0.15	0.12	0.06	37.17	97.81
V3WP	9.98	2.13	2.21	0.14	1.43	43.61	0.83	0.4	0.15	0.13	0.25	36.97	98.22
V21WP	9.28	1.57	0.72	0.06	1.83	45.03	0.71	0.19	0.13	0.1	0.1	38.16	97.88
WP1	6.38	1.59	0.73	0.06	1.68	46.72	0.57	0.4	0.12	0.14	0.05	39.44	97.88
Average	**9.62**	**1.76**	**0.92**	**0.13**	**1.71**	**44.59**	**0.82**	**0.26**	**0.13**	**0.13**	**0.09**	**37.81**	**97.97**
K1 Unit.													
K1-XX	41.99	7.81	3.13	0.23	1.91	22.23	2.09	1.09	0.49	0.16	0.02	18.85	100.02
K1-X	11.08	2.13	0.98	0.37	1.64	43.72	1.01	0.24	0.15	0.12	0.09	36.61	98.13
K1-AA	60.7	13.91	6.57	0.05	3.25	2.4	1.25	3.39	0.87	0.19	0.19	6.18	98.8
K1-A	52.44	7.23	2.39	0.07	1.51	15.51	2.57	0.74	0.39	0.12	0.12	13.44	97.43
K1-B	57.8	7.37	1.85	0.07	1.29	13.2	2.06	1.26	0.75	0.08	0.08	11.52	98.09
K1-H	10.86	1.81	0.91	0.25	1.7	43.93	0.89	0.19	0.13	0.15	0.15	37.01	97.94
Average	**39.15**	**6.71**	**2.64**	**0.17**	**1.88**	**23.50**	**1.64**	**1.15**	**0.46**	**0.14**	**0.11**	**20.60**	**98.40**

Cross Section.

Sample.	d18O(PDB.)	d13C (PDB.)
71.1m	-5.673	-6.102
223.5m	-14.155	-7.606
400.0 m	-13.213	-7.572
486.0m	-12.985	-7.288
922.0m	-13.264	-7.481
963.1m	-14.155	-7.776
Average:-	*-12.241*	*-7.304*

K1 Wonoka Formation.

Sample.	d18O(PDB.)	d13C (PDB.)
K1-XX	-16.42	-9.861
K1-X	-15.53	-8.194
K1-AA	-13.35	-7.455
K1-AA	-15.668	-7.453
K1-A	-15.222	-8.05
K1-B	-15.655	-8.305
K1-H	-15.74	-7.656
Average:-	*-15.369*	*-8.139*

Wallplaster.

Sample.	d18O(PDB.)	d13C (PDB.)
KMWP	-17.543	-9.075
A1WP	-15.651	-8.498
B6WP	-14.618	-8.863
D12WP	-15.345	-8.64
F15WP	-15.378	-7.854
V3WP	-10.22	-8.839
V21WP	-17.358	-8.55
Average:-	*-12.655*	*-8.541* δ

Eickhoff, 1988.

Sample.	d18O(PDB.)	d13C (PDB.)
E133	-15.26	-9.01
E270	-14.95	-9.4
E275	-14.73	-9.11

E324	-15.18	-8.45
E408	-15.12	-7.2
E425	-15.92	-8.75
Bouldery Mudstone - Wallplaster Clasts		
E123	-15.67	-10.1
E240	-15.68	-9.22
E253	-16.02	-9.08
E255	-15.75	-8.3

Note: due to the limitations of the computer program delta notation is expressed as d18O, d13C.

SPEC. COLL.
THESIS
Q9S.B
H636

UNIVERSITY OF ADELAIDE
30-7-98

The Geology of the Pamatta Pass Canyon Complex, Flinders Ranges, South Australia.

Drafted by Jonathan Higgins
University Of Adelaide, 11/97.

Locality Map.

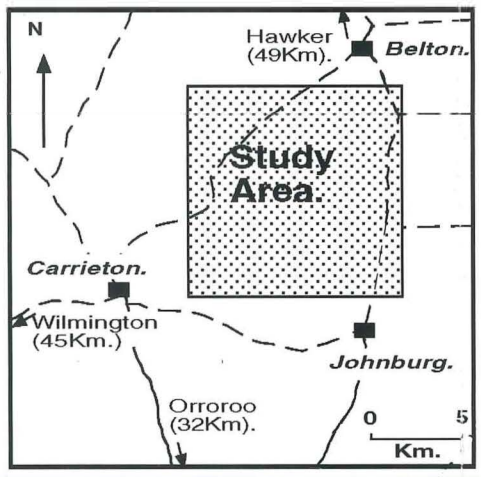

MN

0 1 2
Km.

138°41'

32°23'

"Weira Downs."

"Sandal Park."

"Wilchata."

LEGEND

- Syncline with plunge direction. (12)
- Anticline with plunge direction. (08)
- Please note that only the major fold axes are indicated. Parallelling these axes are numerous smaller scale, parasitic folds.
- Unsealed road.
- Track.
- Homestead.
- Dip and strike of bedding (S0). (45)
- Dip and strike of S2. (45)
- Dip and strike of S3. (45)
- Fault Boundaries: Observed
- Geological Boundaries: Observed / Inferred / Trend Line.

LITHOLOGY

- Alluvium.
- Depot Springs Subgroup.
- Wonoka Formation.
  - Unit 5.
  - Unit 4.
  - Wall Plaster.
  - Basal Sands Unit.
  - Basal Conglomerate Unit.
  - Olistostrome Unit.
  - K1 Unit.
- Aruhna Subgroup.
  - Bunyeroo Formation.
  - Wilcolo Sandstone.
- Sandison Subgroup.
  - ABC Range Quartzite.
  - Ulupa Siltstone.
- Umberatana Group.